Arid Land Condition Assessment and Monitoring Using Multispectral and Hyperspectral Imagery

By

Reza Jafari

Thesis submitted in fulfilment of the requirements for the degree of

Doctor of Philosophy

Discipline of Soil and Land Systems

School of Earth and Environmental Sciences

June 2007

TABLE OF CONTENTS

ABSTRACT

Arid lands cover approximately 30% of the earth's surface. Due to the broadness, remoteness, and harsh condition of these lands, land condition assessment and monitoring using ground-based techniques appear to be limited. Remote sensing imagery with its broad areal coverage, repeatability, cost and time-effectiveness has been suggested and used as an alternative approach for more than three decades. This thesis evaluated the potential of different remote sensing techniques for assessing and monitoring land condition of southern arid lands of South Australia. There were four specific objectives: 1) to evaluate vegetation indices derived from multispectral satellite imagery for prediction of vegetation cover; 2) to compare vegetation indices and field measurements for detecting vegetation changes and assessing land condition; 3) to examine the potential of hyperspectral imagery for discriminating vegetation components that are important in land management using unmixing techniques; and 4) to test whether spatial heterogeneity in land surface reflectance can provide additional information about land condition and effects of management on land condition.

The study focused on Kingoonya and Gawler Soil Conservation Districts that were dominated by chenopod shrublands and low open woodlands over sand plains and dunes. The area has been grazed predominately by sheep for more than 100 years and land degradation or desertification due to overgrazing is evident in some parts of the region, especially around stock watering points. Grazing is the most important factor that influences land condition. Four full scenes of Landsat TM and ETM+ multispectral and Hyperion hyperspectral data were acquired over the study area. The imagery was acquired in dry seasons to highlight perennial vegetation cover that has an important role in land condition assessment and monitoring.

Slope-based, distance-based, orthogonal transformation and plant-water sensitive vegetation indices were compared with vegetation cover estimates at monitoring points made by state government agency staff during the first Pastoral Lease assessments in 1991. To examine the performance of vegetation indices, they were tested at two scales: within two contrasting land systems and across broader regional landscapes. Of the vegetation indices evaluated, selected Stress Related Vegetation Indices using red, near-infrared and mid-infrared bands consistently showed significant relationships with vegetation cover at both land system and landscape scales. Estimation of vegetation

cover was more accurate within land systems than across broader regions. Total perennial and ephemeral plant cover was predicted best within land systems (R^2=0.88), while combined vegetation, plant litter and soil cryptogam crust cover was predicted best at landscape scale (R^2=0.39).

The results of applying one of the stress related vegetation indices (STVI-4) to 1991 TM and 2002 ETM+ Landsat imagery to detect vegetation changes and to 2005 Landsat TM imagery to discriminate Land Condition Index (LCI) classes showed that it is an appropriate vegetation index for both identifying trends in vegetation cover and assessing land condition. STVI-4 highlighted increases and decreases in vegetation in different parts of the study area. The vegetation change image provided useful information about changes in vegetation cover resulting from variations in climate and alterations in land management. STVI-4 was able to differentiate all three LCI classes (poor, fair and good condition) in low open woodlands with 95% confidence level. In chenopod shrubland and Mount Eba country only poor and good conditions were separable spectrally.

The application of spectral mixture analysis to Hyperion hyperspectral imagery yielded five distinct end-members: two associated with vegetation cover and the remaining three associated with different soils, surface gravel and stone. The specific identity of the image end-members was determined by comparing their mean spectra with field reflectance spectra collected with an Analytical Spectral Devices (ASD) Field Spec Pro spectrometer. One vegetation end-member correlated significantly with cottonbush vegetation cover (R^2=0.89), distributed as patches throughout the study area. The second vegetation end-member appeared to map green and grey-green perennial shrubs (e.g. Mulga) and correlated significantly with total vegetation cover (R^2=0.68). The soil and surface gravel and stone end-members that mapped sand plains, sand dunes, and surface gravel and stone did not show significant correlations with the field estimates of these soil surface components.

I examined the potential of a spatial heterogeneity index, the Moving Standard Deviation Index (MSDI), around stock watering points and nearby ungrazed reference sites. One of the major indirect effects of watering points in a grazed landscape is the development around them of a zone of extreme degradation called a piosphere. MSDI was applied to Landsat red band for detection and assessment of these zones. Results

showed watering points had significantly higher MSDI values than non-degraded reference areas. Comparison of two vegetation indices, the Normalized Difference Vegetation Index (NDVI) and Perpendicular Distance vegetation index (PD54), which were used as reference indices, showed that the PD54 was more sensitive than NDVI for assessing land condition in this perennial-dominated arid environment. Piospheres were found to be more spatially heterogeneous in land surface reflectance. They had higher MSDI values compared to non-degraded areas, and spatial heterogeneity decreased with increasing distance from water points.

The study has demonstrated overall that image-based indices derived from Landsat multispectral and Hyperion hyperspectral imagery can be used with field methods to assess and monitor vegetation cover (and consequently land condition) of southern arid lands of South Australia in a quick and efficient way. Relationships between vegetation indices, end-members and field measurements can be used to estimate vegetation cover and monitor its variation with time in broad areas where field-based methods are not effective. Multispectral vegetation indices can be used to assess and discriminate ground-based land condition classes. The sandy-loam end-member extracted from Hyperion imagery has high potential for monitoring sand dunes and their movement over time. The MSDI showed that spatial heterogeneity in land surface reflectance can be used as a good indicator of land degradation. It differentiated degraded from non-degraded areas successfully and detected grazing gradients slightly better than widely used vegetation indices. Results suggest further research using these remote sensing techniques is warranted for arid land condition assessment and monitoring in South Australia.

DECLARATION

This work contains no material which has been accepted for the award of any other degree or diploma in any university or other tertiary institution and, to the best of my knowledge and belief, contains no material previously published or written by another person, except where due reference has been made in the text.

I give consent to this copy of my thesis being available for loan and photocopying.

Signed:……. Date:……..

Reza Jafari

ACKNOWLEDGEMENTS

I would like to take this opportunity to acknowledge many people who have given their time to facilitate the completion of this thesis. To those who I have not mentioned their name, I say thank you.

My supervisors, Dr. Megan Lewis and Dr. Bertram Ostendorf, have both provided continual guidance and support. In particular Dr. Megan Lewis has enabled me to get on with it, and for that I thank her warmly.

Joel Denton from Mount Vivian station and Wayne Rankin from McDoual Peak station and all the other pastoralists who allowed me to access their properties.

The assistance and support of my colleagues in the Spatial Information Group: Anna Dutkiewicz, David Summers, Sean Mahoney, Dorothy Turner, David Mitchell, Neville Grossman, Christina Gabrovsek, Paul Bierman, Ramesh Raja Segaran, Rowena Morris, Kenneth Clarke, Dave Hart, Gregory Lyle is appreciated. In particular, I thank Kenneth Clarke for his assistance in the field work and Anna Dutkiewicz and David Summers for their assistance with the ASD Fieldspec Pro Spectrometer.

A range of data providers is acknowledged for their support of the research. James Cameron at Department of Environment and Heritage (DEH) for his help in selecting appropriate Landsat and Hyperion imagery. Amanda Brook, Paul Gould, Ben Della Torre, and Brendan Lay at the Department of Water, Land and Biodiversity Conservation (DWLBC) provided rainfall, field and spatial data.

I thank my dear wife, Mansoureh Malekian, who supported the study in so many ways. Without her constant support and encouragement, completion of this thesis would have not been possible.

PUBLICATIONS ARISING FROM THIS THESIS

Refereed Publications

Jafari, R., Lewis, M.M. and Ostendorf, B., 2007. Evaluation of vegetation indices for assessing vegetation cover in southern arid lands in South Australia. *The Rangeland Journal* 29(1), 39-49.

Jafari, R., Lewis, M.M. and Ostendorf, B., 2007. An image-based diversity index for assessing land degradation in an arid environment in South Australia. *Journal of Arid Environments* (submitted January 2007, under review).

Other Publications

Jafari, R., Lewis, M.M. and Ostendorf, B., 2006. Analysis of vegetation indices for assessing and monitoring vegetation cover in an arid environment in South Australia, Proceedings of the 14th Biennial Australian Rangeland Society Conference, Renmark, South Australia, , September 2006, pp. 229-232.

Jafari, R., Lewis, M.M. and Ostendorf, B., 2006. An image-based diversity index for assessing land degradation in an arid environment in South Australia, Proceedings of the 13th Australian Remote Sensing and Photogrammetry Conference (ARSPC), The Photogrammetry Association of Australia, CD publication, November 2006, Canberra, Australia.

Jafari, R., Lewis, M.M. and Ostendorf, B., 2006. Use of EO-1 hyperspectral imagery for discriminating arid vegetation, Proceedings of the 13th Australian Remote Sensing and Photogrammetry Conference (ARSPC), The Photogrammetry Association of Australia, CD publication, November 2006, Canberra, Australia.

1 INTRODUCTION

Arid lands occupy nearly one-third of the world's total land surface (Figure 1.1) and support about 13 percent of the world's population (Matlock, 1981). Drought, low and variable rainfall and high temperature and evaporation are the main characteristics of these dry lands. Arid lands are defined as areas falling within the rainfall range of 0-300 mm (FAO, 1987). Because of variability in rainfall and the short growing period of around less than 74 days (FAO, 1987), these areas are not suitable for cultivated agriculture. The main land use in these regions is grazing that depends entirely on native vegetation cover. Research by FAO in 36 dry countries showed that without changes in grazing areas, the numbers of stock increased from 400 million head in 1961 to 600 million in 1995 (FAO, 1996). As a result, the increase of stock numbers has been one of the main reasons for land degradation in these low productive lands. Overgrazing has been documented widely as one of the main causes of land degradation in arid and semi-arid regions (Hostert *et al.*, 2003b; Archer, 2004; Farahpour *et al.*, 2004; Hahn *et al.*, 2005; Kinloch and Friedel, 2005a; Kinloch and Friedel, 2005b; Zhao *et al.*, 2005; Ruthven III, 2007; Zhao *et al.*, 2007). It has been reported that approximately 80 percent of arid and semi-arid land degradation in Australia has been caused by overgrazing (Figure 1.2).

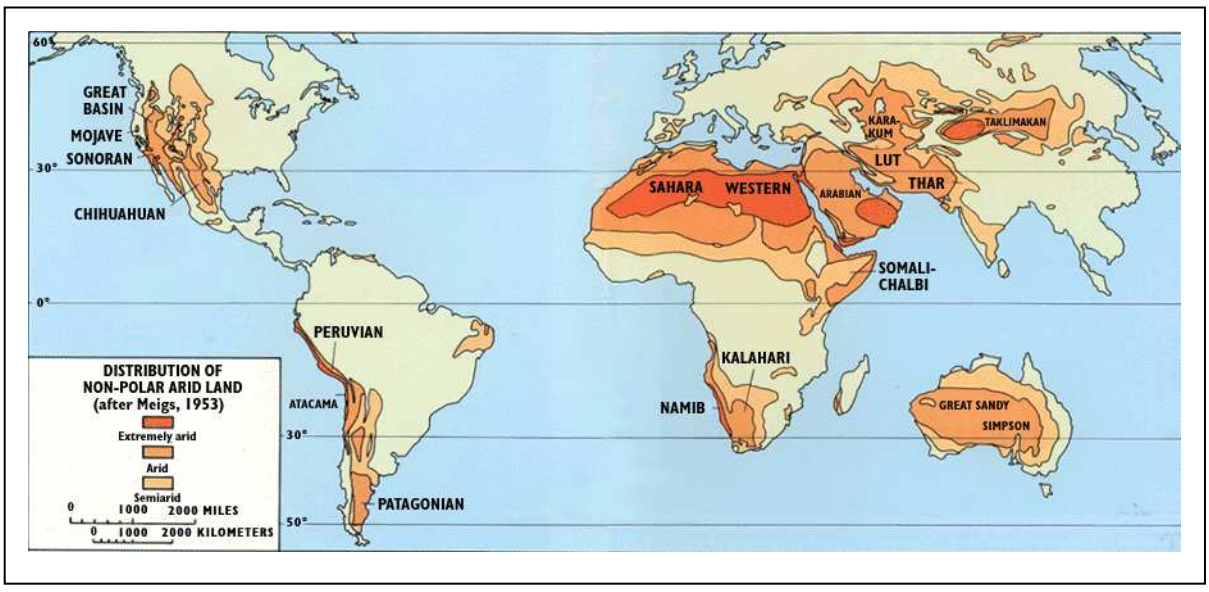

Figure 1.1 The distribution of arid lands in the world (Fraser, 1997)

NOTE: This figure is included on page 2 of the print copy of the thesis held in the University of Adelaide Library.

Figure 1.2 Arid and semi-arid Rangeland degradation from 1945 to 1995. Percentages indicate contribution of overgrazing to total degraded area (Sidahmed, 1996)

Land degradation in arid lands, also called desertification, is a term that became widely known through the 1969-1973 drought in the Sahel region of Africa that caused the starvation of millions of people and livestock (Dregne, 1983). Since then have been documented widely the causes, processes, and consequences of this phenomenon (Dregne, 1983; Chisholm and Dumsday, 1987; Pickup, 1990; Schlesinger *et al.*, 1990; Kassas, 1995; Rubio and Bochet, 1998; Arnalds and Archer, 2000; Dregne, 2002; Reynolds and Stafford Smith, 2002; Symeonakis and Drake, 2004; Zhao *et al.*, 2005). The latest definition of desertification that was presented in Brazil in 1992 (UNCED, 1992) is "*land degradation in arid, semi-arid, dry subhumid areas resulting from various factors including climate variations and human activities.*" The term desertification refers to a group of land degradation processes which have the most impact on the productivity of land. They include vegetation degradation, wind erosion, water erosion, salinisation, and soil compaction. The FAO and the United Nations Environment Programme (UNEP) developed a provisional methodology for assessment and mapping of desertification based on various criteria for each of the contributing processes (FAO, 1983). The evaluation of this internationally recognized technique in a pilot project in Kenya showed that applying this method across broad areas is timeconsuming and expensive (Grunblatt *et al.*, 1992). Hence, many studies (Rubio and

Bochet, 1998; Sharma, 1998; Jafari, 2001) have attempted to reduce the number of the criteria provided by FAO/UNEP in order to reduce the cost and use criteria that are more applicable to local scales.

Among the various desertification processes, vegetation degradation is the main process in Australia's arid lands (Stanley, 1982; Woods, 1983; McKeon *et al.*, 2004) (Table 1.1). It often occurs around stock watering points (Lange, 1969) and starts with the reduction of vegetation cover. This can result from single or combined effects of overgrazing, rainfall deficits. The effects of these are the appearance of barren soils and an increased susceptibility to wind and water erosion.

Table 1.1 Vegetation degradation in Australian arid lands (Chisholm and Dumsday, 1987)

NOTE: This table is included on page 3 of the print copy of the thesis held in the University of Adelaide Library.

The arid lands of Australia cover about 75% of the continent. Half of these areas are not suitable for grazing, while the rest of them are used for stock grazing (Chisholm and Dumsday, 1987). Arid and semi-arid grazing lands cover 85% of South Australia. The grazing history of this area followed the settlement by Europeans about 100 years ago (Condon, 1982). Since then, because of mismanagement, a large amount of the arid lands in South Australia have been overgrazed and moved towards degradation. It has been estimated that approximately 35% of Australia’s arid lands were degraded within a few years of European settlement (Stanley, 1982), and a substantial loss of perennial vegetation and soil was reported in south Australian grazing lands in the 1920s (McKeon *et al.*, 2004). To protect these areas from degradation the south Australian Pastoral Land Management and Conservation Act was enacted in 1989. The land care objectives of the Act are to: (1) "*ensure that all pastoral lands in the state are well managed and utilized prudently so that its renewable resources are maintained and its*

yield sustained; and (2) provide for the effective monitoring of the condition of pastoral lands, the prevention of degradation of the land and its indigenous plant and animal life, and the rehabilitation of the land in cases of damage."

A major problem that all landholders, administrators and researchers have confronted is the lack of suitable techniques to assess and monitor arid rangeland condition. Rangeland condition here refers to the health and stability of the land. It is determined by comparing soil and vegetation characteristics at different sites within the same area. The main aim of assessing rangeland condition is to determine the effect of grazing on land condition (Lay and Evans, 1973). A variety of different field assessment and monitoring methods have been used to evaluate land condition in rangelands, both in Australia and internationally (Lay and Evans, 1973; Wilson *et al.*, 1987; Mesdaghi, 1998; Arizona University, 2001). In South Australia, two field methods have been used for assessing and monitoring rangeland condition: the land condition index (LCI) and permanent monitoring sites. The LCI is used to provide a long term assessment of average land condition in the southern arid lands of South Australia every 14 years. It categorises land into three condition classes (poor, fair, and good) using visual assessments against defined criteria at many random sites. In contrast to the LCI, permanent monitoring sites have been established to determine shorter temporal trends in land condition (Department of Water Land Biodiversity and Conservation, 2002). Although these ground-based methods provide detailed data at small sites, they can not adequately cover the vast areas of the arid rangelands, and in addition they are time-consuming, expensive and subject to human error (Walker, 1970; Friedel and Shaw, 1987a; Friedel and Shaw, 1987b).

Vegetation cover is one of the most important components of the earth's surface. It strongly influences evapotranspiration, infiltration, runoff and soil erosion. Vegetation cover is also the principal factor limiting stocking rates in managed grazing lands. It has been widely recognized as one of the best indicators for determining land condition (Bastin *et al.*, 1998; Booth and Tueller, 2003; Bastin and Ludwig, 2006; Wallace *et al.*, 2006). Therefore, land condition can be assessed and monitored according to vegetation cover and its variations in time and space. This component is often used as the key indicator in the remote sensing of land condition.

Use of remote sensing for land condition assessment and monitoring started with the launch of the first Landsat satellite in 1972. Since then many other polar orbiting Earth-observation satellites such as the Landsat series, Earth Observation-1 (EO-1), Satellite Pour l'Observation de la Terre (SPOT), National Oceanic and Atmospheric Administration (NOAA), Advanced Spaceborne Thermal Emission and Reflection Radiometer (ASTER), Moderate Resolution Imaging Spectroradiometer (MODIS) have been launched and their imagery have been used for a wide range of applications. The broad swaths and regular revisit frequencies of these multispectral satellites mean that they can be used to rapidly detect changes in land cover. However, their limited spectral resolution reduces the capability of these multispectral sensors for discriminating different land cover components. Airborne hyperspectral sensors such as the NASA Airborne Visible-InfraRed Imaging Spectrometer (AVIRIS) with high spectral and spatial resolution have overcome this problem (Asner and Heidebrecht, 2003). Furthermore, because of their high spectral resolution, their images can be calibrated to absolute reflectance and compared with field and laboratory spectra. However, despite the many advantages of airborne imagery, its application to arid lands, with their extensive areas, is limited by high cost. Spaceborne hyperspectral sensors such as Hyperion on board of NASA's Earth Observing-1 (EO-1) satellite seem to overcome some of the limitations of both mutispectral and airborne hyperspectral sensors.

Remotely sensed data has been applied successfully to the assessment and monitoring of vegetation cover, land degradation, forestation and deforestation, floods, fire and many other applications (Johannsen and Sanders, 1982; Yool, 2001; Metternicht *et al.*, 2002; Miller and Yool, 2002; Ostir *et al.*, 2003; Symeonakis and Drake, 2004). The reason for using this technology in environmental studies is that it can provide calibrated, objective, repeatable and cost-effective information for broad regions and it can be empirically related to field data such as vegetation cover, collected by ground-based methods (Graetz, 1987; Tueller, 1987; Pickup, 1989).

Due to the importance of vegetation cover in the determination of land condition, a large number of remote sensing techniques have been suggested and used to extract vegetation information from the remotely-sensed images. One of the most widely used techniques is vegetation indices (Pickup *et al.*, 1993; Bannari *et al.*, 1995; Purevdorgy *et al.*, 1998; Thiam and Eastman, 2001). These indices are based on numeric combinations of a sensor's spectral bands, mainly red and near-infrared, which are used to highlight

vegetation cover. The Normalized Difference Vegetation Index (NDVI) is the most commonly used vegetation index that has been used in environmental studies, globally (Myneni *et al.*, 1997), continentally (Townshend and Justice, 1986) and at regional scales (Foran and Pearce, 1990; Al-Bakri and Tayor, 2003; Wang *et al.*, 2004). However, most of the widely used vegetation indices have been shown to be inappropriate in arid and semi-arid lands of Australia (O' Neill, 1996). This appears to be the result of the low red and near-infrared spectral contrast in the perennial plants that are dominant in these areas. This makes it difficult to distinguish vegetation from soil background (Huete, 1988). Several indices have been proposed and demonstrated as more appropriate in Australian arid and semi-arid grazing lands (Pickup and Nelson, 1984; Pickup *et al.*, 1993). In addition to vegetation indices, other remote sensing techniques such as spectral mixture analysis (Smith *et al.*, 1990) and landscape spatial heterogeneity indices (Tanser and Palmer, 1999) have been applied successfully for assessing and monitoring arid environments. Spectral mixture analysis estimates the fractional vegetation contribution to the reflectance measured by a sensor, thus it appears to be more applicable than vegetation indices in arid and semi-arid environments (Smith *et al.*, 1990; Elmore *et al.*, 2000). In contrast with vegetation indices and spectral mixture analysis, the spatial heterogeneity index may be less sensitive to the underlying substrate and does not depend on measurement of absolute reflectance. In other words, it does not require that imagery be calibrated to absolute reflectance and this is an important advantage for remote sensing of land conditions in areas with highly variable land cover.

The application of remote sensing in land management in Australia has a long history. Australia became one of the first users of remote sensing data shortly after the launch of the first earth observation satellite (Graetz, 1987). However, most of state-wide and national scale programs such as the Statewide Landcover and Trees Study (SLATS), Land Cover Change Project of the Australia Greenhouse Office National Carbon Accounting System (AGONCAS), and Australian Grassland and Rangeland Assessment by Spatial Simulation project (Aussie GRASS) have been developed in recent years. At state-wide scale, the SLATS project provides information about woody vegetation cover and their changes over time in Queensland based on the Landsat archive (Danaher, 1998). Another Landsat-based program is the land cover change project of the AGONCAS. As one of the largest satellite monitoring programs in the world,

AGONCAS provides comprehensive information of land cover and its change over the Australian continent for the past 30 years (Richards and Furby, 2002). The Aussie GRASS project is a state-wide and national level project that is led by Queensland Department of Natural Resources, Mines and Water. It uses advanced simulation modelling techniques for assessing the land condition of Australia's grazing lands or rangelands (Queensland Department of Natural Resources Mines and Water, 2006). This model uses NOAA NDVI vegetation images in its modelling.

At regional levels there has been considerable research in the use of remote sensing data to assess and monitor arid land condition (Pickup and Nelson, 1984; Foran and Pearce, 1990; Bastin *et al.*, 1993a; Holm *et al.*, 2003a; Karfs *et al.*, 2004; Karfs and Trueman, 2005). Bastin *et al*. (1998) applied a grazing gradient method (Pickup and Chewings, 1994) to northern arid rangelands of South Australia (cattle grazing country) to assess land condition. They found that land condition can be successfully detected using this remote sensing approach.

In southern arid lands of South Australia, which are mainly sheep grazing country only field techniques are used to determine rangeland condition. This current study examines the potential for use of remote sensing techniques to augment these field measurements in land condition assessment and monitoring. To date there have been no studies that have evaluated the capability of different remote sensing techniques in these areas. Therefore, this research investigates the potential of different remote sensing techniques for arid land condition assessment and monitoring in the southern rangelands of South Australia.

1.1 Research aims

The overall aim of this research was to evaluate the potential of different remote sensing techniques for assessing and monitoring arid land condition in the southern rangelands of South Australia. The specific objectives of this study were:

1. to evaluate vegetation indices based on multispectral satellite imagery for prediction of vegetation cover;

2. to compare satellite imagery and field measurements as means for detecting vegetation changes and assessing land condition;

3. to test whether it is possible to separate vegetation reflectance from soil surface background and to discriminate more vegetation components using hyperspectral imagery; and

4. to examine whether spatial heterogeneity in reflectance can provide additional information about land condition and the impact of the management on land condition.

1.2 Research significance and hypothesis

The land condition index and sampling methods at permanent monitoring sites are used for determining land condition in the southern arid lands of South Australia. The first assessment of land condition, using the LCI, started in 1990 and continued until 2000. According to the Pastoral Land Management and Conservation Act (1989), this assessment must be repeated every 14 years. In addition to the limitations of field methods, land condition assessment and monitoring is labour-intensive and very expensive. Therefore, this project aimed to address this problem by reviewing and evaluating the suitability of different remote sensing techniques for assessing and monitoring land condition of southern arid rangelands of South Australia. The hypothesis was that remote sensing techniques can provide qualitative and quantitative information on land cover and they can be used as an adjunct to field methods to aid the assessment and monitoring of land condition in southern South Australia.

1.3 Research structure

This thesis is divided into seven chapters. A brief summary of the content of each chapter has been given below. Chapters 3, 4 and 5 focus on the remote sensing techniques in which information about vegetation and soil cover is derived from the spectral characteristics of these components, whereas Chapter 6 deals with the spatial heterogeneity in surface reflectance and investigates the potential of this factor in land condition assessment.

Chapter 2 introduces the environment of the study area, history of land condition assessment and monitoring, satellite imagery and preliminary processing of imagery used in the study.

Chapter 3 focuses on vegetation indices. It reviews and classifies different vegetation indices based on the concepts underlying their formation. It investigates relationships

between vegetation indices and field measurements of land cover. This chapter has been accepted for publication as Jafari, R., Lewis, M.M. and Ostendorf, B., 2007. Evaluation of vegetation indices for assessing vegetation cover in southern arid lands in South Australia, *The Rangeland Journal* 29 (1) 39-49.

Chapter 4 uses the most suitable vegetation indices identified in Chapter 3 to monitor vegetation changes over time. It compares imagery against field cover data and land condition classes for monitoring changes in vegetation cover and land condition in the study area. This chapter also evaluates the suitability of vegetation indices for discriminating land condition classes identified by the current field assessment methods.

Chapter 5 validates vegetation and soil components derived from the hyperspectral imagery against field measurements of spectral reflectance and abundance of ground cover. The components of the research in this chapter have been published as Jafari, R., Lewis, M.M. and Ostendorf, B., 2006. Use of EO-1 hyperspectral imagery for discriminating arid vegetation, Proceedings of the 13th Australian Remote Sensing and Photogrammetry Conference (ARSPC), The Photogrammetry Association of Australia, November 2006, Canberra, Australia.

Chapter 6 uses a spatial heterogeneity index for assessing arid land degradation. It compares spatial heterogeneity in degraded and non-degraded areas and also investigates the spatial scale of variability around stock watering points by examining spatial heterogeneity with increasing distance from watering points. This chapter has been submitted to the *Journal of Arid Environments* as Jafari, R., Lewis, M.M. and Ostendorf, B., An image-based diversity index for assessing land degradation in an arid environment in South Australia.

Chapter 7 reviews the results and findings for each chapter of the thesis, highlights the implications of the research findings in arid land condition assessment and monitoring and provides recommendations for future research.

2 STUDY AREA, FIELD AND SATELLITE IMAGE DATA

2.1 Study area

The study area was located in the southern arid lands of South Australia. It comprises 123,600 km^2 within two Soil Conservation Districts, including Kingoonya Soil Conservation District and Gawler Soil Conservation District. The region lies between latitudes 29° 00′ S and 33° 00′ S and longitudes 133° 00′ E to 138° 00′ E. Figure 2.1 shows the location of the study area and also the extent of imagery that was used in this research. The information of the environment of the study area that is presented in this chapter has been drawn from the Kingoonya Soil Conservation District plan and lease assessment overview report on the Kingoonya and Gawler Soil Conservation Districts (Kingoonya Soil Conservation Board, 1991; Tynan, 1995; Kingoonya Soil Conservation Board, 1996).

The choice of study area was influenced by the history of land condition assessment and availability of spatial and ecological data. The Pastoral Management Branch of Department of Water, Land and Biodiversity Conservation of South Australia established permanent monitoring sites throughout these districts in 1991 to record changes in land condition over time using sampling and photographic methods. They also recorded land system characteristics of the area and assessed land condition using the land condition index method. A second round of land condition assessment of the area was conducted in 2002 at a smaller sample of permanent monitoring sites. This time span from 1991 to 2002 enabled detection of changes in vegetation cover and land condition over time (Chapter 4). To meet the requirements of the Pastoral Land Management and Conservation Act, a comprehensive assessment of land condition of the entire Kingoonya and Gawler districts has commenced in 2004, using land condition index at random sites on each property. The field data that was collected in 1991, 2002 and 2004 as a part of these assessments was used to validate remote sensing techniques that were applied in this study to the study area.

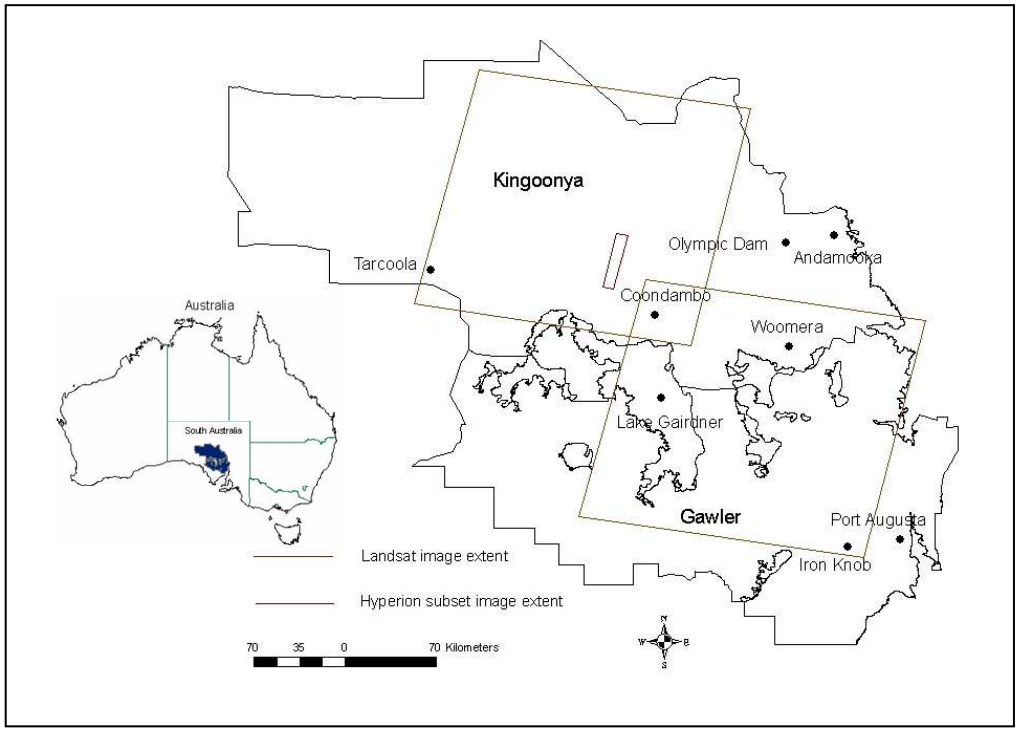

Figure 2.1 Location of study area

2.1.1 Climate

The climate in the study area is characterised by hot summers and cool mild winters. The mean daily maximum temperature ranges from 35°C in summer to approximately 17°C in winter and mean daily minimum temperature ranges from 15°C in summer to about 5°C in winter. The mean annual evaporation rate is approximately 2500 mm. Winds are usually from the southeast in the north and southwest in the south of the study area. Rainfall is highly variable from year to year in this region. It varies across the districts from less than 150 mm in the north to about 300 mm in the south. Figure 2.2 shows the annual rainfall at Coondambo station in the study area recorded from 1990 to 2003 with a notable maximum in 1992. This station is located almost in the centre of the region. Because of the high variability in the rainfall, various water resources are used for domestic, industrial and pastoral purposes. These include local ground water (e.g. wells), local surface water (e.g. dams), network systems originating outside the area, temporal natural water, and rainfall tanks.

NOTE: This figure is included on page 12 of the print copy of the thesis held in the University of Adelaide Library.

Figure 2.2 Yearly rainfall at Coondambo station (Pastoral Board, 2002)

2.1.2 Land use

Because of the low and variable rainfall, the study area has not been cultivated. Grazing is the main land use in this area and sheep and wool production is one of the most important sources of income. Like other pastoral lands in South Australia, the study area has been divided into stations and held under pastoral leases. The region has been divided into 58 stations ranging from 35 to 6,000 km2. The stations have been fenced into smaller paddocks ranging from less than one to 252 km2. The paddocks are the main management units; they are mostly provided with artificial water sources such as dams, tanks and troughs, and that grazing is focused on these water points. The average number of sheep in the region over a 24-year period (1976-2000) was approximately 325,000. Pastoralists often aim to increase income by increasing stocking rates and this may have negative effects on land condition. Inappropriate grazing reduces the cover of living and dead vegetation (plant litter) and this increases the susceptibility of the soil to erosion by water and wind. Overgrazing has been recognised as a main cause of land degradation in the area, though other factors such as mining and mineral exploration and military operations have caused some degradation in specific parts of the region.

2.1.3 Geology and geomorphology

Overall the study area is flat to undulating, with an elevation of about 300 m above sea level. Sand dunes with eastern-western ridges dominate the northern parts of the region. Plains of sandy loams and sandy soils, usually covered with gravel and stone (gibber) occur in different parts of the study area. The dominant vegetation cover on sand dunes

and sand plains is chenopod shrubs and open woodlands. Low hills, rock outcrops and salt lakes are distributed throughout the area, while tablelands occupy most of the Woomera and Arcoona regions towards the centre. These gently rolling tablelands are generally dominated by chenopod shrubs.

The low topography of the area reflects the dominance of relatively young, flat-lying sediments, which have not been changed due to major earth movements. The rocky rises and hills along the western margin of the Lake Gairdner are the oldest outcrops formed from a succession of sedimentary, volcanic, and metamorphic rocks between 1600 and 2600 million years ago. The younger volcanic rocks formed the Gawler Ranges in the southeast of the area about 1600 million years ago.

Deposition of sandstone, siltstone and mudstone sediments occurred about 150 million years ago between the outcrops of the older rocks to the north of Lake Gairdner, northwest of Tarcoola and near Andamooka. The north and northeast of the Kingoonya district are mostly covered with gibbers or pebbles which were formed approximately two million years ago after the erosion of the sediments that contained silica elements. These gravels are usually brown due to high iron oxide concentration. The latest sediments which were commonly sand, silt, gypsum, and clay were deposited in hills, alluvial plains and salt lakes.

2.1.4 Soil

Sandy and calcareous soils dominate the study area. The sandy soils are infertile and coarse-textured with high rainfall infiltration rates. Although wind erosion and dune formation may occur in these soils, they have low susceptibility to erosion because of substantial covering with perennial vegetation. Calcareous soils are relatively infertile, with coarse to medium textures. They are less susceptible to wind erosion than sandy soils and mainly are covered with chenopod shrublands. Other soil types within the study area are cracking clay soils, loamy soils, lithosols (shallow stony soils), ironstone gravels and saline alluvia associated with salt lakes (Stanley, 1982).

2.1.5 Land systems

Soils, plants and geology are associated and create different landscapes or land systems in the environment. Land system here refers to a combination of land units with specific

patterns and land unit is an area that includes similar vegetation, soil type and landform (Rangeland Assessment Unit, 1988). Figure 2.3 shows the distribution of land systems in the Kingoonya and Gawler districts. The main land units of the study area are sand plains with open woodland, calcareous plains with pearl bluebush (*Maireana sedifolia* F.Muell) and bladder saltbush (*Atriplex vesicaria* Benth.), sand dunes with native pine (*Callitris glaucophylla* Joy Thoms and L.A.S.Johnson) or mulga (*Acacia aneura* F.Muell. ex Benth), tableland with bladder saltbush and samphire (*Halosarcia pergranulata* J.M.Black) and low hills with low bluebush (*Maireana astrotricha* L.A.S.Johnson) and mulga and granitic hills (White and Gould, 2002). Appendix 1 shows photographs of these and other plant species that have been mentioned in coming chapters. Further details of specific land systems in which the research was based are given in Chapters 3, 5 and 6.

NOTE: This figure is included on page 14 of the print copy of the thesis held in the University of Adelaide Library.

Figure 2.3 The distribution of land systems in Kingoonya and Gawler districts (Pastoral Board, 2002)

2.2 Land condition assessment and monitoring in the study area

The system of land condition assessment in the South Australian arid rangelands comprise long term assessment of trends using the Land Condition Index and short term assessment at permanent monitoring sites (Burnside and Chamala, 1994; Department of Water Land Biodiversity and Conservation, 2002).

2.2.1 Land condition index

The Land Condition Index (LCI) is used to determine average land condition in the southern pastoral lands of South Australia every 14 years. Land condition is determined by visual estimation of land condition state and scored on a 3-point scale: 1= poor, 2= fair and 3= good, according to defined soil erosion status and vegetation criteria at about 80-100 randomly located sites along tracks on each lease. Criteria used for determining land condition class differ according to the pasture type, and include vegetation cover and composition, presence of regeneration, unpalatable species and grazing effects. An average LCI is calculated for each lease by multiplying the percentage of sample sites for each condition state rating by the score. The values in this calculation for each lease range from 100 (high disturbance at all sample sites) to 300 (low disturbance at all sample sites), and then from these lease values, the average condition index of the district and the whole area is determined (Department of Water Land Biodiversity and Conservation, 2002).

The first land condition assessment in the Kingoonya and Gawler districts was performed by the Pastoral Management Branch over 10 years from 1990 to 2000. The survey recognized different pasture types in the region. Chenopod shrublands and low open woodlands were the main pasture types, covering more than 94% of the districts (Table 2.1). The survey showed that about 42% of the Kingoonya district was in land condition class 3, 28% in class 2 and 30% in class 1 and the results for Gawler district were 52%, 32% and 16% respectively. In this round of land condition assessment the LCI was used to determine land condition at monitoring sites, though it is not a site-based technique (White and Gould, 2002). Figure 2.4 shows the LCI classes of the Kingoonya and Gawler Soil Conservation Districts (Tynan, 1995; Kingoonya Soil Conservation Board, 1991). Mean LCI scores for the Kingoonya and Gawler districts were 2.13 and 2.21, respectively. This means that land condition in the study area was laid in a fair condition.

Table 2.1 The percentage of various pasture types within the Kingoonya and Gawler Soil Conservation Districts

Pasture types	**Kingoonya (%)**	**Gawler (%)**
Chenopod shrubland	64	77.42
Low woodland	30	21.03
Mt. Eba country	5	-
Hummock grassland	0.5	1.55
Ephemeral plains	0.5	-
Total	100	100

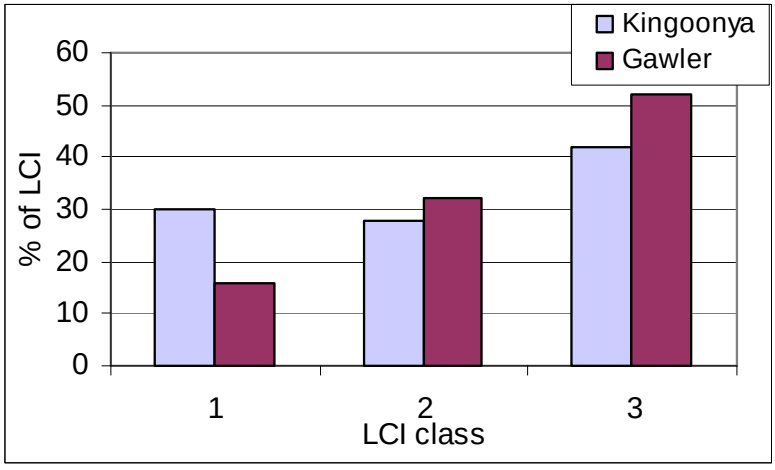

Figure 2.4 Land condition classes in the Kingoonya and Gawler Soil Conservation Districts

White and Gould (2002) used another method, the Functionality Index model (further described in Della Torre, 2005), for assessing land condition at some 180 randomly selected monitoring sites. The determination of land condition classes in the Functionality Index model is similar to the LCI classes. The rangeland condition classes are divided in 5 categories (excellent, good, fair, poor and very poor). These classes are determined according to the plant species composition, plant productivity and soil erosion status. The study observed that only very few sites had excellent and very poor conditions. Therefore, these classes were combined into the good and poor classes respectively. By using three condition classes a score similar to the LCI method was calculated. The mean score of the Functionality Index model for 180 sites in 2002 was 2.36, which shows that the overall land condition in these sites was fair. Using three

similar classes for determining land condition means that the 2002 land condition assessment can be compared with the first 1991 assessment to detect changes in the land condition over time (Chapter 4).

2.2.2 Permanent monitoring sites

During the first land condition assessment using LCI in 1991, permanent monitoring sites were established in each paddock throughout the pastoral country to provide for shorter-term assessment of land condition and trend (Department of Water, Land Biodiversity and Conservation, 2002). There are about 5500 such monitoring sites throughout the South Australian pastoral lands, of which 1900 are located in the study area (Figures 2.5 and 2.6). They were located at moderate distances from water to avoid the heavily grazed areas, but still sample areas are that influenced by stock. In sheep stations the points were located about 1.5 km from water, while in cattle country they were located approximately 3 km from water. At each monitoring site two sampling methods, including Jessup and step-point transects and a photo-point are used for collecting ecological data and documenting changes in land condition. At some of these sites the Pastoral Management Branch records data every 5-7 years (ecological data, photographs, etc) and these data are compiled into a manual and given to landholders and who are encouraged to monitor the sites whenever they see a visible change in the land condition.

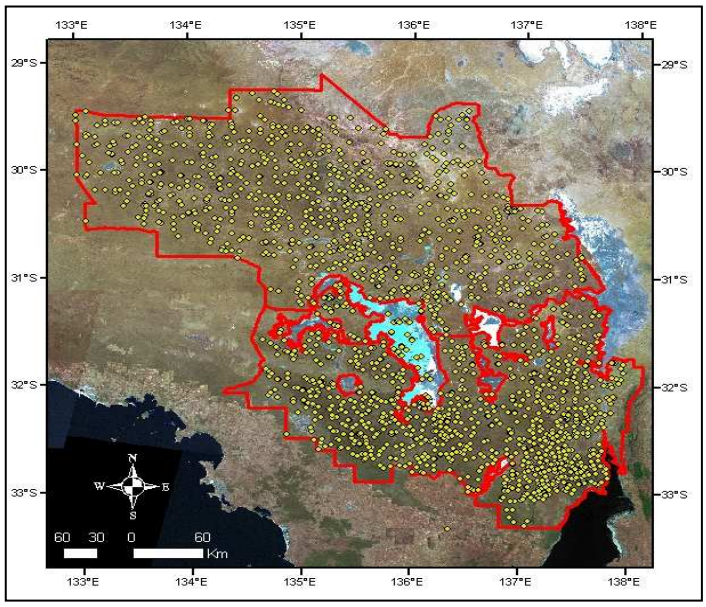

Figure 2.5 The distribution of permanent monitoring sites in the study area

Figure 2.6 An example of a permanent monitoring site established in 1971

The Jessup transect method measures the density and frequency of perennial plants such as chenopods and other shrubs and grasses. It consists of a 100 m transect that is fixed with two pegs at the end. The number of plants is recorded in ten 10×2 m quadrats on both sides of the transect, giving a total sample area of 400 m^2. The quadrats enable subsequent changes in the abundance of perennial plants to be quantified easily. Although this method measures perennial vegetation cover, which is an important criterion in land condition assessment, it is time-consuming and difficult to apply in tall and dense vegetation areas (Cook and Stubbendieck, 1986; Department of Water Land Biodiversity and Conservation, 2002).

The step-point method is used for determining the percentage of vegetation cover. Vegetation cover is the proportion of ground surface that is covered by a vertical projection of the foliage cover canopy. An observer with a pin or mark at the tip of his boots paces out in the same direction as the Jessup transect or other selected transects. Along these transects the observer records the ground cover components intercepted (plant species, litter, soil, stone etc) by each 'hit' of the 'mark'. The percentage of different ground cover is determined for each monitoring site by the proportions of hits. A minimum of 500 hits or points is usually recorded in each transect. Although the step-point method is simple, easy to use and needs little experience, the results of this method can vary between observers. Furthermore, it is time-consuming in large areas (Cook and Stubbendieck, 1986; Friedel and Shaw, 1987a; Friedel and Shaw, 1987b; Department of Water Land Biodiversity and Conservation, 2002).

The photographic method is used at the permanent monitoring sites as a supplementary tool for monitoring vegetation change. Photographs are taken using a camera at the

photo-point monitoring sites. The photographer stands behind a marker peg that is about 10 m from the Jessup transect and focuses on the centre of a sighter peg at the beginning of the Jessup transect (Department of Water Land Biodiversity and Conservation, 2002). Some of the advantages of these photographs are that they are obtained rapidly and easily, the amount of change in vegetation and other events associated with that change are recorded, and they provide a good archive for monitoring vegetation or land condition over time. The limitations of this method are that photographs can present a biased selection when photographed and they are only useful for small and low growing vegetation areas (Harper *et al.*, 1990).

2.3 Satellite imagery

Multispectral medium-resolution satellite imagery is one of the most widely used forms of remote sensing data for many environmental applications (see Chapter 1). The availability of extensive archives of this imagery makes it suitable for broad-area, operational monitoring programs. This current study used four full scenes of Landsat imagery and a Hyperion image, obtained from the Australian Centre for Remote Sensing (ACRES) (Table 2.2 and 2.3). The extent of the imagery is shown in Figure 2.1. All the images were acquired in dry seasons to minimize the contribution of green ephemeral vegetation, maximise solar irradiance and land surface reflectance and also exclude cloud cover from the imagery. The October 1991 Landsat image was used to derive vegetation indices and investigate their suitability in the Kingoonya region (Chapter 3). The index identified as being most suitable in Kingoonya was applied to the 2002 image to detect changes in vegetation cover over an eleven-year period (Chapter 4). It was also applied to the 2005 image to evaluate the usefulness of this index for discriminating LCI classes which were collected by the staff of the South Australian Pastoral Program in 2005. The January 1991 image was used in Chapter 6 to examine the capability of a remotely-sensed diversity index to assess land degradation in the Kingoonya and Gawler districts. The 2005 hyperspectral Hyperion image was used to discriminate vegetation types that are important in land management (Chapter 5).

Table 2.2 Acquisition dates of Landsat 5(TM), Landsat 7 (ETM+) and Hyperion images

Image	Acquisition date	Path	Row
Landsat TM	20/10/1991	100	81
Landsat ETM+	13/01/2002	100	81
Landsat TM	14/02/2005	100	81
Landsat TM	31/01/1991	99	82
Hyperion	29/12/2005	100	81

Table 2.3 Spectral and spatial resolution of the Landsat-5 and Landsat-7 ETM+ sensors

Band number	Wavelength (μm)	Spectral region	Spatial resolution (m)
1	0.45 – 0.52	Visible blue	30
2	0.52 – 0.6	Visible green	30
3	0.63 – 0.69	Visible red	30
4	0.76 – 0.79	Near infra-red	30
5	1.55 – 1.75	Middle infra-red	30
7	2.08 – 2.35	Shortwave infra-red	30

2.3.1 Radiometric calibration of Landsat imagery

To compare multitemporal images, calibration of their radiometric values is needed. This is necessary because atmospheric conditions, sensor characteristics, and image pre-processing influence the values recorded in the digital imagery (Campbell, 1996). Therefore, it is important to separate real changes in land cover components from radiometric changes associated with the images from different dates. Furby and Campbell (2001) used some invariant features which had approximately the same reflectance over time to calibrate a sequences of Landsat images. They recommended that 20-30 invariant features are required for image to image calibration and the features should be selected from a range of dark, middle and bright targets. The calibration involves identifying invariant features in the scenes and developing calibration relationships between them.

In this current study, image-to-image radiometric calibration was done by selecting a reference image (2002 image) and calibrating the 1991 image by using some invariant targets. As the 2002 image was recorded before the failure of the Scan Line Corrector (SLC) of the Landsat 7 Enhanced Thematic Mapper plus (ETM+) on May 31 2003, this

malfunction did affect on the selected image. 24 invariant targets including roads, buildings, mine factories and bare soil were chosen as invariant features. Vegetation and dry salt lakes were excluded as invariant targets because they tend to show seasonal trends. In addition, targets with the digital values of 255 (i.e., very bright or radiometrically saturated targets) were excluded from calculations. A mean of 3-5 pixels for each target was calculated for both images. Linear regressions were established between these, with the 2002 image as the reference (dependent variable) and 1991 image as the independent variable. The resulting linear regression coefficients were then used to convert the 1991 image values to 2002-equivalent values. The linear equations and relationships (R^2 values) between the 2002 and 1991 image reflectance values for invariant targets are shown in Table 2.4.

Table 2.4 Relationship between the reflectance of invariant targets in the 2002 and 1991 images

Spectral bands	**Linear equations**	**R^2 values**
Band 1	y = 1.12x - 5.52	0.95
Band 2	y = 1.97x - 4.41	0.96
Band 3	y = 1.98x - 12.28	0.96
Band 4	y = 1.08x - 3.03	0.97
Band 5	y = 1.31x - 31.01	0.96
Band 7	y = 1.68x - 10.64	0.95

2.3.2 Pre-processing of Hyperion hyperspectral imagery

The Hyperion sensor is the first hyperspectral imager on-board NASA's Earth Observing-1 (EO-1) satellite that was launched on 21 November 2000. The EO-1 satellite follows the same orbit as Landsat 7 by about one minute. The spatial resolution of Hyperion is 30 m and standard scene is 7.7 km wide and 42 km long. This sensor has 242 spectral bands ranging from 400 nm to 2500 nm, recorded at 12-bit radiometric resolution (Appendix 2). Some of the bands of the image that was used in this study were affected by noise that might have been as a result of atmospheric or sensor effects. CSIRO's Hyperspectral Processing Software was used to reduce noise in the image (Mason, 2002; Quigley *et al.*, 2004). In addition to this software, Atmospheric Correction Now (ACORN) software (ImSpecLLC, 2004) and several standard hyperspectral processing techniques in ENVI (Research Systems Inc, 2000) were used

to reduce noise in the Hyperion scene and covert the radiance at sensor values to surface reflectance (Chapter 5).

2.3.3 Georegistration

Georegistration is needed to enable comparison of images from different dates and to accurately relate image values to field and other spatially-referenced data. A reference image that had been georectified to a 1:250,000 map (Map Grid of Australia, MGA 94) was used as a base to georegister the imagery of current study. 31 Ground Control Points (GCPs) were selected throughout the reference image and raw image (2002 Landsat image). Road intersections or other man-made features were appropriate targets for this purpose. The final Root Mean Square (RMS) error for the selected points was 0.49 pixels. The raw image was transformed to the georectified image using a first order polynomial, then resampled using the nearest neighbour method to preserve radiometry. The same method was used to register the remaining Landsat images to the reference image. The Hyperion image was registered to the reference image using the same technique as above. The RMS error for registration of the Hyperion image using 15 Ground Control Points was 0.10 pixels.

2.4 Spatial data

Several forms of Geographical Information Systems data were used in this research. These spatial data were used for interpreting the imagery, extracting information from the imagery, and determining the location and boundaries of areas of interest. These data were provided by the Department of Water, Land Biodiversity and Conservation and included land system boundaries, district boundaries, station boundaries, paddock boundaries, locations of permanent monitoring sites and water points, and meteorological stations. All spatial data were geometrically rectified to Map Grid of Australia (MGA 94).

2.5 Summary

The study area was located in the southern arid lands of South Australia. A region covered with young sedimentary deposits. The soil in this area has low fertility and sandy and calcareous soils dominate, mainly covered with open woodlands and chenopod shrublands. The climate is characterized by low and variable rainfall and high temperature and evaporation. The main land use is grazing of sheep for the production

of wool and meat on extensive pastoral leases which are subdivided into large, fenced paddocks. One of the indirect effects of grazing in the study area is land degradation, especially near the stock watering points.

In South Australia two main field methods have been used in rangeland condition assessment and monitoring including the Land Condition Index (LCI) and permanent monitoring sites. According to the first land condition assessment in 1991, land condition status in the study area was fair. Although field methods that have been used for this land condition assessment provide detailed information about conditions at sample sites, this may not be representative of broad areas. Moreover, the application of these methods in broad areas is expensive and time-consuming. Thus, in the following chapters the potential of remote sensing techniques in land condition assessment and monitoring is investigated.

3 VEGETATION INDICES

3.1 Introduction

One of the most common applications of remote sensing is vegetation assessment and monitoring via vegetation indices (Pickup *et al.*, 1993; Bannari *et al.*, 1995; Purevdorgy *et al.*, 1998; Thiam and Eastman, 2001; Metternicht, 2003). However, most of the widely used vegetation indices appear to be less applicable in arid and semi-arid lands of Australia (Pickup *et al.*, 1993; O' Neill, 1996). Indices that are less dependent on infrared response, such as the Perpendicular Distance (PD54) and Soil Stability Index (SSI) have been shown to be more appropriate spectral indices in Australian arid and semi-arid lands (Foran and Pickup, 1984; Pickup and Nelson, 1984; Pickup and Foran, 1987; Pickup *et al.*, 1993; McGregor and Lewis, 1996; O' Neill, 1996; Edwards, 2001).

Although ground-based methods provide detailed data about specific sites at infrequent monitoring intervals, they represent a very limited sample of the full extent and spatial variation within much broader areas of arid lands. Furthermore, such field assessment is time-consuming, expensive and subject to observer variation (Friedel and Shaw, 1987a; Friedel and Shaw, 1987b). Consequently, the aim of this part of the study was to evaluate the suitability of vegetation indices derived from multispectral satellite imagery as an adjunct to field methods for assessing and monitoring vegetation cover, and consequently land condition, in the southern arid lands of South Australia. Specifically, this component of the study aimed to identify the most suitable image indices for recording vegetation cover in these landscapes, to determine the scales at which they may be applied, and the components of vegetation cover that they best predict. The approach was to determine the relationships between a range of widely used spectral indices and vegetation cover as measured by the South Australian Pastoral Lease assessment program, with the intent of producing image maps that more fully document spatial and temporal variation in vegetation cover.

3.1.1 Vegetation indices

Vegetation indices combine reflectance measurements from different portions of the electromagnetic spectrum to provide information about vegetation cover on the ground (Campbell, 1996). Healthy green vegetation has distinctive reflectance in the visible and near-infrared regions of the spectrum. At visible, and in particular red wavelengths,

plant pigments strongly absorb the energy for photosynthesis, whereas in the near-infrared region, the energy is strongly reflected by the internal leaf structures. This strong contrast between red and near-infrared reflectance has formed the basis of many different vegetation indices. When applied to multispectral remote sensing images, these indices involve numeric combinations of the sensor bands that record land surface reflectance at various wavelengths. Pearson and Miller (1972) first presented the near infrared/red ratio for separating green vegetation from soil background. Since then, numerous vegetation indices have been proposed, modified, analysed, compared and classified (Perry *et al.*, 1984; Huete, 1988; Qi *et al.*, 1994; Bannari *et al.*, 1995; Rondeaux *et al.*, 1996; Thiam and Eastman, 2001; Gilabert *et al.*, 2002). In this current study vegetation indices have been grouped into four types including slope-based, distance-based, orthogonal transformation and plant-water sensitive vegetation indices on the basis of the spectral bands they use and the means by which these are combined. Definitions of these indices are provided in Table 3.1.

3.1.1.1 Slope-based vegetation indices

These vegetation indices comprise simple arithmetic combinations of reflectance measurements, contrasting the high infrared and low red reflectance that characterises photosynthetic vegetation. This contrast has been used widely to generate several vegetation indices such as the Simple Vegetation Index (SVI) (Pearson and Miller, 1972), Normalized Difference Vegetation Index (NDVI) (Rouse *et al.*, 1974), and Soil Adjusted Vegetation Index (SAVI-A) (Huete, 1988). Pixel values in this group produce vectors with differing slopes through the origin of the red and NIR bi-spectral plot. Figure 3.1 shows the distribution of pixel values in the NDVI. The NDVI has been used widely in many applications including regional and continental-scale monitoring of vegetation cover (Satterwhite and Henley, 1987; Huete, 1988; Foran and Pearce, 1990; Sattle and Drake, 1993; Rondeaux *et al.*, 1996; Purevdorgy *et al.*, 1998; Minor *et al.*, 1999; Schmidt and Karnieli, 2001; Al-Bakri and Tayor, 2003; Runnstorm, 2003; Wang *et al.*, 2004; Wessels *et al.*, 2004).

Table 3.1 Vegetation indices applied to the 1991 Landsat image

Vegetation index group	Vegetation Index	Acronym	Author	Formula	Landsat TM bands
Group 1 (Slope-based)	Simple	SVI	Pearson & Miller, 1972	NIR/R	4/3
	Normalised Difference	NDVI	Rouse, 1974	(NIR-R)/(NIR+R)	(4-3) / (4+3)
	Soil Adjusted-A	SAVI-A	Huete, 1988	[(NIR-R)/(NIR+R+L)] × (L+1) L= Soil adjusted factor	[(4-3)/(4+3+0.25)] ×1.25
Group 2 (Distance-based)	Perpendicular Vegetation Index-3	PVI-3	Qi *et al*., 1994	A×NIR– B×R A= the intercept of soil line B= the slope of soil line	A×4-B×3
	Perpendicular Distance	PD54	Pickup *et al*.,1993	Perpendicular distance from soil line toward vegetation line	2 v 3
	Soil Stability Index	SSI	Pickup & Nelson, 1984	Perpendicular distance from soil line toward vegetation line	2/4 v 3/4
Group 3 (Orthogonal transformations)	Soil Brightness Index	SBI	Kauth & Thomas, 1976	Orthogonal Transformation	All bands except band 6
	Green Vegetation Index	GVI	Kauth & Thomas, 1976	Orthogonal Transformation	All bands except band 6
Group 4 (Plant-water sensitive)	Stress Related-1	STVI-1	Thenkabail *et al*. 1994	(MIR×R)/NIR	(5×3)/4
	Stress Related-3	STVI-3	Thenkabail *et al*. 1994	NIR/(R+MIR)	4/(3+5)
	Mid-infrared-1	MSVI-1	Thenkabail *et al*. 1994	NIR/MIR	4/5
	Mid-infrared-2	MSVI-2	Thenkabail *et al*. 1994	NIR/SWIR	4/7
	Mid-infrared-3	MSVI-3	Thenkabail *et al*. 1994	NIR/(MIR+SWIR)	4/(5+7)

3.1.1.2 Distance-based vegetation indices

The second group consists of distance-based vegetation indices. These indices have been designed to remove the influence of soil brightness in sparsely vegetated areas;

they are more effective at discriminating vegetation from bright soils when the two are mixed within the sensor field of view.

NOTE: This figure is included on page 27 of the print copy of the thesis held in the University of Adelaide Library.

Figure 3.1 The distribution of pixel values in Normalised Difference Vegetation Index (Harison and Jupp, 1990)

These indices take advantage of the fact that most soil-dominated pixels fall along a line in a red/near-infrared bi-spectral plot, with vegetation increasing with distance perpendicular to this line. The soil line can influenced by surface roughness, moisture, texture and colour (Huete *et al.*, 1984; Baret *et al.*, 1993). The Perpendicular Vegetation Index (PVI) (Richardson and Wiegand, 1977) was the first of this type of index (Figure 3.2). The PD54, which has been used with considerable success in Australian perennialdominated arid vegetation, also falls within this group (Pickup *et al.*, 1993). All of the vegetation indices in this group require definition of the slope and intercept of the soil line.

3.1.1.3 Orthogonal transformation vegetation indices

The slope-based and distance-based vegetation indices generally use two spectral bands, most usually red and infrared. Orthogonal transformation vegetation indices, the third group, use multiple spectral bands to derive a new set of image components that are uncorrelated with one another and ordered with respect to the amount of scene variation they capture from the original band set (Kauth and Thomas, 1976; Fung and LeDrew, 1987). The first component usually represents overall land surface brightness or albedo while the second component often represents variation in vegetation cover. This group has been used in numerous environmental studies, mostly in agricultural and forest

environments (Byrne *et al.*, 1980; Richards, 1984; Ingebritsen and Lyon, 1985; Fung and LeDrew, 1987; Deer and Longmore, 1994; Ribed and Lopez, 1995; Hirosawa *et al.*, 1996; Wu, 2000; Caren *et al.*, 2002; Price *et al.*, 2002; Lu *et al.*, 2004; Jin and Sader, 2005). The tasselled cap transformation is the best-known of this group (Kauth and Thomas, 1976): its two first components are the Soil Brightness Index (SBI) and the Green Vegetation Index (GVI). This transformation was adapted to the six bands of Landsat Thematic Mapper (TM) data by changing the empirical coefficients from those originally applied to the four bands of Landsat Multispectral Scanner imagery (Crist, 1985).

In addition to the soil brightness that is considered in the second and third group of indices, soil colour can also influence vegetation indices. Red and yellow soils with high red reflectance can particularly interfere with vegetation estimation. To address this problem, Escadafal and Huete (1991) presented a colouration index, the Redness Index (RI), as a correction for the soil colour effect on vegetation indices (Bannari *et al.*, 1995). The index, based on the contrast between red and green reflectance, was shown to double the sensitivity of vegetation indices, especially in sparsely vegetated areas.

Figure 3.2 The perpendicular vegetation index (Richardson and Wiegand, 1977)

3.1.1.4 Plant-water sensitive vegetation indices

The fourth group consists of vegetation indices that include mid and short-wave infrared regions of the electromagnetic spectrum, on the basis that vegetation has lower

reflectance than soil in these regions, a contrast that may assist their discrimination (Kimes *et al.*, 1981; Dusek *et al.*, 1985; Baret *et al.*, 1988; Thenkabail *et al.*, 1994). Since it is water content that largely determines plant reflectance in the near infrared, mid and shortwave infrared regions, these have been called plant-water sensitive vegetation indices. Thenkabail *et al.* (1994) proposed six different plant-water sensitive vegetation indices using Landsat TM mid-infrared and shortwave-infrared bands, including the Mid-infrared Vegetation Index (MSVI 1, 2 and 3) and the Stress Related Vegetation Index (STVI-1, 2 and 3). They found that these indices were as good or better predictors of yield, leaf area index, wet biomass, dry biomass, and plant height than slope-based vegetation indices in corn and soybean fields. O' Neill (1996) applied these indices to chenopod shrublands in western New South Wales and suggested that STVI-1 can be a useful index for vegetation mapping and analysis in these environments.

Most of the vegetation indices that use red and NIR regions of the spectrum appear to be inappropriate in Australian arid and semi-arid lands (O' Neill, 1996). because the perennial vegetation types of these regions do not reflect highly in the NIR (Graetz and Gentle, 1982). Moreover, the sparse cover and low leaf area index of the vegetation also contribute to low reflectance in the NIR channel. To address this problem Pickup *et al.* (1993) developed the Perpendicular Distance vegetation index (PD54). This index falls within group 2, but uses visible green and red reflectance to separate vegetation cover from soil (Bastin *et al.*, 1999). Pickup *et al.* (1993) found that this index is less sensitive than red and NIR indices to differences in plant greenness. The PD54 has been widely used in rangeland monitoring and assessment in Australia (Bastin *et al.*, 1993a; Bastin *et al.*, 1993b; Pickup *et al.*, 1994; McGregor and Lewis, 1996; Bastin *et al.*, 1998). The Soil Stability Index (SSI) is another distance-based vegetation index developed to assess soil condition in Australian arid rangelands (Pickup and Nelson, 1984). Although the SSI provided useful information about soil erosion, stability, and deposition, it was much more sensitive than PD54 to the amount of vigorous green vegetation in the landscape and hence was considered less suitable for assessing perennial dominated landscapes. Due to the longevity and lower sensitivity of perennial plants to seasonal conditions, they are usually used as a key indicator of land condition. As a result, strong relationships between perennial cover and vegetation indices would mean that image indices have capability for land condition assessment and monitoring.

3.2 Methods

3.2.1 Study area

The study area was located in the Kingoonya Soil Conservation District in the arid rangeland of South Australia (Figure 3.3) and was defined by the extent of Landsat scene path 100 and row 81. Detailed information of the environment of the study area has been presented in Chapter 2.

The relationships between vegetation cover and satellite image indices were analysed at two scales: across 34,225 km^2 covered by the Landsat scene, which encompassed ten different land systems, and within two particular land systems: Buckshot and Gina. Buckshot land system (498 km^2) comprises "buckshot" gravel (iron-oxide coated gravels) plains and watercourses of mulga low woodland, while Gina land system (1,601 km^2) is dominated by sandy calcareous plains of pearl bluebush (Table 3.2).

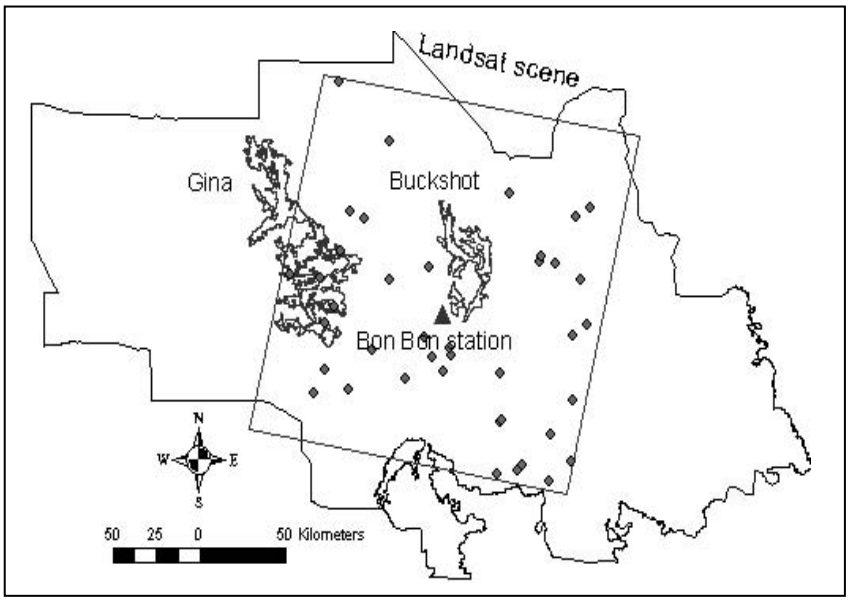

Figure 3.3 The study area defined by Landsat scene path 100, row 81 within the Kingoonya Soil Conservation District. Shown also are the location of monitoring sites and Buckshot and Gina land systems which were used for land-system scale analysis.

Table 3.2 Characteristics of Buckshot and Gina land systems (Pastoral Board, 2002)

NOTE: This table is included on page 31 in the print copy of the thesis held in the University of Adelaide Library.

3.2.2 Field cover data

The vegetation cover data used in this study were collected at permanent monitoring sites throughout the Kingoonya Soil Conservation District as part of lease assessments in 1990-1991: sites within Gina and Buckshot were recorded in October 1990 and April 1991, while sites across the district were recorded in October and December 1990 and between March and June 1991. Rainfall in the study area was below average during these years (140 and 102 mm recorded at Bon Bon station in 1990 and 1991). Monthly rainfall during and immediately preceding the data collection periods was generally low, with some localised falls during January and May 1990 (Figure 3.4).

NOTE: This figure is included on page 31 in the print copy of the thesis held in the University of Adelaide Library.

Figure 3.4 The distribution of monthly rainfall in Bon Bon station centrally located within study area (Pastoral Board, 2002)

The field data comprised estimates of ground cover derived from step point transects with a minimum of 500 points or hits (Department of Water Land Biodiversity and

Conservation, 2002). Linear transects originated from the permanent monitoring sites, although the specific direction was not recorded. For this study the cover data were aggregated into three groups to compare with image indices: perennial plant cover, combined perennial and ephemeral plant cover, and total vegetation plus litter and soil-covering cryptogam cover. Forty monitoring sites from across the district representing ten different land systems with varying land form, vegetation and soils were used to evaluate relationships of perennial plants and other cover components with image indices across the extent of the Landsat scene (landscape scale) (Figure 3.3), while eight and 19 sites were used to test relationships within Buckshot and Gina land systems. These two land systems were chosen for analysis because they are extensive, they have contrasting landscapes, and because they contained sufficient monitoring points to allow statistical comparisons of field and image variables.

Total vegetation cover averages were similar for the two land systems, at 20% and 21% in Gina and Buckshot respectively, compared with a mean of 19% for all sites (Table 3.3). Buckshot had higher ephemeral and grass cover (13%) and lower perennial cover (8%) than Gina and the regional average (12%). Litter and cryptogam cover were significant contributors to total ground cover at 23 and 30% for Buckshot and Gina, and 27% for all sites, bringing total ground cover to 45-50%.

Table 3.3 Vegetation cover components at landscape and land system scales

Vegetation components	**% cover Study area Sample size= 40**		**% cover Buckshot land system Sample size= 8**		**% cover Gina land system Sample size= 19**	
	Mean	StdDev	Mean	StdDev	Mean	StdDev
Perennial species	12.1	7.4	7.9	6.2	12.4	6.5
Ephemeral & grass species	6.8	5.3	13.5	12.3	8	5.4
Total vegetation (perennial, ephemeral and grass species)	18.9	8.7	21.4	16.3	20.4	8.1
Litter and cryptogams	27	14.5	22.7	9.3	29.5	10.1
Total vegetation plus litter & cryptogams	45.9	16.6	44.1	19.3	49.9	9.9

3.2.3 Satellite image data

The Landsat Thematic Mapper (TM) scene from 20 October 1991 (path 100, row 81) was used for this component of the study. Because field data collection spanned several

months in 1990-1991 it was not possible to acquire an image that coincided with all field data dates. The imagery captured similar dry conditions, however, with only 10 mm of rain falling during the preceding four months. Preliminary radiometric calibration and georegistration of the image are described in Chapter 2.

The vegetation indices detailed in Table 3.1 were calculated using the Landsat image bands. In addition to these indices, a new Stress Related Vegetation Index (STVI-4) was devised (Equation 3.1). This index is a variant of the plant-water sensitive group, and was designed to respond positively to increasing vegetation response, whereas the existing STVI indices decrease with increasing vegetation influence. It was calculated using Landsat red band 3 (0.63-0.69μm), near-infrared (NIR) band 4 (0.76-0.90μm) and mid-infrared (MIR) band 5 (1.55-1.75μm) with the following formula:

$$STVI\text{-}4 = NIR-(RED \times MIR) / (NIR+MIR) \qquad (3.1)$$

The index contrasts the higher NIR reflectance of vegetation with chlorophyll absorption in the red and water absorption in the MIR. Because of xeromorphic adaptations and low chlorophyll levels the visible red reflectance of arid plants may be high, but the MIR reflectance may be low in response to moisture content, particularly of semi-succulent chenopods. Therefore, in this study, the (NIR-(RED×MIR)) operation instead of (NIR-RED) that was used in the NDVI formula was used to highlight vegetation cover. By normalizing the (NIR-(RED×MIR)) operation over (NIR+MIR) instead of (NIR+RED) as in the NDVI formula, the effects of soil background were significantly reduced and highlighted the sparse vegetation cover in this arid environment. This normalization retains the ability of the index to minimize topographic and atmospheric effects.

This index was also corrected using the Redness Index (Bannari *et al.*, 1995). This index calculates the difference between red and green reflectance, normalised by their sum, defined by the following equation:

$$\text{Redness Index} = (R-G)/(R+G) \qquad (3.2)$$

where

R= the mean reflectance in the red channel

G= the mean reflectance in the green channel

The method uses the slope "K" obtained from the correlation between RI and the vegetation index, in this case the STVI-4. This produced a corrected vegetation index, VI* as shown in the Equation 3.3:

VI*= STVI-4 – KRI (3.3)

Each of the permanent monitoring sites was located on the rectified satellite image and average pixel values extracted for each of the vegetation indices within a 150 m radius from the point. Field data were collected from transects up to 750 m from the monitoring sites, although the direction of these was not recorded. Consequently there was some uncertainty about the precise image location and area that coincided with the field transects. To address this, the mean values from buffers of 100, 150, 300, and 400 m were extracted around the monitoring points, and the comparative strength of relationships between the image and field data was evaluated. This preliminary assessment showed that the 150 m radius buffer yielded the strongest relationships with the field data.

3.2.4 Data analysis

The relationships between field cover data, aggregated into different categories, and vegetation indices were tested with linear regression analysis. Vegetation indices were used as independent variables and the dependent variables were different categories of field cover data. To investigate the influence of spectral variations on the vegetation indices, relationships between field cover data and vegetation indices were tested at two different scales: landscape scale, using the 40 monitoring sites across the whole Landsat scene, and land system scale with less spectral variation, using the 8 and 19 samples in Buckshot and Gina.

3.3 Results

The regression relationships between field cover data and vegetation indices across the Landsat scene are given in Table 3.4.

Table 3.4 Relationships between field cover (N=40) and vegetation indices at landscape scale across the whole Landsat scene. Relationships significant at p< 0.05 are highlighted.

Vegetation index group	**Vegetation Index**	**% Cover Perennial plants**		**% Cover Total vegetation**		**% Cover Total vegetation & litter & cryptogams**	
Group 1 (Slope-based)		R^2	p	R^2	p	R^2	p
	SVI	0.22	0.002	0.26	0.001	0.37	0.001
	NDVI	0.22	0.002	0.27	0.001	0.39	0.001
	SAVI-A	0.22	0.002	0.26	0.001	0.38	0.001
Group 2 (Distance-based)	PVI-3	0.04	0.208	0.14	0.019	0.20	0.003
	PD54	0.06	0.117	0.15	0.015	0.18	0.006
	SSI	-0.02	0.333	-0.01	0.387	-0.01	0.774
Group 3 (Orthogonal transformation)	SBI	-0.09	0.061	-0.19	0.005	-0.22	0.002
	GVI	0.08	0.069	0.20	0.003	0.30	0.001
Group 4 (Plant-water sensitive)	STVI-1	-0.17	0.009	-0.26	0.001	-0.23	0.002
	STVI-3	0.28	0.001	0.12	0.029	0.01	0.917
	STVI-4	0.10	0.048	0.21	0.003	0.26	0.001
	MSVI-1	0.10	0.045	0.01	0.561	-0.09	0.063
	MSVI-2	0.04	0.225	-0.01	0.490	-0.24	0.001
	MSVI-3	0.07	0.091	-0.01	0.964	-0.17	0.009

At this scale, an area that includes 10 different land systems, all the slope-based vegetation indices were correlated significantly with field cover data, with the strongest relationships of NDVI with combined plant, litter and cryptogam cover explaining up to 39% of the variation in field measurements. The PVI-3 and PD54 of the distance-based vegetation indices were also correlated significantly with total vegetation and total organic cover, explaining 18-20% of cover variation, but their relationships with perennial plant cover were not significant. Similar results were obtained with the orthogonal vegetation indices (SBI and GVI). The SBI, a weighted sum of the Landsat image bands, equating to total ground reflectance or albedo, correlated negatively with total ground cover, while the GVI showed a stronger positive relationship. The PVI-3

and PD54 predicted total vegetation cover and total organic ground cover, but the SSI from the same group of distance-based vegetation indices was not related significantly to any of the field cover components. The plant-water sensitive vegetation indices (group 4) showed variable relationships with field data. Among these indices, the Stress Related Vegetation Indices (STVI-1 and 4) were correlated significantly (R^2=0.1-0.3) with all combinations of field cover components, although they explained relatively low proportions of the variance in the field measurements. Other vegetation indices in this group were less consistent predictors of field cover.

Within the two land systems, as expected, there were stronger relationships between vegetation indices and field cover data than at the broader scale. Table 3.5 shows these relationships in Buckshot land system. The STVI-1 showed the strongest relationship with total vegetation cover (R^2=0.88), followed by the SBI (R^2=0.82) and STVI-4 (R^2=0.78). There were significant correlations between the slope-based indices and total vegetation cover (R^2=0.6) but these indices were very poor predictors of perennial vegetation cover or total organic cover. In contrast to the regional analysis, all the distance-based and orthogonal transformation indices were correlated significantly with all categories of field cover data in this land system, although the strongest relationships were with total vegetation cover. However, the STVI-3 and MSVI versions 1, 2 and 3 showed no significant correlations with field cover data.

In Gina land system all the relationships were significant at the 95% confidence level with the exception of the slope-based indices that were poorly related to total ground cover (Table 3.6). The vegetation indices generally best predicted total plant cover, followed by perennial plant cover. The strongest relationships were between GVI and total vegetation cover (R^2=0.74) followed by STVI-4 (R^2=0.66).

3.4 Discussion and conclusions

The prediction of vegetation cover was stronger within the two land systems studied, rather than across the range of land systems within the region. Across the study area up to 39% of the variation in cover was explained, whereas within land systems the vegetation indices explained up to 90% of variation in cover measurements. The stronger predictive power of the vegetation indices within land systems is not unexpected, as soils and vegetation are usually more homogeneous and resultant spectral variations are lower at this scale. At regional or landscape scale the

relationships between cover and spectral response are more varied, and although they may be strong within land systems, are weaker when the land systems are aggregated together.

Table 3.5 Relationships between field cover data (N=8) and vegetation indices in Buckshot land system. Relationships significant at p< 0.05 are highlighted.

Vegetation index group	**Vegetation Index**	**% Cover Perennial plants**		**% Cover Total vegetation**		**% Cover Total vegetation & litter & cryptogams**	
Group 1 (Slope-based)		R^2	p	R^2	p	R^2	p
	SVI	0.02	0.325	0.57	0.030	0.24	0.215
	NDVI	0.03	0.314	0.58	0.020	0.26	0.196
	SAVI-A	0.01	0.329	0.57	0.031	0.24	0.217
Group 2 (Distance-based)	PVI-3	0.71	0.008	0.78	0.003	0.61	0.022
	PD54	0.61	0.013	0.72	0.008	0.62	0.021
	SSI	-0.44	0.044	-0.61	0.022	-0.62	0.020
Group 3 (Orthogonal transformation)	SBI	-0.71	0.008	-0.82	0.001	-0.63	0.018
	GVI	0.68	0.012	0.64	0.017	0.55	0.036
Group 4 (Plant-water sensitive)	STVI-1	-0.64	0.011	-0.88	0.001	-0.65	0.015
	STVI-3	-0.07	0.260	-0.08	0.500	-0.12	0.404
	STVI-4	0.71	0.008	0.78	0.003	0.62	0.019
	MSVI-1	-0.01	0.437	-0.01	0.914	-0.04	0.633
	MSVI-2	-0.39	0.057	-0.20	0.267	-0.20	0.264
	MSVI-3	-0.16	0.178	-0.06	0.554	-0.11	0.421

Across the region the vegetation indices best predicted total cover comprising the combination of perennial and ephemeral plants with surface plant litter and cryptogam crust, followed by the less abundant total plant cover and perennial plant cover, suggesting that it is the reduction in overall landscape reflectance brought about by the organic cover that is influencing the spectral indices. By contrast, the cover components predicted best within the two land systems were total plant cover and perennial plant

cover, with the combined cover components predicted poorly. The strength of the cover prediction is noteworthy, since the total plant cover was only 20-21% and the perennial cover 8% and 12% in Buckshot and Gina. The poorer relationships between the spectral indices and total cover (plants, litter and cryptogams) within the land systems suggest that the indices are indeed responding to the reflectance characteristics of photosynthetic vegetation, rather than the simple "darkening" effect of cover on the soil.

Table 3.6 Relationships between field cover data (N=19) and vegetation indices in Gina land system. Relationships significant at p< 0.05 are highlighted.

Vegetation index group	**Vegetation Index**	**% Cover Perennial plants**		**% Cover Total vegetation**		**% Cover Total vegetation & litter & cryptogams**	
Group 1 (Slope-based)		R^2	p	R^2	p	R^2	p
	SVI	0.37	0.005	0.65	0.001	0.12	0.146
	NDVI	0.36	0.006	0.64	0.001	0.10	0.168
	SAVI-A	0.36	0.006	0.64	0.001	0.12	0.145
Group 2 (Distance-based)	PVI-3	0.49	0.001	0.61	0.001	0.47	0.001
	PD54	0.40	0.003	0.54	0.001	0.54	0.001
	SSI	-0.32	0.013	-0.22	0.040	-0.60	0.001
Group 3 (Orthogonal transformation)	SBI	-0.53	0.001	-0.64	0.001	-0.32	0.004
	GVI	0.60	0.001	0.74	0.001	0.33	0.010
Group 4 (Plant-water sensitive)	STVI-1	-0.49	0.001	-0.60	0.001	-0.29	0.018
	STVI-3	-0.21	0.045	-0.22	0.004	-0.54	0.001
	STVI-4	0.51	0.001	0.66	0.001	0.41	0.001
	MSVI-1	-0.32	0.011	-0.46	0.001	-0.53	0.001
	MSVI-2	-0.24	0.035	-0.49	0.001	-0.37	0.006
	MSVI-3	-0.30	0.015	-0.52	0.001	-0.48	0.001

Across the land systems the best vegetation indices were the slope-based group, which explained up to 39% of total cover variation, followed by some of the stress-related indices and the Green Vegetation Index (20-30% of cover variation). There was little

difference between the performance of NDVI, the simple red/infrared ratio vegetation index (SVI) and the soil-adjusted vegetation index (SAVI-A) in predicting total cover at this scale. The distance-based indices performed less well at this scale, explaining only around 20% of total cover variation. These poor correlations result from the dependency of these indices on specific landscape spectral characteristics in the image. All distance-based vegetation indices rely on the definition of a soil line, with vegetation cover estimated by the perpendicular distance from it in bi-spectral space. This soil line depends on soil type and colour and varies between different land systems. Thus, it would be poorly defined for the whole scene, which included 10 different land systems. In addition, these indices (e.g. PD54) require definition of a point of maximum vegetation cover in bi-spectral space, also a feature that is likely to vary across different land systems.

Within Gina and Buckshot, many of the vegetation indices were correlated strongly with total plant cover, explaining 60-90% of the variation in the monitoring point cover measurements. Strong relationships were recorded for both land systems, despite their marked differences in soil type and colour and dominant vegetation species. The best image indices were from the orthogonal and stress-related (STVI) group, followed by the distance-based and slope-based indices. Predictions of total plant cover were somewhat stronger in Buckshot land system, even though it had lower perennial plant cover (8% vs 12%), and the soils are covered by iron-oxide coated “buckshot” gravels which considerably add to the visible red reflectance and may interfere with vegetation discrimination. However, the Buckshot predictions should be used with caution, since they were based on only eight sample sites.

Of the orthogonal indices, both the Soil Brightness Index and the Green Vegetation Index correlated strongly with all cover components, the Soil Brightness Index showing negative relationships with plant cover, as expected, because it is a weighted sum of the satellite image bands, recording brightness that is usually related to exposed soils. The orthogonal indices were somewhat poorer predictors of combined vegetation, litter and cryptogam cover, compared with vegetation cover alone. This may be because the spectral responses of dry plant litter and dark cryptogam crust are more likely to be found in the third component of the tasselled cap transformation rather than the first and second ones.

Responses of the stress-related indices were variable. The mid-infrared indices (MSVI 1,2, and 3) were significantly correlated with all cover components in Gina, but were very poor predictors in Buckshot. Examination of the vegetation index images suggested that these indices were highly influenced by the variations in the soil background in this arid environment. However, the stress related indices, in particular STVI-1 and 4, were good predictors of cover in both land systems. The STVI-4, here applied with the soil colour correction, showed little improvement over existing indices of this type (STVI-1) in Buckshot, but performed better in Gina. Although the STVI-4 did not perform statistically significantly better than STVI-1, it had positive relationships with vegetation cover and this made STVI-4 imagery easier to interpret than STVI-1. In addition, cover mapping using the red-corrected STVI-4 showed better discrimination of vegetation patterns.

The distance-based indices were good predictors of total vegetation cover, and to a lesser degree of perennial vegetation cover within the two land systems. Within a land system soil types are more consistent and better represented by a single soil line in a bi-spectral space. As a result, distance from the soil line was a better indicator of vegetation cover. Several of distance-based vegetation indices (e.g. PD54) have been used successfully as indicators of perennial plant cover which has important role in land condition assessment and monitoring, irrespective of plant greenness. The correlations here confirm their utility within land systems, but not across broader landscapes.

In considering predictive relationships between image spectral indices and the field cover measurements at the monitoring points, it must be remembered that the cover data was collected over several months, and that the imagery has captured landscape conditions at one time during this period. The Gina and Buckshot field data were collected in two months, although they were six months apart, while the monitoring points across the whole region were measured over a nine-month period. Consequently temporal variation in vegetation cover and its photosynthetic status, resulting from continuing grazing and from response to changing weather and rain, must be considered as contributors to variability in the field data. In addition, slight mismatch between the precise area sampled in the field and the pixels extracted from the imagery could also potentially reduce the strength of relationships between the two data sets. The field cover data was collected from transects radiating up to 750 m from the monitoring points, while the image values came from areas of approximately 7 ha around the points

in order to include corresponding location. Finally, the field measurements were made by several different field workers, adding another source of variation to the data. For example, it has been shown that there may be up to 20% difference in measurements of plant cover made by experienced field workers, using objective methods similar to those made at the pastoral lease monitoring sites (Friedel and Shaw, 1987b; Wilson *et al.*, 1987).

The findings of this study have several implications for the use of multispectral vegetation indices in vegetation cover assessment and monitoring in this environment. Firstly, it is clear that predictive relationships can be established between image-derived indices and vegetation cover assessed by familiar field techniques. While total organic ground cover and total plant cover can be quantified by some image indices, it is most significant that perennial plant cover can be predicted, since this is the vegetation that is most important in assessment of rangeland condition and monitoring of long term trend. This means that image indices could be used to determine vegetation cover and document its distribution across broad landscapes, providing more information about spatial variation than is possible with current ground-based methods. Image-derived maps can show variations in plant cover within paddocks, properties and land systems, and can direct grazing and land management. Image-based assessment of vegetation cover also opens the way for more frequent monitoring of land condition at land system level. At present the vegetation cover at some of the permanent monitoring points is surveyed at infrequent intervals, while the overall property and district condition is assessed on a 14 year cycle, as required by the Pastoral Land Management and Conservation Act. More frequent assessment and monitoring using conventional field methods would be prohibitively expensive. However, image-based assessment could be performed more frequently and cheaply to track short and longer-term trends in land condition.

Secondly, prediction of vegetation cover from image indices is best approached on a land system basis, rather than across broader landscapes comprising a wider range of terrain, soils and vegetation. Comparisons of cover derived from image indices can be made within land systems, but should be used with caution across different land systems, since the relationships between plant cover and image indices vary with vegetation and soil types. Stratification into land systems should be undertaken if vegetation cover is to be quantified from image indices. For similar reasons, such

stratification has been an integral part of the image-based grazing-gradient approach to pastoral land condition assessment that has been implemented in northern arid rangelands of South Australia and in Central Australia (Bastin *et al.*, 1993a; Bastin *et al.*, 1998).

One of the main objectives of this component of the research was to identify vegetation indices that were the best predictors of vegetation cover, and hence land condition, in the land systems of the Kingoonya Soil Conservation District. Criteria that make an image-based vegetation index suitable for regional monitoring are strong relationships with perennial cover in the vegetation types of the district, ability to predict this cover within land systems and across broader regional landscapes, and an objective means of computation to ensure consistent application across different images and dates.

Although simple red-infrared contrast indices, in particular NDVI, have been widely used with success in arid land studies throughout the world, the results confirm that they are not the best indices for recording perennial plant or total plant cover within the Gina and Buckshot chenopod shrub-dominated land systems of southern Australia. However, this study found they were the best predictors of combined plant, plant litter and cryptogam cover at a broad landscape scale that included a diversity of land systems across the 34,225 km^2 study region. This suggests that NDVI and simple red-infrared indices are useful for general cover monitoring regardless of more localised soil and vegetation variation.

Although distance-based indices, in particular the PD54, have been used with success in other Australian rangeland studies, they were not the strongest predictors of perennial or total plant cover in the land systems studied, even though these were dominated by chenopods and other perennial shrubs, and had relatively low ephemeral plant cover. A further difficulty with distance-based vegetation indices that inhibits their use in broad-scale repeated monitoring programs is the need to subjectively define a soil line and vegetation dominated pixels in bi-spectral space. This process requires considerable expertise in image analysis, is subjective and may lead to inconsistencies in application of the index.

Of the indices evaluated, the Stress Related Indices 1 and 4 (STVI-1, 4) performed best in relation to the criteria of this study. They showed high to very high correlations with vegetation cover within land systems and significant relationships with cover at

landscape scale. Generally, they best predicted combined perennial and ephemeral plant cover, as did O'Neill (1996) in a vegetation community dominated with chenopod shrublands in western New South Wales. However, they were also good predictors of perennial vegetation and of total ground cover. Their consistency of performance at different landscape scales suggests that these indices are less sensitive than others to variations in soil and vegetation within the Kingoonya District. An additional strength of these indices is that they are calculated using arithmetic combination of Landsat TM image bands, and hence do not require subjective interpretation of soil and vegetation spectral expressions. Consequently, they are well suited for operational programs of broad-scale land cover monitoring.

The results of this study provide a strong foundation for use of vegetation indices as an adjunct to field methods for assessment of land condition in southern Australia with stratification at land system level. Stress-related Vegetation Indices that use multispectral image bands in the red, near-infrared and mid-infrared appear to be good predictors of vegetation cover as measured by traditional monitoring methods at both land system and landscape scales within the Kingoonya District. Image-based monitoring can provide more information about vegetation condition and variation in space and time, and is more cost-effective than field methods. Image maps can provide a means of extrapolating from the current network of monitoring point locations, thus could potentially supplement field-based land condition assessments.

4 VEGETATION MONITORING AND LAND CONDITION ASSESSMENT

4.1 Introduction

Monitoring vegetation cover is an essential step in land management, because it is the single most effective indicator for preventing land from degradation. Accurate monitoring of this component provides information that helps to understand climatic and human impacts on the land condition. Monitoring is thus a very useful tool for land holders, government and different non-government organizations because it helps to detect potential problems and make better decisions for the future.

Ground-based monitoring techniques used currently in arid lands are too inefficient and expensive for broad-scale applications. Interpolation of data to cover areas beyond sample sites is difficult because of the spatial and temporal variability of vegetation in arid environments. Satellite remote sensing with its broad coverage, frequent repetition and cost-effectiveness is apparently a clear choice.

Monitoring land cover using satellite imagery has been recognized since the launch of the first earth resources technology satellite (ERTS-1) in 1972. The NOAA AVHRR NDVI imagery with its low spatial resolution (nominally 1.1 km) and high temporal frequency have been used widely for monitoring broad areas. For example, Tucker *et al*. (1983) used a sequence of AVHRR NDVI imagery to monitor green vegetation at continental scales (see also Myneni *et al.*, 1997; Hountondji *et al.*, 2006). Sequences of the NDVI imagery have been used also for monitoring long-term trends in the rangelands of Australia at state and national levels (Queensland Department of Natural Resources, Mines and Water 2006). Landsat imagery with its moderate spatial resolution (30 m) is another source of satellite data that has been used extensively for long-term monitoring purposes. Most of the Landsat-based monitoring programs in Australia such as Australia Greenhouse Office National Carbon Accounting System project and Victoria River District project have been reviewed by Wallace *et al*. (2006). The Victoria River District (VRD) project was conducted by the Australian Collaborative Rangeland Information System (ACRIS) and the Northern Territory Government in the rangelands of Victoria River pastoral district in the Northern Territory. The project mapped vegetation changes successfully using a 20 year sequence

of Landsat cover index imagery (Karfs and Trueman, 2005). VegMachine is another monitoring project which uses time-series of imagery from different sensors for monitoring long-term trends in Australian rangelands. It is under way currently in the Northern Territory, southern Queensland and northern Western Australia (Karfs *et al.*, 2004).

In addition to long-term monitoring using sequences of satellite imagery, a number of studies have used satellite imagery to monitor vegetation cover and land condition during specific periods (Graetz *et al.*, 1983; Chavez and Mackinnon, 1994; Peters and Eve, 1995; Edwards, 2001; Al-Bakri and Tayor, 2003; Murwira and Skidmore, 2006; Johansen *et al.*, 2007). Foran and Pearce (1990) applied the NOAA NDVI imagery to arid rangelands of central Australia and found that by using imagery from suitable dates it is possible to detect seasonal changes in vegetation cover. Bastin *et al*., (1998) used the grazing gradient approach to determine vegetation trends with increasing distance from stock watering points in dry and wet conditions. The assumption was that if the vegetation was not restored after a good rainfall grazing has had a deleterious effect on land condition. The result of the study showed that vegetation response to rainfall can be used as an appropriate indicator of land condition.

To detect changes in vegetation cover, different change detection techniques can be applied to cover index images (i.e. simple spectral bands or vegetation indices). Such change detection techniques that use cover indices from different dates to detect trends in vegetation cover have been reviewed widely in the literature (Singh, 1989; Yool *et al.*, 1997; Johnson and Kasischke, 1998; Mas, 1999; Rogan *et al.*, 2002; Coppin *et al.*, 2004; Dewidar, 2004; Lu *et al.*, 2004; Nackaerts *et al.*, 2005). Of the change detection techniques mentioned in the literature, visual interpretation of true and false colour composites, image differencing, image ratios, image regression, change vector analysis, and principal component analysis have been used widely. Each technique has its advantages and disadvantages, thus there is no single method that is best used for monitoring purposes. Image differencing is however one of the most popular change detection techniques. In this method two spatially registered cover index images of two different times are subtracted to create a new difference image that represents the changes between those two dates. Pixels that show extreme change lie in the tails of the histogram of the difference image and pixels that show no change lie around the mean (Figure 4.1). Amongst the different methods, image differencing is simple, easy to

interpret and is one of the practical techniques that is used commonly for vegetation cover change detection (Chavez and Mackinnon, 1994; Lu *et al.*, 2004). I adopted this approach for analysis of vegetation change with Landsat imagery.

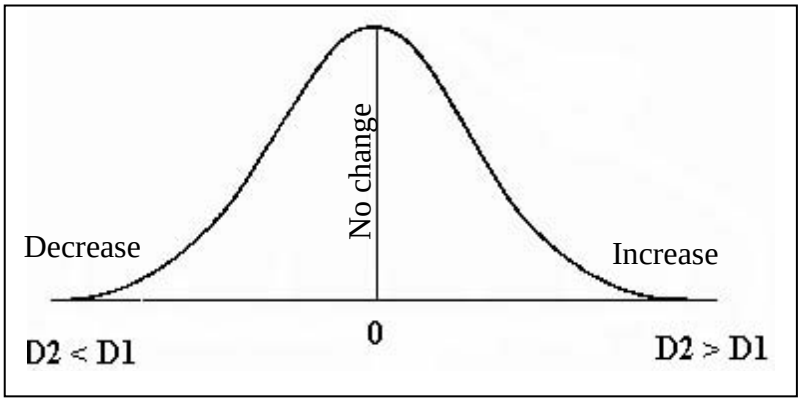

Figure 4.1 Histogram of values differencing resulting from two dates of imagery (date 1 values subtracted from date 2 values)

This component of my research aimed first to detect changes in vegetation cover in the Kingoonya Soil Conservation District between 1991 and 2002 by using Landsat vegetation indices that showed strongest correlations with vegetation cover (Chapter 3). The second aim was to compare field measurements and vegetation indices as different means of documenting changes in land cover. My third aim was to compare the Land Condition Index classes (Chapter 2) with vegetation indices to evaluate whether vegetation indices can be used to assess rangeland condition.

4.2 Methods

This section of the research, like Chapter 3, was conducted in the Kingoonya Soil Conservation District. Detailed information about characteristics of the environment of the study area can be found in Chapter 2.

4.2.1 Field data

Vegetation cover and land condition data used in this component of the study were collected by the Pastoral Management Branch in 1991 and White and Gould in 2002 at the permanent monitoring sites (Chapter 2). These data were compared with image data to see whether the Landsat imagery can detect changes in field cover data and land condition over time. Of the sites assessed in these field studies, 40 fell within the study area covered by the Landsat scene (Figure 4.2). Comparisons between the LCI from

1991 and Functionality Index from 2002 at these sites showed 5 sites improved in condition, 7 sites degraded and 28 sites remained unchanged.

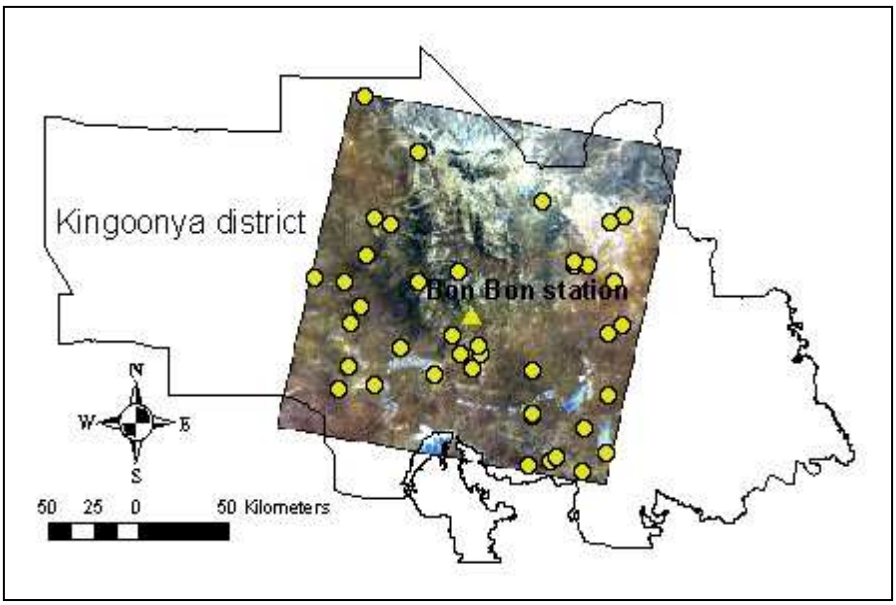

Figure 4.2 The distribution of permanent monitoring sites in the Kingoonya district

The second round of assessment of all monitoring sites in Kingoonya and Gawler Soil Conservation districts began in late 2004. At these sites, the staff of the SA Pastoral Program measured perennial vegetation density using the Jessup transect. In addition to plant density, they determined land condition using the LCI at random sites on each station or property (Chapter 2). In contrast with the first round assessments in 1991, the location of all sites was recorded using a Global Positioning System (GPS). This makes it possible to compare field scores of the LCI with image indices for corresponding locations. Figure 4.3 shows the distribution of LCI sites in the Kingoonya District. Of LCI sites recorded in this district, 885 sites fell within the study area. The LCI scores recorded at these sites were compared with vegetation indices to see whether these indices were good indicators of land condition.

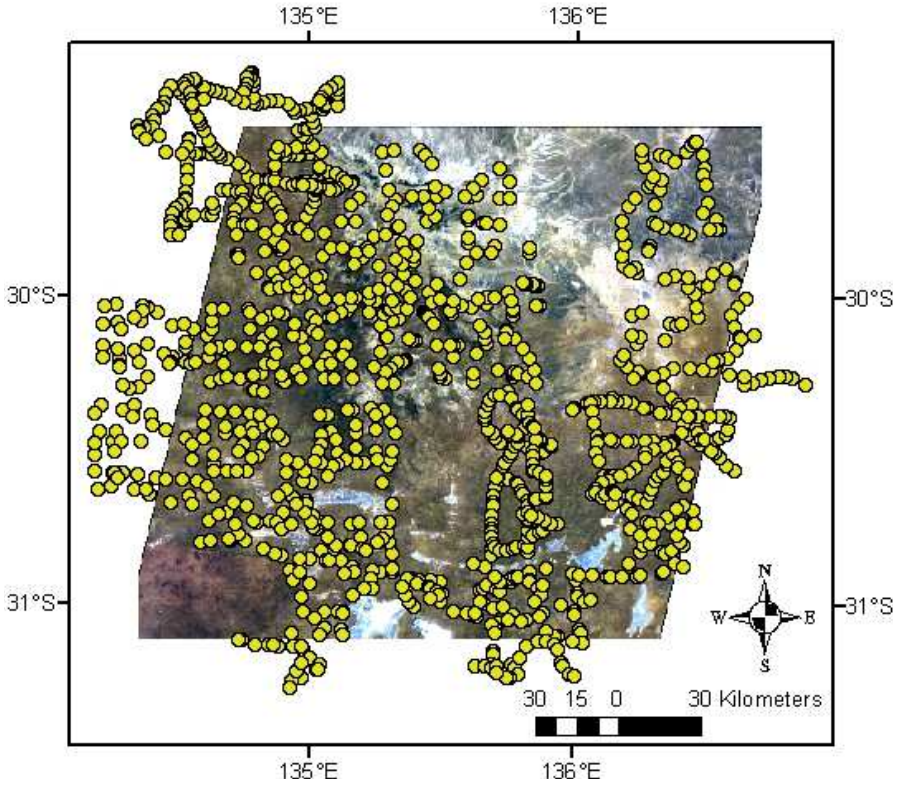

Figure 4.3 The distribution of LCI sites in the Kingoonya district

Determination of land condition at a site using the LCI involves (1) identification of pasture type, and (2) determination of land condition score (LCI-1 (poor condition), LCI-2 (fair condition), and LCI-3 (good condition)) based on reference descriptions and photographs in the LCI manual (Department of Water Land Biodiversity and Conservation, 2002). Major pasture types in the study area are chenopod shrublands, low woodlands and Mount Eba country (plains covered by gravels and dominated with shrubs such as chenopod shrubs). Each of these pasture types was stratified into different sub-types according to the species composition and land forms in which they occurred. Species composition and abundance and also soil surface condition are the main land condition indicators that are used to determine the LCI classes. The criteria for determining the classes of LCI in an example pasture component within each major pasture type is given in Table 4.1.

Table 4.1 Criteria for determining land condition in examples of pasture components in dominant pasture types within Kingoonya Soil Conservation District (Department of Water Land Biodiversity and Conservation, 2002). CSR= crown separation ratio, a measure of plant density.

Pasture type	Pasture component	Condition class descriptions
Chenopod shrublands	*Atriplex vesicaria* /*Maireana astrotrica* on treeless plains	**3:** Shrubland of *A. vesicaria* and *M. astrotrica*, dense to rather spare (CSR 4-6). Some *M. triptera*, *M. pyramidata* and *M. aphylla* commonly occur also in parts. Scalds appear natural (no dead bush remains). **2:** Stands of *M. astrotrica* remain (CSR 1-4); however no *A. vesicaria* apart from isolated or heavily grazed plants. *Sclerolaena spp* more abundant than in 3; some accelerated (man-induced) scalding evident. **1:** No *A. vesicaria*, *M. astrotrica* also absent apart from isolated remnants (CSR 1). Reduced stands of *M. triptera*, *M. pyramidata* etc, may remain. Extensive *Sclerolaena spp*; scalding and / or drifting and dead bush remains.
Low woodlands	*Acacia ramulosa*/*A. aneura* on sandy countries	**3:** No obvious browse line on *A. anueura* trees. Regeneration occurring of *Acacia ramulosa*/ or *A. aneura*, perennial grass cover includes palatable species e.g. *Monachather sp*. Palatable shrubs intact. No increase of unpalatable shrubs. **2:** No *A. aneura* regeneration; excising trees grazed. Reduction in palatable grasses, with an increase in unpalatable annuals. Palatable shrubs missing or damaged. Noticeable increase in unpalatable shrubs and fire bushes, or general reduction in plant cover. **1:** *A. Aneura* old and senescent, or mostly dead. No palatable perennials within grazing reach. *Eragrostis eriopoda* the only perennial grass remaining. Often significant woody weed encroachment of unpalatable shrubs. Annual growth dominates, especially *Aristida sp*., *Salsola kali*, melons.
Mt. Eba country	Mt. Eba gibber plains (plains with fine black and brown gibbers or sometimes coarser); groves of *Acacian aneura* and *A. tetragonophylla*	**3:** *Acacian aneura* (where present) regenerating, palatable shrubs ungrazed. These include *Cassia oligophylla* and *Maireana astrotrica*. Annual growth of *Aristida contorta* with few *Sclerolaena spp*. Natural bare gibber areas occur in this country. **2:** *Acacian aneura* regeneration absent or grazed back; palatable shrubs grazed back or missing; annual grasses with significant *Sclerolaena spp* and cannonballs present. **1:** Country bare, with dominance of *Sclerolaena spp* or cannonballs, increase in *A. tetragonophylla* and *Ptilotus obovatus*. Any *A. aneura* present old and senescent with no regeneration.

4.2.2 Satellite image data

I used the 1991 and 2002 TM and ETM+ scenes from path 100, row 81 to assess vegetation changes over an eleven-year period. In addition, the February 2005 TM

scene for the same area was used to examine the potential of vegetation indices for differentiating LCI scores that were collected in 2005.

Monthly rainfall distribution prior to the 1991 and 2002 images is shown in Figure 4.4. According to the data recorded at Bon Bon station between January and April 2005, approximately 13.5 mm fell in February 2005, prior to the February 2005 image date.

NOTE: This figure is included on page 50 of the print copy of the thesis held in the University of Adelaide Library.

Figure 4.4 The monthly rainfall distribution in Bon Bon station in 1991, 2001 and 2002 (Pastoral Board, 2002)

4.2.3 Vegetation change analysis

Analysis of different vegetation indices in relation to field cover measurements in 1991 (Chapter 3), showed that the STVI-1 and STVI-4 were the best indices for predicting vegetation cover in the study area. Because the positive correlation of STVI-4 with vegetation cover was easier to interpret than the negative correlations of STVI-1, the STVI-4 was selected to investigate changes in vegetation cover over time.

The STVI-4, corrected with the Redness Index (Equation 3.3), was applied to the 1991 and 2002 images and then image differencing was used to highlight changes in vegetation cover. A significant problem with image differencing is selecting suitable thresholds to identify the change areas. Two methods for selecting thresholds have been used: 1) manual trial-and-error; and 2) statistical procedures (Khoudiedji, 1998; Lu *et al*., 2004; Singh, 1989). The statistical method bases change thresholds on standard deviations of values around the mean, although there is no general rule about the number of standard deviations to use. In this study, I found that the mean plus or minus one standard deviation identified extreme but not subtle changes in vegetation index,

therefore I used manual trial-and-error to distinguish all vegetation changes in the region.

The agreement between changes in image and field cover data and also the agreement of changes in the LCI classes with the image and field data was assessed using the Kappa statistical test at 40 monitoring sites. This test compares the strength of agreement between different categories (in this study, vegetation cover, LCI and image data) with that expected by chance. Kappa statistics or coefficients range from 0 to 1. A Kappa coefficient of less than 0.2 means slight agreement, $\hat{K}$=0.21-0.4 is interpreted as fair agreement, $\hat{K}$=0.41-0.6 means moderate agreement, $\hat{K}$=0.61-0.8 means substantial agreement, and $\hat{K}$=0.81-1 means near perfect agreement (Landis and Koch, 1977). The suitability of image data for predicting quantitative changes in vegetation was investigated also using linear regression analysis. For the purpose of this study, the vegetation cover data collected by step-point in 1991 and 2002 was aggregated into three groups including perennial plant cover, combined perennial and ephemeral plant cover (total vegetation cover), and total vegetation plus litter and soil-covering cryptogam cover (total organic cover). Image data were extracted using a 150 m buffer around permanent monitoring sites to enable comparison with corresponding field data.

To extract vegetation values around LCI observation sites the same buffer was applied to the 2005 STVI-4 image and an independent-samples t-test was used to test for significant differences in the STVI-4 values in different LCI classes. To examine whether LCI classes can be discriminated using vegetation indices, analyses were applied in two steps: firstly all the sites with the same LCI class were grouped regardless of pasture type (non-stratified vegetation cover); secondly the LCI classes were stratified according to pasture type into chenopod shrublands (e.g. saltbushes and bluebushes), low woodlands (e.g. mulga) and Mount Eba country which included black and brown gibbers with different vegetation types (e.g. mulga, dead finish and chenopods). The same stratification was applied to the STVI-4 values for comparison with LCI.

4.3 Results

4.3.1 Monitoring vegetation cover over time using STVI-4 vegetation index

Figures 4.5 and 4.6 show STVI-4 vegetation index values across the study area in 1991 and 2002, respectively. As can be seen from the Figures, this index shows different values in each land system due to differences in vegetation, soil and land form types. Very low index values relate to bare soil, mostly white shales (Figure 4.5 (a)) that dominate in the north, especially in Painted land system, and in the north east of the study area (e.g. north of Roxby Downs land system). Relatively high vegetation index values in the centre of the image represent high vegetation cover, mostly tree covers, in sand plains and watercourses that are associated with black gravels or buckshots (Figure 4.5 (b)). Visual image inspection and also field checks showed that the STVI-4 appears to overestimate the amount of vegetation cover in buckshot country.

Changes in the vegetation cover have been highlighted by subtracting 1991 vegetation index values from 2002 values (Figure 4.7). It appears that increased vegetation cover in the east and north east of the difference image (e.g. Roxby Downs land system) mostly corresponds with areas where rain fell prior to the 2002 image acquisition. Parakylia station which is located in this region recorded 47.6, 29 and 42 mm in October, November and December 2001 (Pastoral Board, 2002). This was almost more than 1.7 times more than the rainfall in corresponding months at Bon Bon station 88 km to the west, as a result, it seems that ephemeral plant growth in these areas was much greater than other parts of the study area and has caused an increase in the STVI-4 values.

For further investigation of vegetation changes in response to land management, a subset of the difference image of the southern part of the study area is presented in Figure 4.8. In this subset difference image, changes in vegetation cover can be seen easily within and along some of the paddock boundaries. These boundaries provide clear evidence for management related differences in vegetation cover.

To illustrate vegetation changes within paddocks, three regions that showed the highest changes in vegetation index values are shown including area 'a' (a group of paddocks), and paddock 'b' and 'c' (Figure 4.8). These paddocks are located in Bon Bon and Mount Vivian stations in the Vivian land system. This land system comprises low dunes and sand sheets on calcareous plains. The dominant vegetation types include open

woodlands of mulga and western myall and chenopod shrublands of bluebushes and saltbushes.

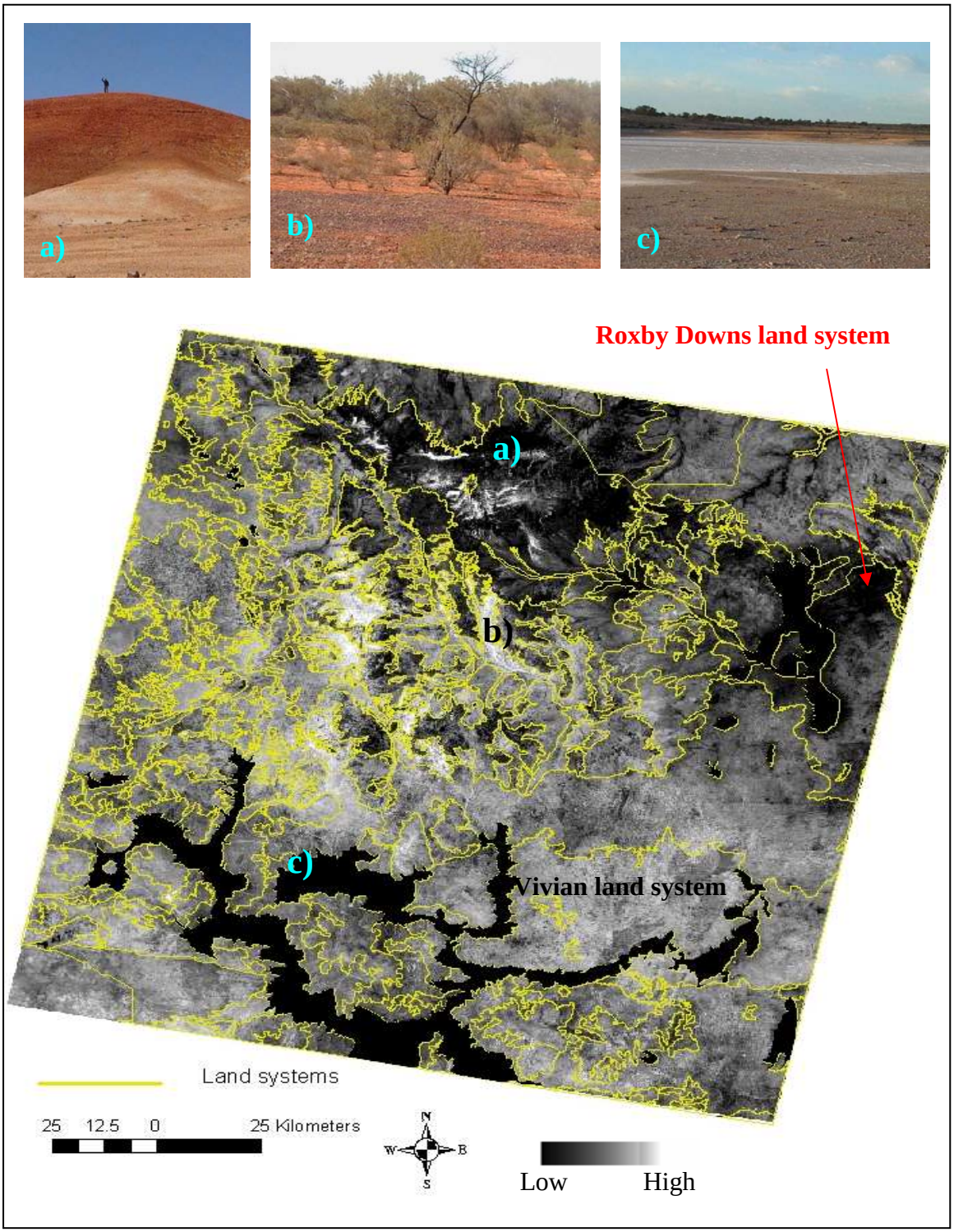

Figure 4.5 Spatial variability of vegetation cover (STVI-4 values) in 1991. Photographs and image locations: a) exposed hills with white shale in Painted land system; b) watercourse of mulga with black gravels in Buckshot land system; c) salt lake masked out.

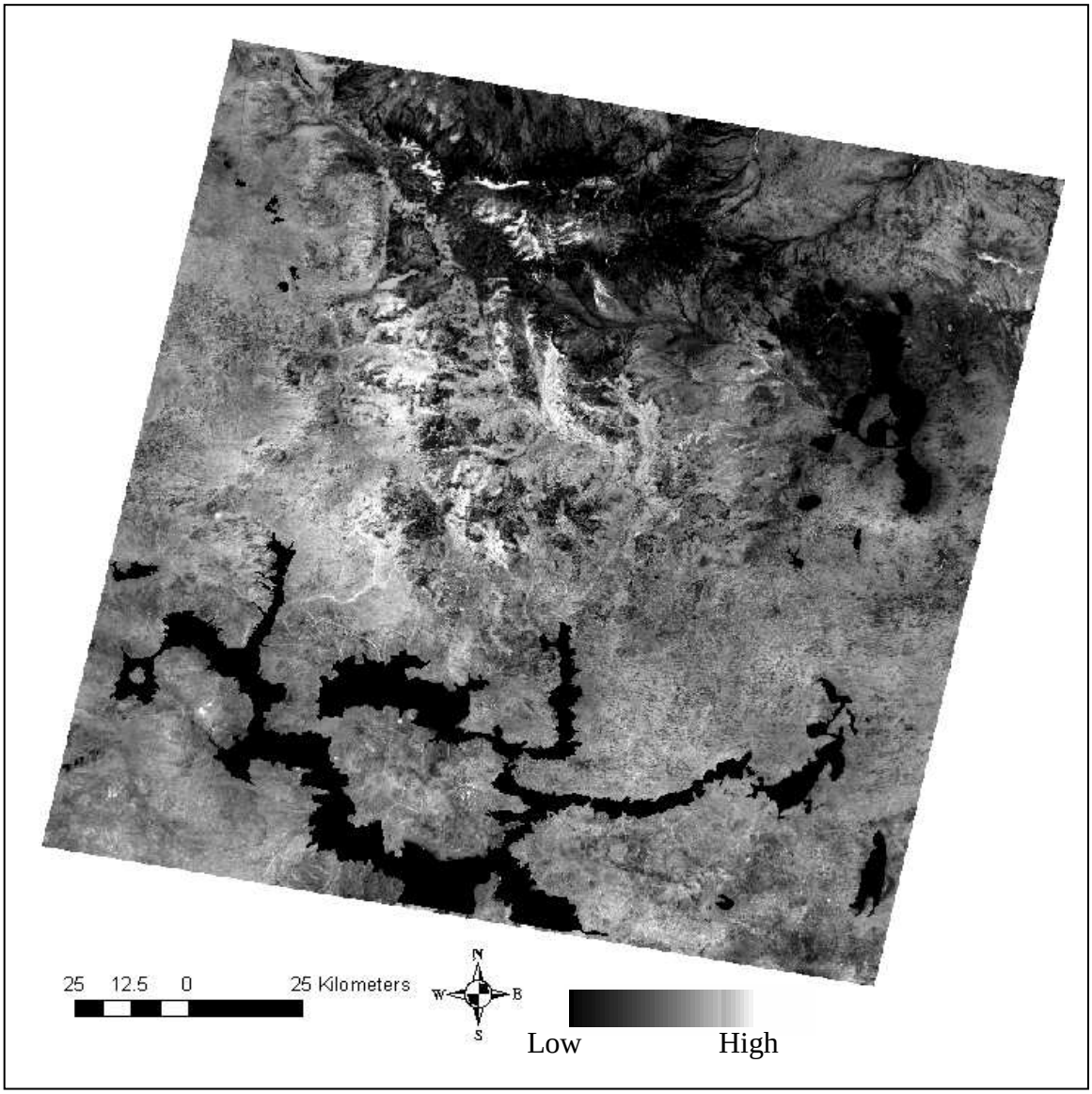

Figure 4.6 Spatial variability of vegetation cover (STVI-4 values) in 2002

Area 'a' shows a high increase in STVI-4 values, suggesting that vegetation cover increased over the eleven-year period between images. The Pastoral Branch reports that all water points were removed (between the two image dates) in these paddocks in response to degradation caused by high grazing pressure (Pastoral Board, 2002). It appears that the removal of stock has allowed some vegetation regeneration in these paddocks.

Very high increase in STVI-4 values was also observed in the south-east corner of the image in paddock 'c'. The main reason for this increase was the regrowth of the vegetation cover after fire that occurred prior to the 1991 image. Because of the

remoteness of the area however, there are no official records of the exact date or extent of this fire (Department for Environment and Heritage, 2007).

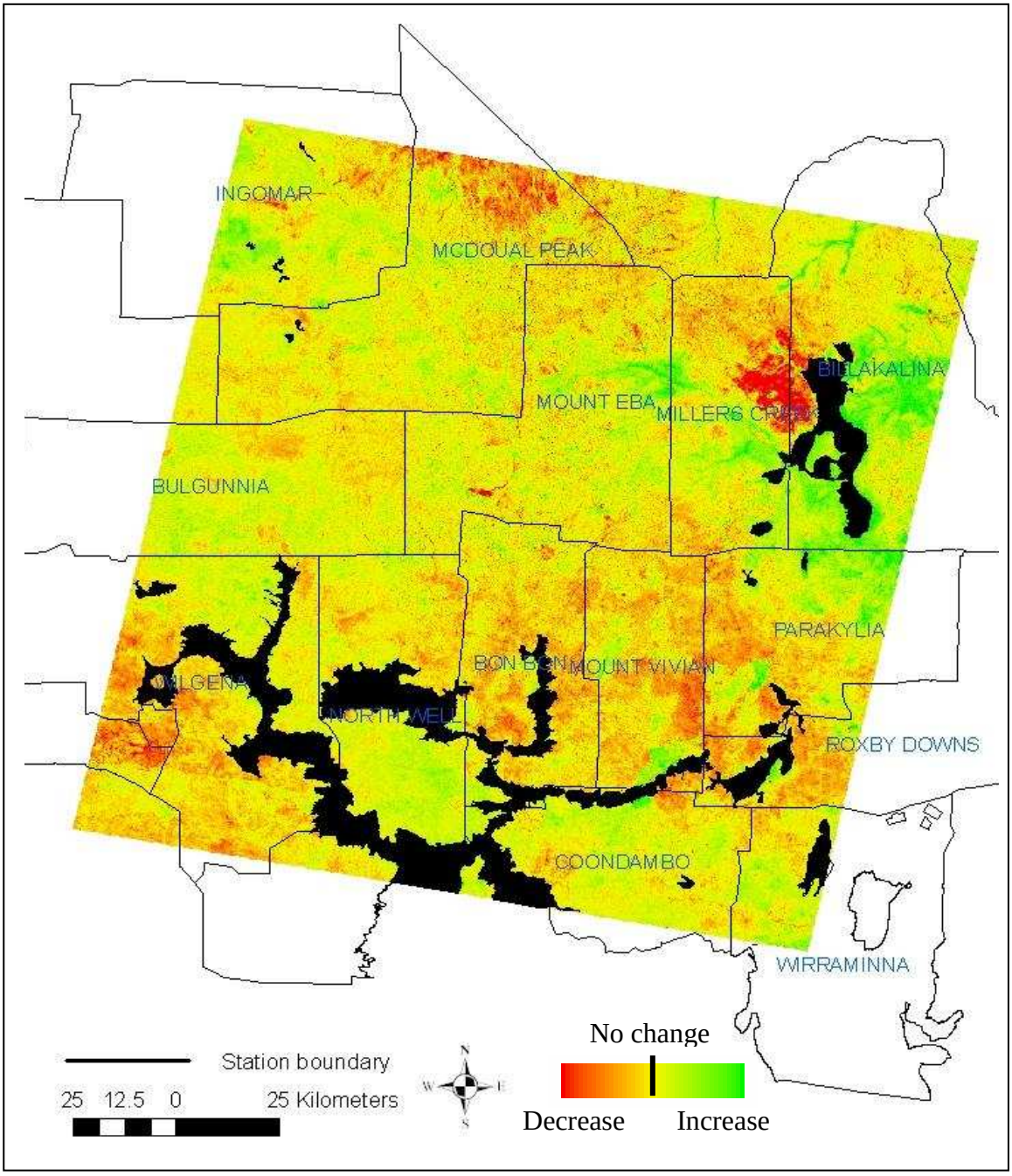

Figure 4.7 Spatial variability of changes in vegetation cover (STVI-4 values) from 1991 to 2002. 1991 STVI-4 was subtracted from 2002 STVI-4, thus high values indicate increase in vegetation cover.

In contrast with the paddocks in area 'a' and paddock 'c', paddock 'b' (east of area 'a') showed a decrease in STVI-4 values. This decrease can be seen clearly at the boundary shared between paddock 'b' and area 'a'. This indicates that management has been the main reason for this vegetation decrease, rather than differences in rainfall. This may be

the result of overgrazing in paddock 'b'. As can be seen from the difference image other areas showed varying levels of increase and decrease in STVI-4 values.

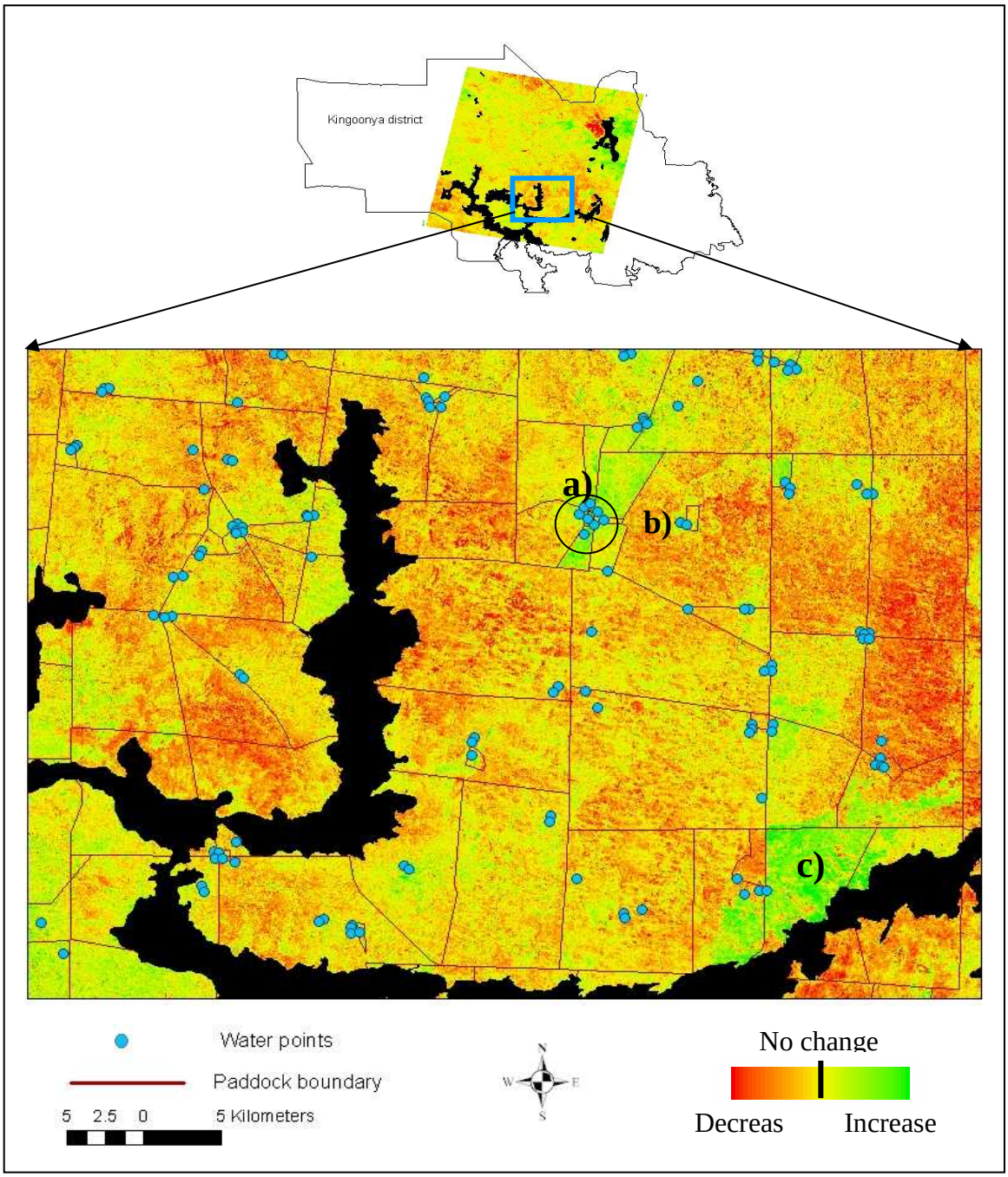

Figure 4.8 Vegetation change (1991 STVI-4 values subtracted from 2002 values) at paddock scale in three selected paddocks.

4.3.2 Comparisons of field cover data and STVI-4 vegetation index for monitoring vegetation changes

1991 and 2002 records of aggregated cover data for 40 monitoring sites are compared in scatter plots in Figures 4.9 (a), 4.9 (b), and 4.9 (c). The diagonal dashed line indicates

the status of no change in cover. The Figure shows that a large number of sites had considerable decreases in cover in all components. Some of the sites showed very little or no change and some sites had increases in cover. Perennial plants had the lowest range of changes from 1991 to 2002 in comparison with other cover components. Perennial vegetation cover increase of up to 5% was recorded at a few sites, and decreases of up to 10% at some sites. In comparison, total vegetation cover decreases of up to almost 20% and total ground organic cover decreases of up to 45% were recorded at some sites. This indicates that perennial plants are less affected by seasonal climate effects and can be used as a good indicator of land condition. Decreases in perennial and ephemeral plants (total vegetation) and total vegetation plus litter and cryptogams (total organic cover) were much higher than perennial plants. These decreases are mainly related to the inclusion of ephemeral plants and cryptogams that are influenced by seasonal conditions.

Changes in the STVI-4 vegetation index generally followed almost the same trends as field cover components (Figure 4.9 (d)). Eight sites showed an increase, some sites with very low changes and the rest of the sites showed large decreases in STVI-4 values. As can be seen from Figure 4.9 (d), the index shows a narrower range of deviation from no change from 1991 to 2002. More sites showed an increase in STVI-4 values (eight sites) than in total plant cover (four sites, Figure 4.9 (b)) and total organic cover (six sites, Figure 4.9 (c)) but less than the number of sites with increase in perennial plants (13 sites, Figure 4.9 (a)). Figure 4.9(d) shows that one of the sites has had very low vegetation cover in both dates. The reason is that this site is located in a poorly vegetated area, mostly dominated by white shales in the north east of the study area in Roxby Downs land system.

Of the 40 sites, 27 sites showing decrease in perennial cover in the field data also showed decrease in the vegetation index, and six of the 13 sites showing increase in perennial plants also showed increase in the vegetation index. Likewise for the total plant cover and total ground cover in comparison with vegetation index, corresponding decreases in the vegetation index were recorded in most of the cases, although increases in both cover components and vegetation index were lower compared with perennial cover.

STVI-4 vegetation index change from 1991 to 2002 are presented in Figure 4.10. As the Figure shows, a large number of sites fell within 5% variation in both field cover and image data, except in total ground cover in which only six sites showed no change over time.

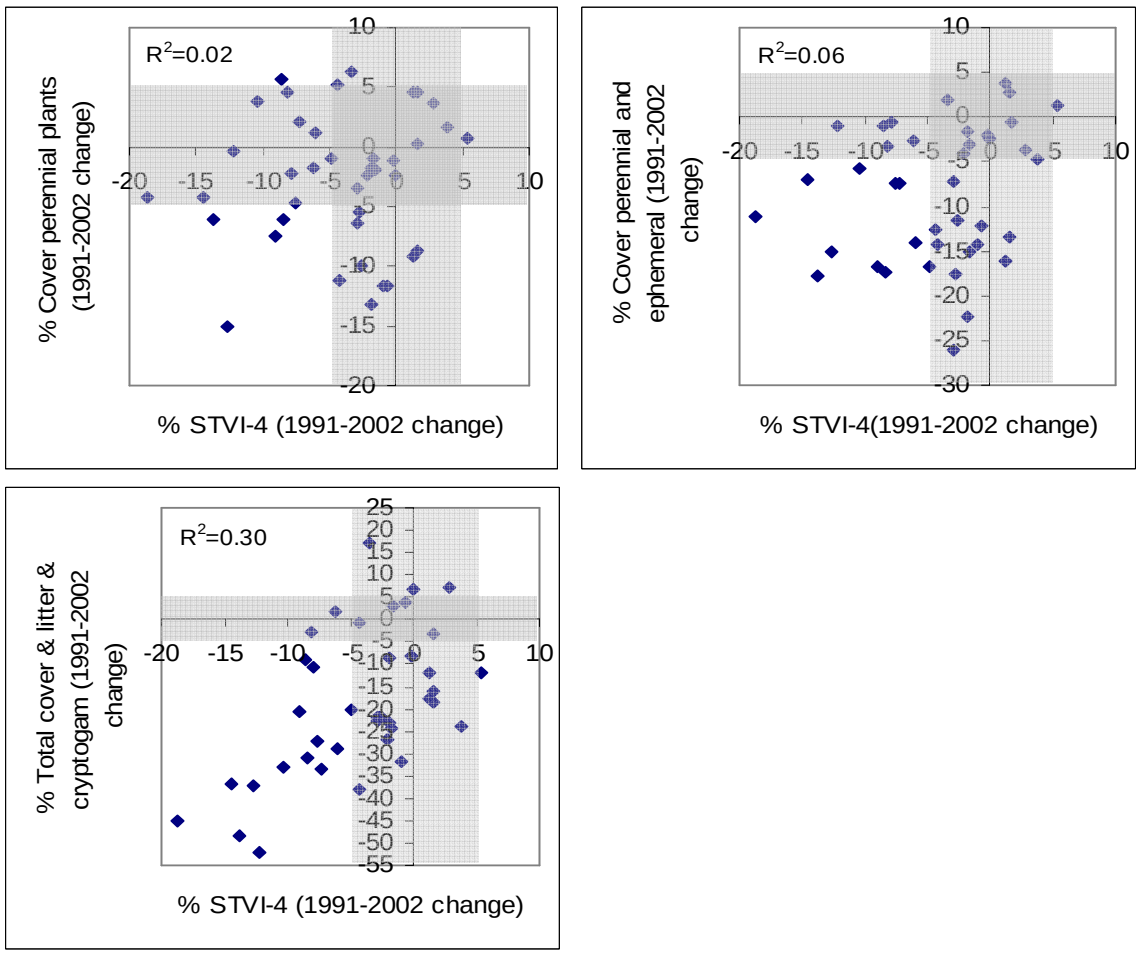

Figure 4.10 Comparisons between changes in STVI-4 and different vegetation cover components from 1991 to 2002 (no change shaded grey)

To assess the extent of agreement between STVI-4 vegetation index quantitatively, field cover components, and LCI data in the change detection, they were grouped into three classes including increases, no changes and decreases. The result of applying the Kappa test to the classified data showed there was not a high agreement between changes in STVI-4 and vegetation cover classes. The STVI-4 change classes had a slight agreement with all cover components. The STVI-4 index change classes had the best agreement with total vegetation cover change classes ($\hat{K}$=0.1), followed by total ground cover change ($\hat{K}$=0.07) and perennial plant cover change ($\hat{K}$=0.01). The level of agreement of the change in LCI classes with change in vegetation cover and STVI-4 variables

appeared to be slightly better than STVI-4 and ground cover data (Table 4.2). Changes in LCI classes showed the highest agreement coefficient with changes in STVI-4 classes ($\hat{K}$=0.14). It had almost similar agreement with total vegetation cover ($\hat{K}$=0.13), followed by perennial plant cover ($\hat{K}$=0.1) and its lowest agreement was with total ground cover ($\hat{K}$=0.08).

Table 4.2 Changes in Land Condition Index (LCI) in comparison with changes in different cover components and STVI-4 vegetation index from 1991 to 2002

Land Condition Index (LCI)					
Perennial plants	*class*	Increases	No change	Decreases	Total
	Increases	0	3	0	3
	No change	4	18	3	25
	Decreases	1	7	4	12
	Total	5	28	7	40
Land Condition Index (LCI)					
Perennial and ephemeral	*Category*	Increases	No change	Decreases	Total
	Increases	0	0	0	0
	No change	3	13	1	17
	Decreases	2	15	6	23
	Total	5	28	7	40
Land Condition Index (LCI)					
Total cover & litter & cryptogam	*class*	Increases	No change	Decreases	Total
	Increases	1	2	0	3
	No change	1	4	0	5
	Decreases	3	22	7	32
	Total	5	28	7	40
Land Condition Index (LCI)					
STVI-4 vegetation index	*class*	Increases	No change	Decreases	Total
	Increases	1	0	0	1
	No change	2	19	4	25
	Decreases	2	9	3	14
	Total	5	28	7	40

Kappa coefficients revealed that changes in the STVI-4 vegetation index had a slight agreement with changes in cover components and LCI classes. To examine the suitability of this vegetation index for predicting quantitative changes in vegetation

components, the changes in index values were regressed against changes in cover components from 1991 to 2002. As expected, the linear relationships were not strong because they were based on 40 sample sites located in different land systems. Changes in the STVI-4 showed very poor relationships with changes in perennial plant cover (R^2=0.02) followed by total vegetation cover (R^2=0.06). The predictive power of the STVI-4 change index was much higher when compared with changes in total organic cover (R^2=0.30).

4.3.3 Comparisons of LCI classes and STVI-4 vegetation index

In this section the suitability of the STVI-4 applied to the 2005 Landsat TM image as an indicator of land condition was examined. The means of STVI-4 for all pasture types in different LCI classes are given in Table 4.3 and Figure 4.11. As it can be seen from the Figure, the STVI-4 has a higher mean value in LCI-2 and LCI-3 than LCI-1, suggesting vegetation cover in these classes is greater than LCI-1. LCI-3 sites which would be expected to have greater vegetation cover showed a lower mean STVI-4. The standard errors indicate however that vegetation index values are very highly variable due to vegetation variations within the LCI classes. The t-test comparisons of mean STVI-4 in different LCI classes showed that this index was unable to separate different LCI classes when vegetation cover was not grouped according to pasture types (p=0.129).

Table 4.3 Results of t-tests for differences between mean STVI-4 in different LCI land condition classes

LCI classes	No. of sample sites	STVI-4 comparisons	P-value
1 (poor)	156	LCI-1 vs LCI-2	0.129
2 (fair)	266	LCI-1 vs LCI-3	0.726
3 (good)	463	LCI-2 vs LCI-3	0.178

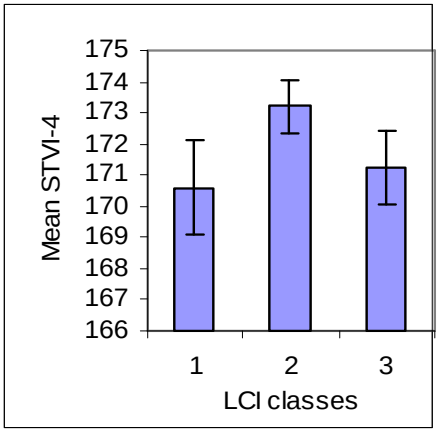

4.11 Mean STVI-4 with standard error bars in different LCI land condition classes

In the second analysis, the STVI-4 values were grouped in each LCI class according to the pasture type that dominated in the study area (Table 4.4). By stratifying pasture

type, the STVI-4 followed the same trend as the LCI results (Figure 4.12): the STVI-4 index increased with the improvement of the land condition from poor to a fair to good. The t-tests revealed that the STVI-4 values between LCI-1 and LCI-3 were significantly different in all the pasture types ($p<0.05$). The STVI-4 also showed significant differences between all LCI classes in the low woodlands ($p<0.05$). However, this index did not differentiate between LCI-1 and LCI-2 in chenopod shrublands and nor between LCI-2 and LCI-3 in Mt. Eba country.

Comparisons between standard errors in stratified and non-stratified pasture types generally showed that the STVI-4 had low variations within and across LCI classes in stratified pasture types compared with combined vegetation types.

Table 4.4 Results of t-tests for mean STVI-4 in different LCI classes based on pasture type

Chenopod shrublands			
LCI classes	**No. of sample sites**	**STVI-4 comparisons**	**P-value**
1 (poor)	49	LCI-1 vs LCI-2	0.134
2 (fair)	234	LCI-1 vs LCI-3	0.007
3 (good)	233	LCI-2 vs LCI-3	0.052
Low woodlands			
LCI classes	**No. of sample sites**	**STVI-4 comparisons**	**P-value**
1 (poor)	82	LCI-1 vs LCI-2	<0.001
2 (fair)	181	LCI-1 vs LCI-3	<0.001
3 (good)	29	LCI-2 vs LCI-3	0.049
Mt. Eba Country			
LCI classes	**No. of sample sites**	**STVI-4 comparisons**	**P-value**
1 (poor)	156	LCI-1 vs LCI-2	0.096
2 (fair)	266	LCI-1 vs LCI-3	0.047
3 (good)	463	LCI-2 vs LCI-3	0.152

4.4 Discussion and conclusions

Vegetation indices as a remote sensing technique have been used widely for monitoring changes in vegetation cover. To evaluate the suitability of these indices in the southern rangelands of South Australia the Stress Related Vegetation Index (STVI-4) was

applied to Landsat images to detect vegetation changes in this area. Results showed that STVI-4 may be used as an appropriate vegetation index for identifying trends in vegetation cover.

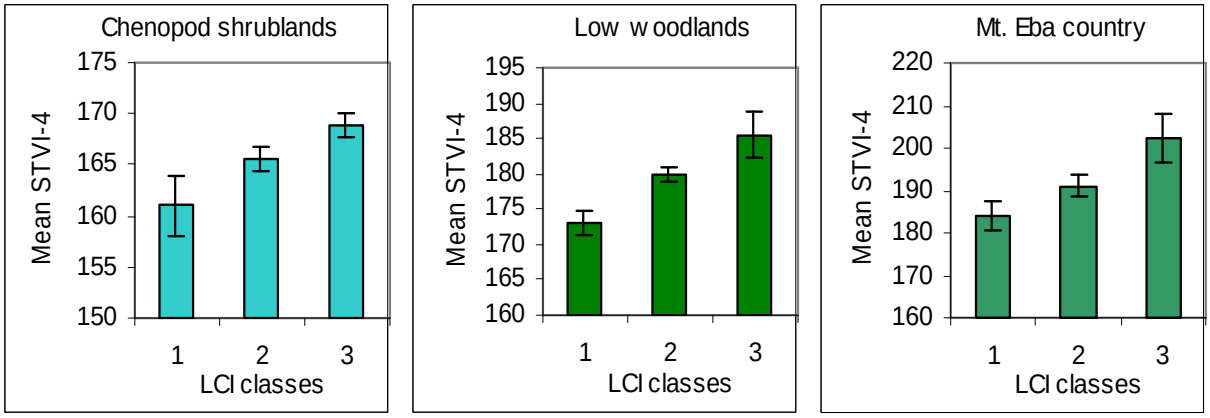

Figure 4.12 Results of STVI-4 with standard error bars in different LCI classes based on pasture type

Changes in vegetation cover across the study area appeared to be the results of seasonal effects and differences in paddock management. Although the 2002 image was selected to represent the dry season and reduce the influence of ephemeral plants, the rainfall for the few months prior to this image was greater than that preceding the 1991 image. Visual inspection showed that this increased rainfall had little effects on most parts of the study area except in the east and north east where the rainfall was approximately 1.7 times greater than Bon Bon station in the southern part of the region. High STVI-4 values in these regions due to the presence of ephemeral plants were clearly observed. Examination of the STVI-4 difference image in the southern region showed clear evidence that changes in vegetation cover within and along some paddocks were the result of alterations in land management and that rainfall had little effect on the changes in land cover. The management influence on vegetation cover in this region was particularly evident in areas around some water points which displayed an increase in STVI-4 values after removal of grazing. The STVI-4 difference image also highlighted the regrowth of vegetation cover in the southeast part of the study area where a bushfire occurred prior to 1991 image.

In spite of the good performance of STVI-4 in the detection of vegetation changes over time, the level of statistical agreement between changes in this vegetation index and different vegetation cover components was not high. All the Kappa coefficients between

STVI-4 and cover data were less than 0.2, which indicates slight agreement. Changes in STVI-4 index showed approximately 10% agreement with changes in total vegetation cover followed by approximately 0.7% and 0.1 % agreement with total ground cover and perennial plants, respectively. It seems the low agreement between image and field cover data in the detection of changes over time relates to the contribution of different classes in Kappa analysis: the number of sites in many classes was very low and this has influenced the strength of the statistical agreement. Kappa results should therefore be taken with caution. The regression analysis showed changes in the values of this index were not a strong predictor of changes in cover components. It had its highest relationships with changes in total ground cover, explaining up to 30% of the variation in this component. These results here confirmed the finding in Chapter 3 that STVI-4 is a better predictor of total ground cover than other vegetation components at broad scales. This analysis considered 40 sample sites from a range of land systems, and as the results of Chapter 3 showed, the STVI-4 is not best applied to the prediction of cover at this broad scale. The Chapter 3 results suggest it might better to predict cover change if analysed within land systems, however there were not sufficient sample sites assessed in 2002 to allow this stratification.

The comparison of LCI classes from 1991 to 2002 revealed that changes in the LCI were in a slight agreement with changes in field cover components and image data ($\hat{K}<0.2$). The LCI had the highest agreement with STVI-4 vegetation index (14%) followed by the total cover component (13%) and perennial plants (10%). LCI had lowest agreement with total ground cover (0.8%). The low agreement may relate to the limited classes of the LCI method. The LCI has three broad classes that are unlikely to be changed with small changes in the field cover components and image data. The relatively low agreement may relate alternatively to changes in abundance of unpalatable increasers and invader plant species. This causes an increase or decrease in the percentage of vegetation cover components and consequently vegetation index values, but may not lead to a change in the land condition class. Lastly, the low agreement may relate to the presence and absence of palatable plants. A site with a high number of small juveniles of palatable species would be classified as fair or good LCI class, whereas the vegetation index values in this site would be very low.

Irrespective of the low Kappa coefficients of LCI compared with field cover components and the STVI-4 vegetation index, the field data showed that the majority of

sites had very little or no change in perennial plants (the most important ones for land condition assessment) and LCI, and that only a few sites showed minor increases in plant cover. The STVI-4 change image showed also that there was little change in cover, and increases, where they occurred, were very small. For management purposes, changes in perennial cover are of concern, and the STVI-4 change image followed the same trends of perennial cover at more than 40% of the sample sites. Land condition change in the area presented by the imagery is consistent overall with the LCI (at approximately 50% of the sites) and field cover data, although the imagery provided much more information about the degree and direction of cover change across the whole region, versus the 40 sample sites used in this analysis.

The results of comparisons between the 2005 STVI-4 vegetation index and LCI classes recorded that year showed that this index had high potential to differentiate different land condition classes in stratified pasture types, which were low woodlands, chenopod shrubland and Mt. Eba country. The STVI-4 differentiated all LCI classes in low woodlands and extreme classes (LCI-1 and LCI-3) in chenopod shrublands and Mt. Eba country. The reason for the good performance of STVI-4 in differentiating LCI-1 and LCI-3 in all pasture types relates to the criteria that are used to differentiate these classes (see Table 4.1): vegetation density, regardless whether it is palatable or unpalatable, in LCI-3 is much higher than LCI-1. The crown separation ratio of vegetation cover in chenopod shrublands in LCI-3, for instance, is 4-6 in comparison with LCI-1, which is equal to one. This low vegetation cover in LCI-1 means that a higher level of eroded and bare soil areas increase the contrast between this class and LCI-3. Vegetation condition or quality is another factor that might influence this separation. Because senescent and heavily grazed vegetation in LCI-1 differs in reflectance from the fresh and ungrazed vegetation in LCI-3. As can be seen from Table 4.1, the low differences between these factors in LCI-1 and LC-2 and also LCI-2 and LCI-3 has affected on the performance of STVI-4 and this index was unable to differentiate these classes in chenopod shrublands and Mt. Eba country. It appears that because of the dominance of tree cover in low woodlands and strong reflectance differences between this pasture type and background soil, the STVI-4 was able to separate all LCI classes.

Among the indicators used to determine land condition in the LCI method (i.e. vegetation composition and abundance, palatability and soil surface condition), the

vegetation abundance, regardless of palatability, and exposure of bare soil appear to be determinable using image-based methods. It is clear that the abundance of vegetation cover is the most important factor that influences land condition and protects it from wind and water erosion. Results presented here indicate that STVI-4 is responsive to the same vegetation cover that forms the basis of the LCI classes. The STVI-4 index was able to discriminate LCI land condition classes in low woodlands and chenopod shrublands that comprise more than 90% of the pastures in the region. This shows that the STVI-4 with its broad coverage, simplicity and repeatability could be used to aid the LCI technique in land condition assessment. If the primary aim is, for example, to determine the density of vegetation cover, especially in its extreme crown separation ratio classes, then the STVI-4 could be very useful. Moreover, the STVI-4 can provide information about vegetation condition in areas far from the network tracks where direct observation for application of the LCI is impossible. Use of STVI-4 imagery would enable a more accurate and spatially-explicit estimate of land condition. It would be possible to more specifically identify the actual location or areas on a property or in a district that are in different condition classes. The STVI-4 vegetation index could therefore be used, not as a replacement, but as a valuable supplementary method to LCI in land condition assessment and monitoring.

As shown in Chapter 3, almost all vegetation indices including STVI-4 had stronger relationships with different cover components at land system versus landscape scale due chiefly to the greater similarity in vegetation cover type within land systems. The STVI-4 revealed the same results with the LCI classes in the stratified vegetation cover. This means that in areas with similar vegetation type, not only can vegetation indices be used as useful tools for predicting and monitoring vegetation cover, but they can also be used for determining land condition. Using these tools in large areas is more cost-effective and may overcome some of the limitations of field methods such as subjectivity and inconsistency.

5 ARID LAND CHARACTERISATION WITH HYPERSPECTRAL IMAGERY

5.1 Introduction

One of the main characteristics of vegetation cover in arid environments is its sparseness; consequently soil is the dominant land surface component in xeric regions. Remote sensing techniques such as vegetation indices have been used widely for assessing and monitoring vegetation cover (Chapters 3 and 4). It is well known that estimating vegetation cover from vegetation indices is often strongly influenced by soil background effects. Huete *et al*. (1985), for example, found that most of the slope-based vegetation indices (e.g. NDVI) and distance-based vegetation indices (e.g. PVI) overestimate the amount of vegetation cover in darker and brighter soils, respectively. I found similar results (Chapter 4): the Stress Related Vegetation Index (STVI-4), as one the most promising indices for cover assessment in the study area, appeared to overestimate vegetation cover in black gravel areas or buckshot country.

Spectral Mixture Analysis (SMA) may overcome the limitations of vegetation indices by decomposing all the ground cover components within a sensor's ground resolution or pixel (Smith *et al.*, 1990). It makes full use of all spectral bands in an image, rather than relying on combinations of a few selected bands to discriminate particular cover types. For each pixel in the image SMA estimates the proportions of that pixel covered by each component on the ground. The general assumption in spectral mixture analysis is that the reflectance recorded for each pixel is a linear mixture of the reflectance of different components in that pixel. This occurs when the radiation interacts with only one material type on its path between the earth surface and sensor (Campbell, 1996). SMA has been used in different environmental studies including land cover assessment and monitoring, land degradation assessment and mineral mapping. Several studies have shown that unmixed vegetation and soil components and their variations in space and time can be used as indicators of land condition or degradation (Metternicht and Fermont, 1998; Tromp and Epema, 1999; Harris and Asner, 2003; Hostert *et al.*, 2003a). Studies have also shown the benefit of this method in many different geological contexts. For example, Bierwirth (1990) applied spectral mixture analysis to multispectral imagery of a geological site in north Queensland, Australia and concluded that it successfully extracted two vegetation types (green and dry) and four different

mineral types. SMA has been shown to be a superior method to widely used vegetation indices in arid and semi-arid environments (Smith *et al.*, 1990; Elmore *et al.*, 2000). These studies found SMA predicted vegetation cover better than vegetation indices such as NDVI. Elmore *et al*., (2000) found, for example, that spectral mixture analysis determined correctly the changes in vegetation cover at 87% of sample sites while NDVI detected changes in only 67% of these sites.

Known also as linear mixture analysis, linear unmixing and end-member analysis, SMA aims to map the relative abundances of different components present within a pixel. This is done by defining spectrally pure pixels known as end-members of the particular surface component (Bateson and Curtiss, 1996; Tompkins *et al.*, 1997; Garcia-Haro *et al.*, 1999). These end-members are drawn from the image itself, from field spectra, or from spectral libraries. Smith *et al*., (1990) applied SMA to Landsat TM imagery of a semi-arid environment in California and found that green or photosynthetic vegetation, non-photosynthetic vegetation, shade and water, and three soil or rock were common components in this region. Landsat TM imagery produced similar results in an arid region in New South Wales, Australia (Lewis and Wood, 1994). Research has shown, however, that the discrimination of different vegetation species in arid environments with less than 30% cover is limited, even using airborne hyperspectral imagery with high spectral and spatial resolution (Lewis, 2000; Okin *et al.*, 2001).

SMA was developed originally for satellite multispectral imagery (Smith *et al.*, 1990) and various studies have shown the potential of spectral mixture analysis in these sorts of data sets (Adams *et al.*, 1995; Asner and Heidebrecht, 2002; Small, 2004). This approach has also been applied successfully to the satellite hyperspectral imagery. The Hyperion sensor is the first space-borne hyperspectral imager on-board NASA's Earth Observing-1 (EO-1) satellite (Pearlman *et al.*, 2003; Ungar *et al.*, 2003). Since the launch of EO-1, several studies have shown the potential of Hyperion data for vegetation and land degradation assessment in arid and semi-arid environments (Asner and Heidebrecht, 2003; Huete *et al.*, 2003). These studies found that end-members extracted from Hyperion imagery using SMA were able to detect disturbance in the landscape due to grazing and other activities. Another study in woody and grassland landscapes of the southern USA showed Hyperion imagery could be decomposed into four different end-members that were combinations of different ground cover components including senescing foliage, cypress-tupelo trees, and trees without leaves;

shadows and green vegetation; senescing Chinese tallow species (i.e. a tree) with yellow leaves and foliage; and senescing Chinese tallow with red leaves (Ramsey *et al.*, 2005). Chewings *et al*. (2002) applied Hyperion imagery to an arid environment near Alice Springs in central Australia and concluded the data have good potential for characterisation of vegetation components in this arid region. In this Australian study, abundance images of photosynthetic vegetation, non-photosynthetic vegetation and soil were produced using spectral mixture analysis. All the studies mentioned above focused on specific components of interest to decompose Hyperion imagery rather than attempting to extract all possible spectral end-members within this imagery.

Apart from Chewings *et al*. (2002) no research has evaluated the potential of Hyperion data for mapping and assessing Australian arid lands. Niether has any work examined relationships between Hyperion data and ground measurements of vegetation and soil. This component of the study aimed, therefore, to evaluate the potential of Hyperion hyperspectral data to discriminate landscape components of arid rangelands of South Australia. The hypothesis was that Hyperion imagery with high spectral resolution should have greater potential for discriminating various vegetation and soil components than was possible with multispectral analysis. This study aimed, specifically, to discriminate some of the vegetation types such as chenopod shrubs that have an important role in land management.

5.2 Methods

5.2.1 Study area

This component of the research focused on an area of 335 km^2 within the Vivian land system, covered by a Hyperion image swath (Figure 5.1). A summary description of this land system is given in Table 5.1.

5.2.2 Field data

5.2.2.1 Collection of vegetation cover

Quantitative data on ground cover from 52 sample sites were collected in January 2006 using the step-point technique (Appendix 4). Sample sites were chosen to include different vegetation species and physical ground cover components that dominated in

the study area. The location of the sample sites was recorded using a Global Positioning System (GPS).

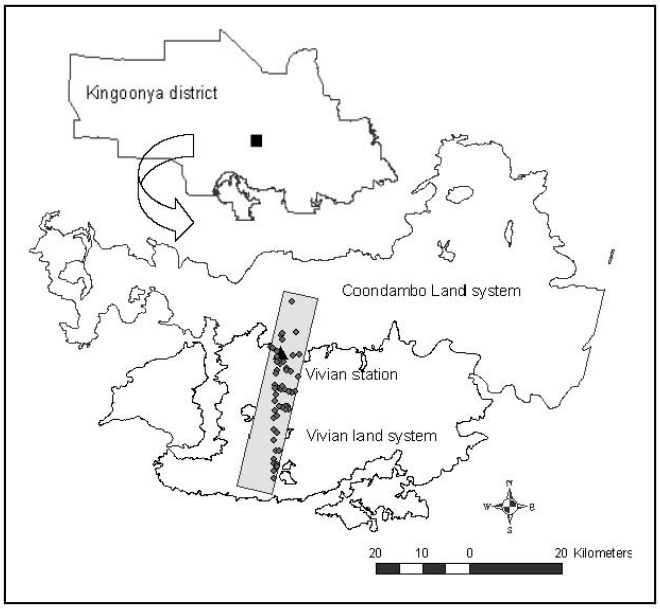

Figure 5.1 Location of study area in Kingoonya Soil Conservation District. Shown also are sample sites across the Hyperion image subset.

Table 5.1 A brief description of Vivian land system (Pastoral Board, 2002)

NOTE: This table is included on page 70 of the print copy of the thesis held in the University of Adelaide Library.

At each sample site a minimum of 1000 points or hits were recorded to estimate field cover components (e.g. perennial and ephemeral vegetation species, litter and lichen, and physical components including soil and surface gravel and stone) along eight radiating transects within a radius of 150 m, sampling an area of approximately 70,650 m^2 (Figure 5.2 (a)). The layout of the radiating transects was chosen to sample relatively homogeneous sites, and avoid mixes of different vegetation and soil types. The average vegetation cover for all sites in the study area was approximately 28 percent. The percentage of different cover components was calculated by dividing the number of hits for each component by the total hits and multiplying by 100.

For comparison with end-member images derived from the Hyperion imagery, field data on abundance of several field cover components were aggregated into groups. Raw and aggregated components included perennial plants with green colour or greenish canopies (e.g. mulga), greenish perennial plants plus grass and herbs (ephemerals), total greenish vegetation cover plus litter and lichen, cottonbush, bluish perennial plants plus litter, total photosynthetic vegetation, bare soil, gravel and stone, and bare soil plus gravel and stone (total physical components).

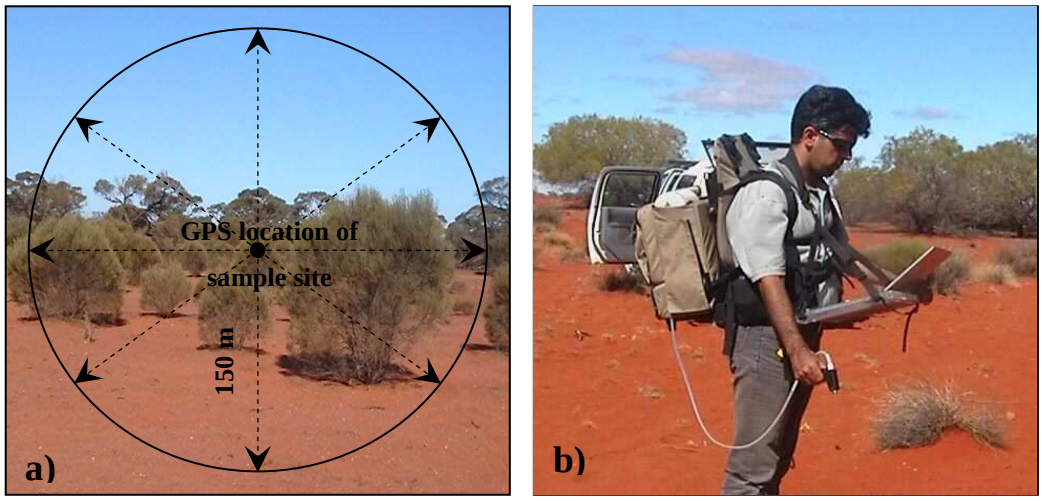

Figure 5.2 Collecting field cover and spectra: a) step-point, b) portable spectrometer

5.2.2.2 Collection of field spectra

Field spectra were obtained with an Analytical Spectral Devices (ASD) Field Spec Pro spectrometer (Figure 5.2 (b)). This instrument includes three spectrometers to sample visible and near infrared (VNIR) and two shortwave infrared (SWIR1 and SWIR2) of the electromagnetic spectrum, from 350 to 2500 nm with a spectral resolution of 10 nm (Hatchell, 1999). The instrument is controlled and data displayed and stored using a notebook computer. In the study area, reflectance spectra of dominant vegetation species (e.g. *Acacia aneura*, *Acacia papyrocarpa*, *Maireana aphylla*, *Maireana sedifolia*, and *Senna ft. petiolaris*) and physical ground cover components such as sandy soil, sandy-loam, and gravel and stone were recorded in April 2006 (Appendix 1 and 3). The field spectra were acquired at a nadir position at 50 cm above the canopy of shrubs, foliage of trees, and physical components which had a plot of 25 cm in diameter on the ground (Hatchell, 1999). For each sample, ten spectra were recorded, with each spectrum being an average of 10 individual measurements that were obtained automatically by field spectrometer. The calibration of the spectrometer was done

approximately every 4-5 minutes using a white spectralon reflectance panel and dark object.

5.2.3 Hyperion hyperspectral imagery

Detailed information about the characteristics of Hyperion imagery and the image acquired over the study on 29 December 2005 has been given in Chapter 2. Figure 5.3 shows the distribution of rainfall which was recorded by the lessee of Vivian station prior to the image capture. Image visual inspection and field checks revealed that rainfall on 17 December 2005 had minimum effect and ephemeral plants were not present at the time of image acquisition.

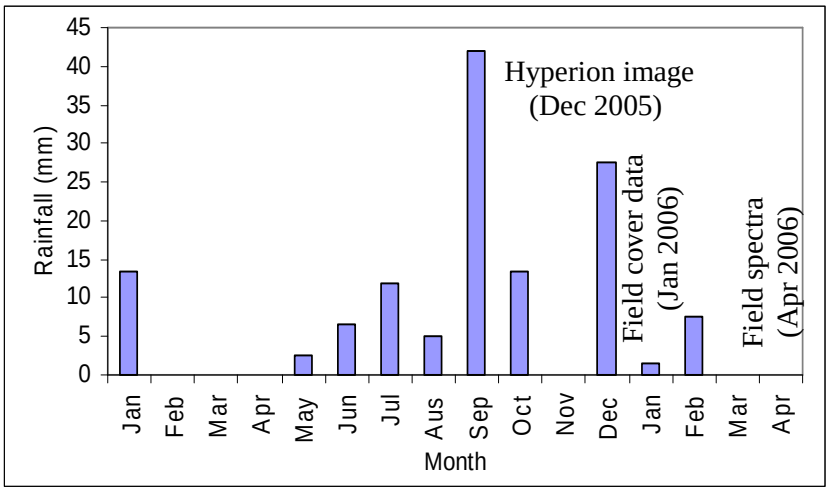

Figure 5.3 Monthly distribution of rainfall from January 2005 to January 2006 in Vivian station in relation to dates of image capture and field data collection

5.2.4 Preliminary image analyses

The image was delivered as a radiometrically calibrated Level 1R product. This image was georegistered using the image to image registration method (Chapter 2). Figure 5.4 shows the sequence of analyses of the Hyperion image that included spatial and spectral subsetting, noise reduction, atmospheric correction, and end-member extraction. The Hyperion image was spatially subset to include study area. Spectral subsetting was performed to remove the first bands 1-7 (355.59-416.64 nm) and the last bands 225-242 (2405.6-2577.07 nm) continuing null values. Bands 8-9 (426.82-436.99 nm) and bands 222-224 (2375.3-2395.5 nm) were removed due to pixel to pixel variation related to sensor detector differences. Other bands excluded were 58-78 (936-1058 and 852-972 nm) to remove the spectral overlap between the two detectors of the Hyperion sensor. A total of 51 bands were excluded with 191 bands remaining for further pre-processing.

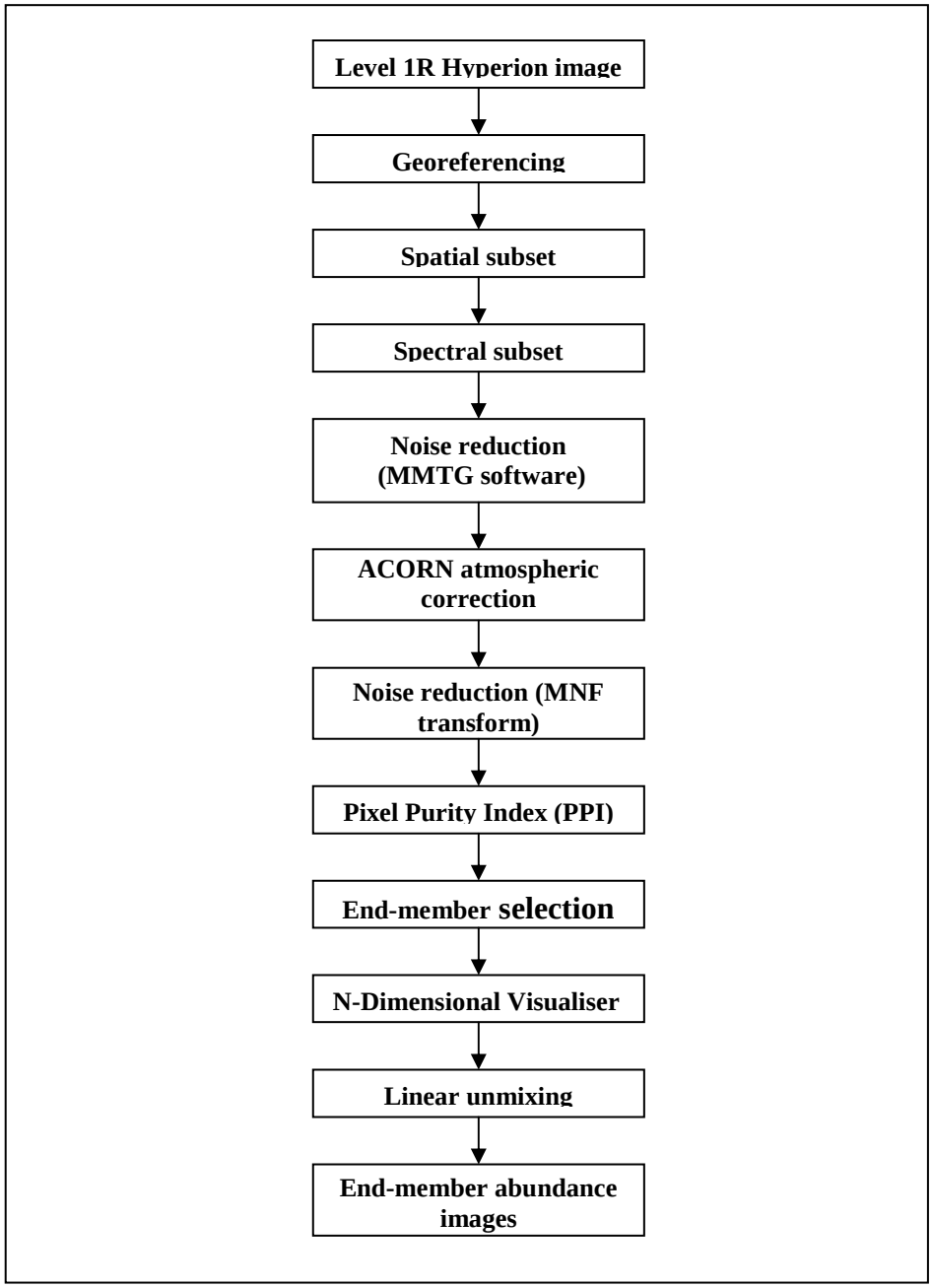

Figure 5.4 Flowchart of Hyperion image analysis

The Commonwealth Scientific and Industrial Research Organization (CSIRO)'s Mineral Mapping Technology Group (MMGT) A-List Hyperspectral Processing Software, as an extension in ENVI (ENVI Research Systems Inc, 2000), was used to reduce noise in the Hyperion image (Mason, 2002; Quigley *et al.*, 2004). The software incorporates different modules including Pushbroom Plugger, Pushbroom Destriper, Outlier Mask Generation, Log Residuals, Normalisation and Background Removal, Spectral Indices, EFFORT Polishing and HyperPPI. From these modules the

Pushbroom Plugger and Pushbroom Destriper were used to remove bad sensor detector cells and stripes from the imagery.

The MMTG Plugger module found noisy pixels or 'bad' pixels throughout the image. A pixel is known as 'bad' if it is completely different from the entire detector-array row based on mean or standard deviation calculations (Mason, 2002). Most of the noisy cells were detected in column 1 and 256 of the detector array. Visual inspection showed that some of the good cells were identified as noisy cells. These cells were deselected from the detector array. After visual correction and testing different window sizes a standard deviation window of (5×5) was used to correct noisy cells. The Plugger uses this window to replace the values of bad cells with ones interpolated from neighbouring good cells.

One of the major problems with the Hyperion image was many along-track stripes in some of the bands. This might result from variations in the calibration of cells in the cross-track direction (Mason, 2002). The MMTG Destriper was applied to the image and it removed the stripes from the image successfully. This module calculates gain and offset values for each 'bad' cell in its row and then these values are applied to normalise the affected cell in the columns of each band.

In order to utilize hyperspectral data for detecting different components on the ground, uncalibrated radiance recorded by the sensor should be corrected for atmospheric and solar illumination effects and converted to surface reflectance. This enables comparisons between image spectra and field or laboratory spectra. There are many methods for atmospheric correction of hyperspectral data that depend on image-based inputs (Green and Craig, 1985; Ben-Dor *et al.*, 1994) and field measurements (Smith and Milton, 1999). Model-based methods such as Fast Line-of-sight Atmospheric Analysis of Spectral Hypercubes (FLAASH) (ENVI Research Systems Inc, 2000) and Atmospheric Correction Now (ACORN) (ImSpecLLC, 2004) rely on image characteristics and atmospheric variables for converting radiance to reflectance and are based on the MODTRAN radiative transfer models (Gao and Goetz, 1990). ACORN atmospheric correction software has been applied successfully to Hyperion data in different studies in Australia (Chewings *et al.*, 2002; Quigley *et al.*, 2004; Dutkiewicz, 2005). One of the important benefits of ACORN over other models is that it removes water vapour and liquid from the imagery and produce separate images of water vapour

and liquid on a pixel-by-pixel basis (ImSpecLLC, 2004). This option reduces the probability of overestimating vegetation cover in areas with high water vapour and liquid.

The noise-reduced image from the CSIRO software pre-processing was corrected for irradiance and atmospheric effects using ACORN atmospheric correction software. Parameters used in ACORN for atmospheric correction are given in Appendix 2. To derive water vapour, the 1140 nm channel was used instead of 940 nm because of high noise and overlapping between the VNIR and SWIR detectors in this region.

To reduce noise in the atmospherically corrected image, subsequent analysis of the image was performed using ENVI software (ENVI Research Systems Inc, 2000). The Maximum Noise Fraction transform (MNF) was used to determine the dimensionality of the data (Green *et al.*, 1988; Boardman and Kruse, 1994). This method produces images ranging from high (the first bands) to low (the last bands) coherence or scene information. The last bands usually have the most noise and least information about the landscape and can be removed from subsequent processing. Visual inspection of the MNF images determined that from 191 bands only 34 bands contained scene information with high Eigenvalues (71.51 to 1.01). These 34 bands were used to extract end-members from the noise-reduced Hyperion image.

5.2.5 End-member generation

The Pixel Purity Index (PPI) was used to extract the most pure pixels in the atmospherically corrected and noise-reduced MNF bands. In this method, the pure pixels are calculated by repeatedly projecting n-dimension data set on to random vectors. The spectrally pure pixels in each projection locate at the apices of the data set and the total number of times each pixel is marked as pure pixel is noted. A "pure pixel" image is created in which the value of each pixel is the number of times that pixel was recorded by these projections. The pure pixel index was run on MNF image with 50,000 iterations and the output image was thresholded to select 800 pixels with high values or numbers of hits marked in the projections.

The n-Dimensional Visualiser function was used to locate and identify the purest pixels (end-members) in an n-dimensional visualisation of pure pixels (n=34, the number of dimensionality or bands of MNF image) (ENVI Research Systems Inc, 2000). Mean

spectra of the end-members were calculated. These potential end-members were used in unconstrained linear unmixing to decompose the MNF Hyperion image into different scene components. The unconstrained linear unmixing calculated an abundance image for each selected end-member. The value of each pixel in the abundance images was the proportion of that end-member in the corresponding pixel of the Hyperion image. A linear stretch enhancement was applied to the abundance images to highlight the high end-member abundance areas. For displaying purposes, in addition to abundance images, an error image was calculated. This image indicates the adequacy of selected end-members., An error image with low values and pattern shows, for example, that all the spectral information relating to scene features in the image has been extracted.

5.2.6 Data analysis

Each of the field sampling sites was located on the rectified end-member images and average pixel values extracted for each of the images within a 150 m buffer, covering an area of approximate 70,650 m^2. In order to evaluate whether the image components could be used to predict field cover data, linear regressions were used to examine their relationships. The abundance of individual and aggregated field cover components was regressed against mean end-member abundance from the corresponding sample sites in the images. Abundance images were used as independent variables and the dependent variables were different categories of field cover data. Preliminary analysis and field checks revealed that one of the image components mostly related to cottonbush vegetation cover (*Maireana aphylla*). This species was one of the dominant vegetation cover at seven sites located in the north of the study area in Coondambo land system. Detailed information about this land system will be given in Chapter 6. It was also a dominant species at two sites in the south. These nine sites were only used, therefore, to correlate the field measurements of cottonbush to that image component and the rest of the sites (45 sites) were used to validate other image components.

5.3 Results

5.3.1 Abundance images

Five spectrally distinct end-members were extracted from the Hyperion subscene in n-dimensional spectral space (Figure 5.5). The five abundance images resulting from linear unmixing using these end-members are shown in Figure 5.6, together with the

residual error image. Two end-members appeared to be associated with photosynthetic vegetation, while the remaining three were associated with soil, surface gravel and stone. The error image had low values and little spatial pattern, which indicates that most of the spectral information about the scene has been extracted from the Hyperion image.

Figure 5.7 compares mean spectra of the image end-members with selected spectra collected in the field using the ASD spectrometer. The selected field spectra were the most similar spectra to image end-member spectra that were chosen after reviewing all related field spectra (Appendix 3). Although the Hyperion mean spectra contain more band to band noise, they are very similar in general form and specific absorption features to selected field spectra. A summary of the end-members and their main spectral absorption features for characterising these end-members is presented below. The specific identity of the end-members was determined by examining their image spectra, distribution and abundance in the images, and by comparing their mean spectra with field spectra and their correlations with field cover data (Figure 5.8).

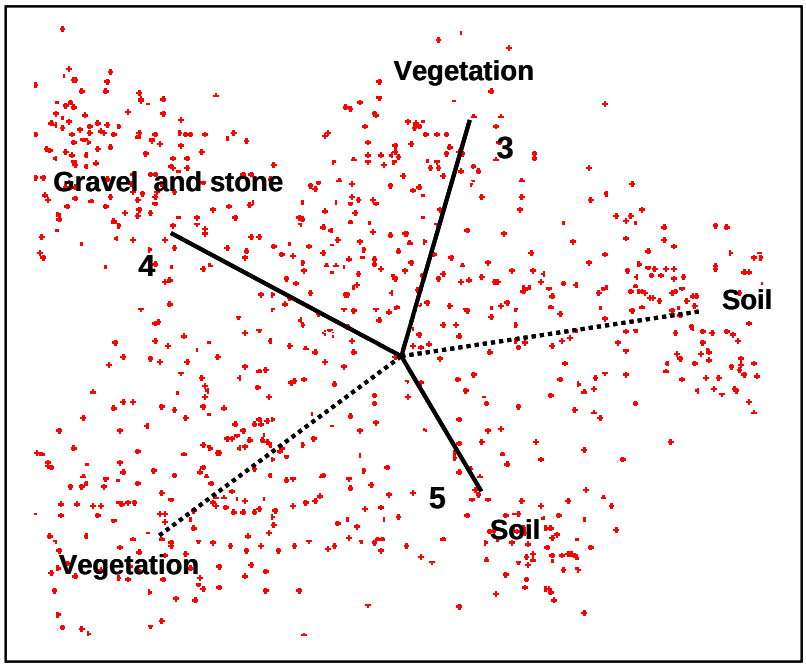

Figure 5.5 End-member extraction in n-dimension visualiser using band 3, 4, and 5 of the MNF Hyperion image.

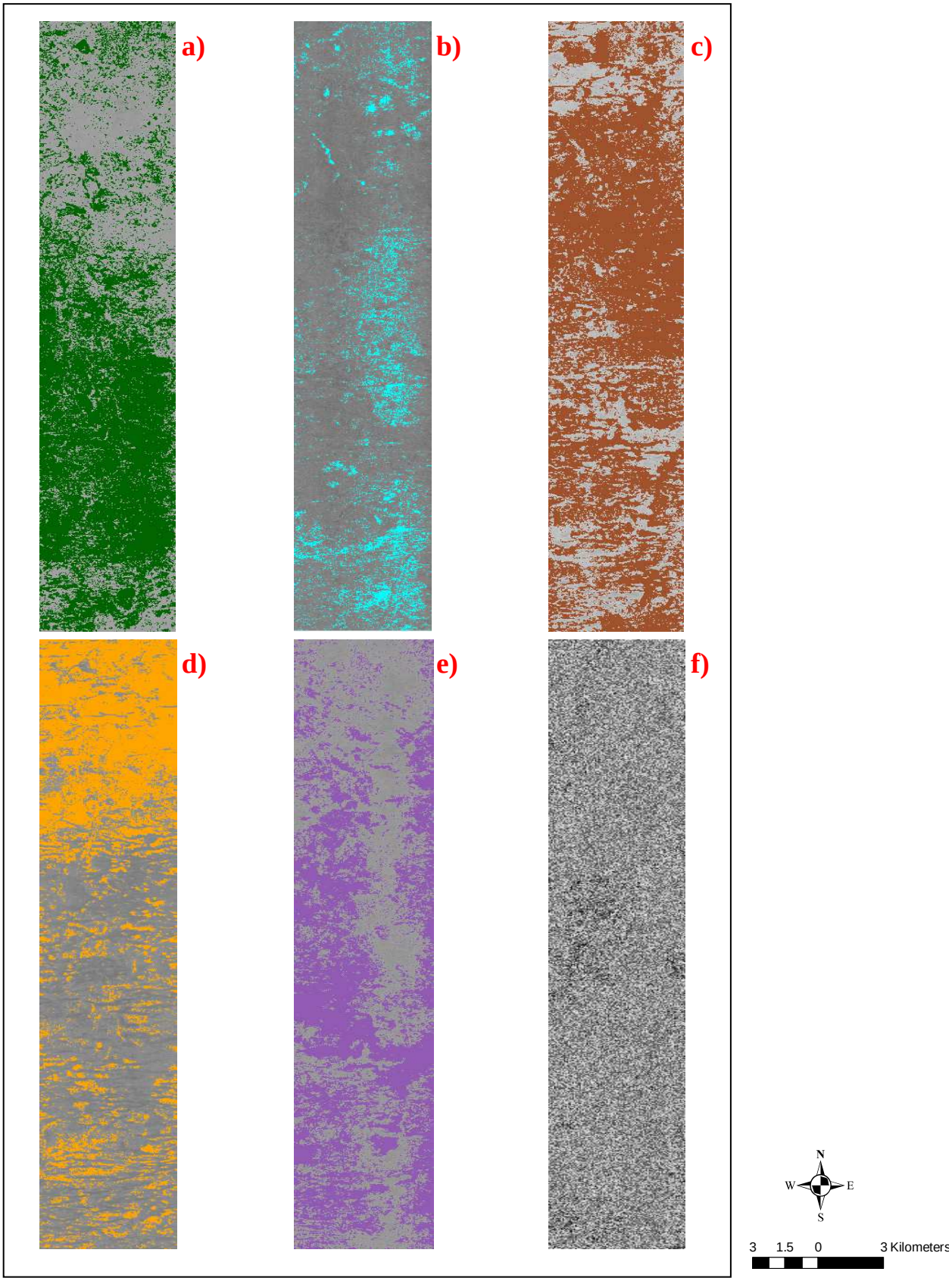

Figure 5.6 Abundance images of end-members resulted from unmixing of the Hyperion imagery: a) Photosynthetic vegetation (PVg), b) Photosynthetic vegetation (PVc), c) sandy soil, d) sandy-loam soil, e) gravel and stone, f) error image. High abundance areas shown as colour masks superimposed on a grey-scale image.

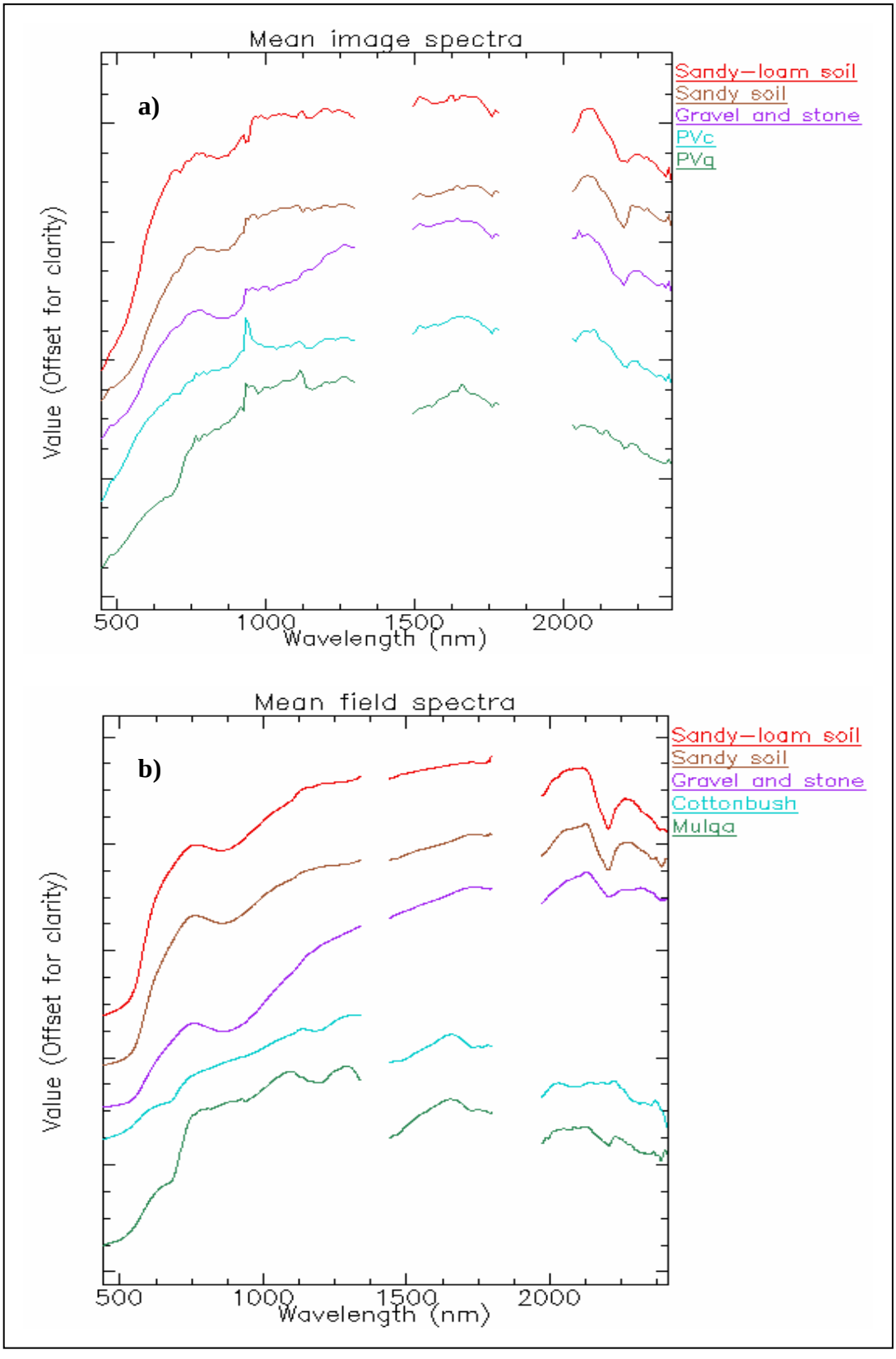

Figure 5.7 Mean reflectance spectra: a) Hyperion image spectra, b) field spectra. Noisy reflectances across water absorption bands (1400 and 1900 nm) have been removed.

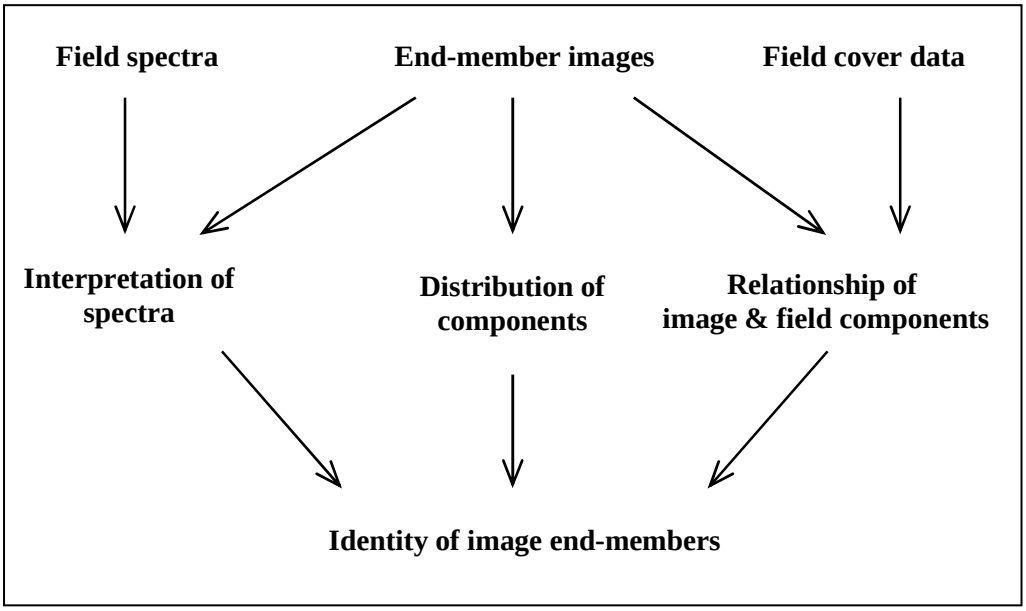

Figure 5.8 Flowchart of steps involved in end-member identification

The first end-member, photosynthetic vegetation (PVg), seems to be associated with a variety of green and grey-green vegetation, with the image spectrum quite similar to field spectra for mulga (*Acacia aneura)*, a dominant plant in the study area. As can be seen from Figure 5.7, both field and image spectra of mulga have significant absorption features at 680 nm caused by the chlorophyll in the leaves, although they also display a clear absorption feature at 2200 nm, most likely attributed to the background soil. Water absorption features were also observed in both field and image spectra at 972-983 nm and 1134-1164 nm. The green and grey green vegetation end-member image (PVg) (Figure 5.9 (a)) appeared to record the distribution of several perennial shrub vegetation types such as *Acacia ligulata* and *Acacia aneura*. It showed high vegetation cover in watercourses and on sand dunes. The PVg image showed higher vegetation cover in the southern parts of the study area compared with the north due to higher green tree cover. In the north chenopod shrublands such as saltbushes (e.g. *Atriplex vesicaria*) and bluebushes (e.g. *Maireana sedifolia*) with grey colour were dominant.

The second vegetation end-member (PVc) was associated with cottonbush (*Maireana aphylla*) that was distributed as patches throughout the study area. The PVc recorded all known patches of this species that were distributed throughout the study area (Figure 5.10 (a)). This image also showed high abundance in sand plains and dunes where dry grasses such as Woollybutt (*Eragrostis eriopoda*) were dominant. The PVc also displayed high values in areas with dense pearl bluebushes. The spectral signature of

PVc was very noisy, especially at 915-983 nm (Figure 5.7). However, there were clear absorption features around 690 nm (680 nm in the field spectra) and at 2080-2100 nm. A shallow absorption feature was also observed at 2314-2351 nm. The absorptions at 2080-2100 nm and 2314-2351 nm correspond to those for starch and cellulose absorption and lignin, cellulose, oil and waxes respectively, suggesting that this end-member has mapped dry grass or non-photosynthetic vegetation and possibly woody chenopod shrubs with high levels of oil, wax, cellulose, and lignin in their canopies (Lewis *et al.*, 2001). Like the PVg end-member, this end-member showed significant absorption at 1134-1164 nm, but the 972-983 nm feature was dominated by noise.

One of the image components mapped the sandy soils in the sandy plains and dunes (Figure 5.11 (a)). This component has been successfully separated from others due to its high albedo. The image spectrum showed similar form and spectral features to the field spectra for sandy soil (Figure 5.7). Both had deep absorption features at 2200 nm that shows these soils have high level of clay minerals. They also showed significant absorption at 870 nm due to high iron oxide concentration.

The second soil end-member recorded bare and eroded regions of the study area (Figure 5.11 (b)). This end-member had a spectrum very similar in form and absorption features to the image spectrum of sandy soil. It appears to have mapped areas with little or no vegetation cover. As this end-member and also the sandy soil end-member both recorded the exposed soils of the study area, they were combined into one soil image and then the combined image was used to examine its relationship with the field estimates of soil cover component. This combined soil image also was combined with the gravel and stone end-member image to evaluate its relationship with the field estimate of total physical components.

The final physical image component mapped black and brown gravels and stones that are distributed in some parts of the study area, especially in the centre (Figure 5.12). This end-member appears to overestimate the amount of surface gravel and stone in the centre of the image, corresponding to areas with dense vegetation cover. The spectral response of the image end-member was similar to field spectra with a distinct absorption feature at 870 nm and shallow absorption at 500 nm due to the concentration of iron oxide. It also showed a significant absorption feature at 2200 nm because of the clay context of the background soil underlying the gravels.

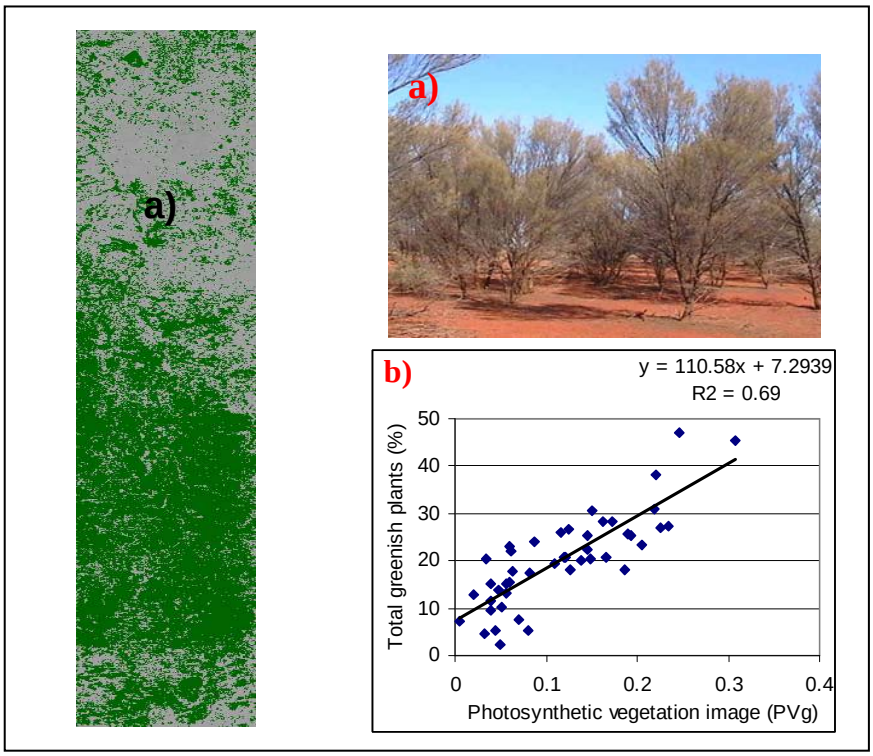

Figure 5.9 Photosynthetic vegetation image (PVg): high abundance areas shown as green mask superimposed on a grey-scale image. a) Photograph and image locations: dense mulga in watercourse; b) regression between total vegetation cover and PVg.

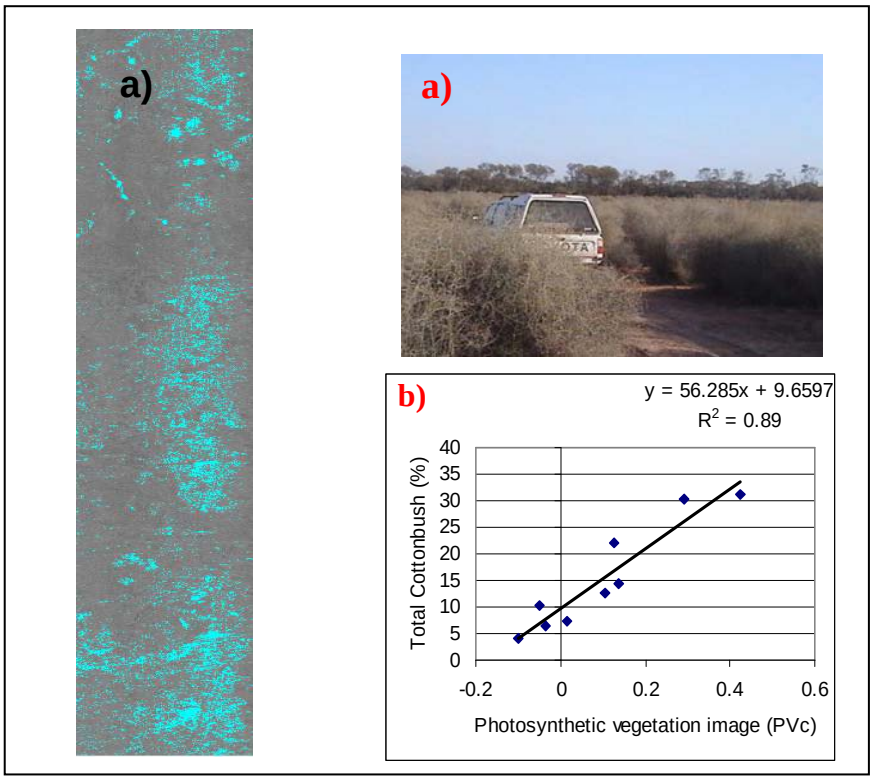

Figure 5.10 Photosynthetic vegetation image (PVc): high abundance areas shown as cyan mask superimposed on a grey-scale image. a) Photograph and image locations: dense cottonbush in watercourse surrounded with mulga; b) regression between total cottonbush cover and PVc.

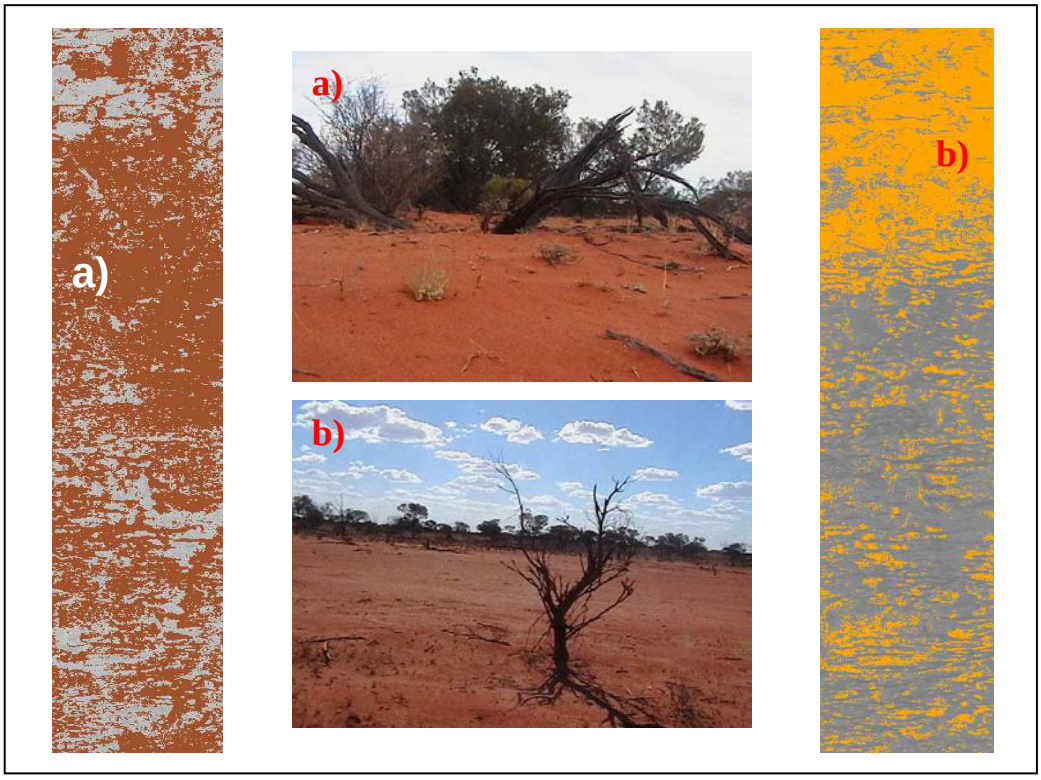

Figure 5.11 Sandy soil and sandy-loam soil abundance images: high abundance areas shown as brown and yellow masks superimposed on a grey-scale image. Photographs and image locations: a) sandy soils (sand plains and dunes); b) exposed soil.

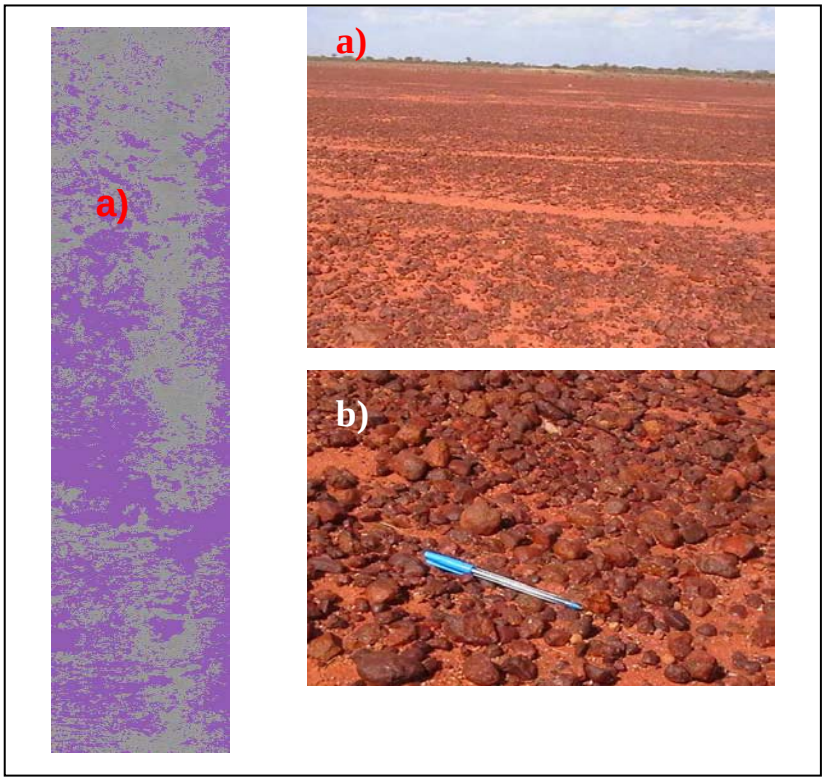

Figure 5.12 Gravel and stone abundance image: high abundance areas shown as green mask superimposed on a grey-scale image. Photographs and image locations: a) area with dense gravel and stone; b) close-up of the gravels and stones.

5.3.2 Relationships between abundance images and field cover components

Relationships between end-member abundance images and field cover components showed several significant correlations that helped confirm the identity of the image spectral components (Table 5.2). The regressions of image components against vegetation cover data have been presented in Figure 5.9 (b) and 5.10 (b). The strongest correlation was found between the image component PVc and field estimates of cottonbush (R^2=0.89), followed by the PVg image end-member with field estimates of greenish perennial plants plus grasses and herbs (R^2=0.69) and greenish perennial plants (R^2=0.58). The PVc also showed some correlation with total cover of bluish perennial plants (e.g. bluebushes and saltbushes) plus litter (e.g. dry grasses and dead shrubs) (R^2=0.23). The weakest relationship was found between PVg and the integration of total greenish cover plus litter and lichen. The combination of PVg and PVc correlated significantly with total photosynthetic vegetation (R^2=0.32) but not as strongly as their individual relationships with greenish and cottonbush vegetation components. Although image visual inspection, mean field spectra and field checks revealed that soil and surface gravel and stone appeared to map corresponding field components, the correlations between these end-members and quantitative measurements of their abundance were not strong. The combination of these image physical components, however, showed better correlation with total field physical components (R2=0.28).

5.4 Discussion and conclusions

The low spectral resolution of multispectral satellite imagery limits its suitability for extracting information in arid environments with sparse vegetation cover. The higher spectral resolution of hyperspectral imagery may improve discrimination of different components especially various vegetation types, even with low cover. This component of the research evaluated the potential of Hyperion hyperspectral imagery to map vegetation and soil components through spectral mixture analysis. Five distinct end-members were produced using this method, including green and grey green photosynthetic vegetation (PVg), cottonbush photosynthetic vegetation (PVc), sandy soil, sandy-loam soil and gravel and stone. To identify the end-members, their image spectral responses were compared with field spectra. Results showed that the image end-members were very similar to field spectra and corresponded to selected components on the ground.

Table 5.2 Relationships between abundance images and field cover

Abundance image	**Field component**	**R^2**	**P-value**	**Sample size**
Photosynthetic vegetation (PVg)	greenish perennial plants	0.58	<0.001	45
Photosynthetic vegetation (PVg)	greenish perennial plants+grass and herbs (total greenish plants)	0.69	<0.001	45
Photosynthetic vegetation (PVg)	greenish perennial plants+grass and herbs + litter and lichen	0.07	0.078	45
Cottonbush photosynthetic vegetation (PVc)	cottonbush	0.89	<0.001	9
Cottonbush photosynthetic vegetation (PVc)	bluish perennial plants+litter	0.23	<0.001	45
PVg+PVc	total photosynthetic vegetation	0.32	<0.001	45
Sandy soil+sandy-loam soil	bare soil	0.21	0.001	45
Gravel and stone	gravel and stone	0.11	0.027	45
Image physical components	field physical components	0.28	<0.001	45

In addition to the soil end-members, the two vegetation end-members also had clear clay absorption features around 2200 nm. This indicates that none of the vegetation end-members were “pure” and that soil has had a detectable influence on their image spectral responses. This might be expected since plant cover in the region was generally less than 30%: end-members derived from Hyperion imagery with 900 m^2 ground resolution will inevitably comprise mixes of cover types. The strong absorption feature at 2200 nm in the soil end-members shows that the soil of the region contains high levels of clay minerals.

The absorption features of the vegetation end-members showed they belonged to different vegetation types in the study area. Although both had clear chlorophyll absorption around 680 nm, this was much stronger in the PVg than PVc. The PVg mapped all the greenish vegetation cover with strong chlorophyll absorption. The high correlation between this end-member and field estimates of total greenish plants (perennials combined with grass and herbs) (R^2=0.69) and its very poor correlation with the aggregation of total greenish cover with litter and lichen (R^2=0.07) revealed that the PVg has only mapped the green and grey green photosynthetic vegetation cover. In contrast with PVg, the PVc showed not only a clear absorption feature around 680 nm

but also shallow absorptions at 2100 nm and 2314-2351 nm. It mapped all cottonbush vegetation cover of the study area with a strong correlation with the field estimates of this component (R^2=0.89). The lower correlation between this end-member and field estimates of total bluish perennial plants plus litter (R^2=0.23) revealed that this end-member may have also mapped other cover components such as chenopod shrubs and non-photosynthetic vegetation cover.

Image physical components including soil and surface gravel and stone that were dominant components in the study area, comprising more than 70% of the land cover, had much clearer absorption features than the vegetation end-members. The spectral similarity between these end-members and field spectra and their distribution in the images revealed that they mapped sand plains, sand dunes, eroded areas, and gravel and stone in the region. However, their relationships with the field estimates of physical components on the ground were not strong. The combined image of physical components accounted for 28% of variation in the ground physical components. It seems that one of the main reasons for these low relationships relates to the different percentages of soil cover that have been recorded by the field measurements and Hyperion sensor: the step-point method used in this study was able to measure very low vegetation cover, for example less than 5%, within the Hyperion sensor's field of view (900 m^2), whereas the sensor may not be able to record this amount of vegetation cover due to high reflectance of soil background. The amount of soil actually recorded by field measurements in sparsely vegetated areas was lower compared with the sensor response and this might have influenced the statistical relationships.

Despite the high spectral resolution of the Hyperion scene, it was not possible to identify more than five meaningful spectral end-members in this arid environment. The number of end-members extracted here was similar to other studies in arid environments (Smith *et al.*, 1990; Lewis, 1999) that used full set of scene spectra from Landsat multispectral imagery. This similarity in the number of end-members suggests that arid landscapes are dominated with few spectral components (usually three soil or rock and two vegetation components) and using imagery with low spatial and high spectral resolution may not produce more land surface components than multispectral imagery. Previous studies (e.g. Okin *et al.*, 2001) conducted in arid environments with low vegetation cover (less than 30%) have also reported that the discrimination of different vegetation types is limited with hyperspectral imagery, even with high spatial

resolution. This may be the result of low vegetation cover of arid regions, the lack of spectral contrast between different arid vegetation types and soil background effects.

The validation of end-members against field spectra and field cover data showed that the end-members corresponded to real vegetation components and soil types on the ground. Where image end-members provide quantitative estimates about the distribution of specific vegetation and soil components they can be used as appropriate metrics in land management in the region. For example, in a study in Utah, a vegetation end-member derived from spectral mixture analysis has been successfully used to assess land degradation around stock watering points (Harris and Asner, 2003). Image-derived end-members such as those mapped in this study have potential as metrics for land condition assessment and monitoring. For example, initial inspections showed that the PVg and soil end-members had low and high values near stock watering points, respectively.

Although the spectral mixture analysis extracted vegetation end-members such as green and grey green vegetation and cottonbush from the Hyperion image, no meaningful end-member was identified to show chenopod shrublands such as saltbushes and bluebushes that are major vegetation types in the study area and have an important role in land management. In addition to the low spectral contrast between vegetation types and soil background effects, one of the reasons that it was not possible to extract more vegetation components may relate to the high level of noise in this image, especially around the 915-983 nm regions. To date, no study has discriminated these kinds of vegetation types using satellite multispectral and hyperspectral imagery. A study that was conducted by Lewis (2000) in an arid environment in New South Wales, Australia showed chenopod shrubs can be discriminated using airborne imagery with high spectral and spatial resolution. It appears that high spatial resolution and also high image quality, because of less atmospheric effects, of airborne imagery are the main reasons for this separation (Harris and Asner, 2003). Despite the potential of airborne hyperspectral imagery for detecting and mapping chenopod shrubs, applying this kind of imagery to arid environments with their extensive areas is expensive and is likely only to be suitable for pilot studies. Therefore, more research is needed to focus on the application of other imagery such as MODIS that are cheap and cover broad areas and have advanced spectral resolution.

6 LAND DEGRADATION ASSESSMENT WITH REMOTELY-SENSED HETEROGENEITY INDEX

6.1 Introduction

Vegetation disturbance is one of the principal degradation processes in arid and semi-arid lands of Australia (Chapter 1). It occurs mostly due to grazing, which is the main land use in these regions. To assist management of extensive arid lands, they have been fenced into paddocks extending from few to hundreds of square kilometres. Depending on the paddock size, one or more artificial watering points provide a source of drinking water for domestic stock, although they are used also by feral and native animals. As a result the watering points provide a focus for animals that lead to localised land degradation. Land degradation that has resulted from high grazing pressure can be seen easily around the watering points in arid and semi-arid regions, both in Australia and internationally (Andrew and Lange, 1986a; Andrew and Lange, 1986b; James *et al.*, 1999; Brits *et al.*, 2002; Heshmatti *et al.*, 2002; Harris and Asner, 2003; Nash *et al.*, 2003; Nangula and Oba, 2004). In this zone, also called the piosphere or sacrifice area (Lange, 1969), grazing changes the distribution, quality and abundance of soil particles and vegetation (Friedel *et al.*, 2003; Tongway *et al.*, 2003).

Previous studies have shown that degraded landscapes or regions in Australian arid lands, especially around watering points, are more spatially homogeneous in cover than non-degraded areas (e.g. Holm *et al.*, 2003b). The reduction in spatial heterogeneity is thought to occur as grazing reduces vegetative patches and causes changes in the soil surface, leading to more homogeneous landscapes. Tanser and Palmer (1999) used a satellite-derived diversity index called the Moving Standard Deviation Index (MSDI) to assess rangeland degradation in South Africa. In contrast to the Australian field studies, they found, however, that degraded areas were more heterogeneous in surface reflectance than non-degraded areas. Guo *et al*. (2004) found also that grazed prairie grasslands in North America had higher spectral variations than conserved regions. In contrast to these findings, a study by Fabricius *et al*. (2002) in the rangelands of South Africa showed that degraded areas were more homogeneous than non-degraded areas, which is similar to the findings of Australian field studies. They found that the coefficients of variation (CV) of image pixels in disturbed areas were smaller than in undisturbed areas.

Remote sensing has been successfully used in land degradation assessment and monitoring (Robinove *et al.*, 1981; Pickup and Nelson, 1984; Pickup and Chewings, 1988; Bastin *et al.*, 1993a; Pickup and Chewings, 1994; Bastin *et al.*, 1998; Harris and Asner, 2003; Geerken and Ilaiwi, 2004; Symeonakis and Drake, 2004; Wessels *et al.*, 2004; Wessels *et al.*, 2007). In most instances the evaluation of land condition has been based on the spectral reflectance of vegetation cover using multispectral vegetation indices (Chapter 3). As an alternative to vegetation indices, spatial heterogeneity in land surface reflectance has potential for assessment of landscape condition and land degradation. In contrast to vegetation indices, MSDI as suggested by Tanser and Palmer (1999), does not rely on the spectral characteristics of vegetation cover and it is calculated simply from the variance of surface reflectance in a moving window across the imagery. Because of this simplicity, MSDI may provide useful information for the assessment of broad areas. MSDI uses image texture or spatial heterogeneity in land cover to assess land condition. Image texture, as an important spatial feature, has been used as a useful tool in other applications. For example, Fabbri *et al.*, (1989) used image texture for exploring and assessing mineral resources, while He and Wang (1990) evaluated different image texture methods for image classification.

This component of the current study investigates whether landscape spatial heterogeneity as recorded by Landsat multispectral imagery can be used to assess land degradation in southern arid lands of South Australia. The first aim was to evaluate spatial heterogeneity status within selected piospheres and nearby reference areas that have minimal grazing impact. In southern Australian arid lands, high grazing pressure generally reduces biodiversity and landscape pattern: this part of the study aimed to evaluate if this leads to findings different from those of Tanser and Palmer (1999). The second aim was to assess the spatial scale of variability around watering points by investigating spatial heterogeneity with increasing distance from watering points. As grazing pressure decreases with distance from watering points, a gradient of change in MSDI is expected. To evaluate the performance of MSDI, two widely used vegetation indices (PD54 and NDVI) were used as reference indices for comparison.

6.2 Methods

6.2.1 Study area

This part of the study was conducted in the same region as that described Chapter 2. This section focussed on four land systems; Coondambo, Yudnapinna, Kolendo and Arcoona, chosen because they were extensive and included reference sites that were not close to salt lakes or roads (Figure 6.1). This excluded the edge effect of these features in the calculation of the MSDI. A summary description of these land systems is given in Table 6.1.

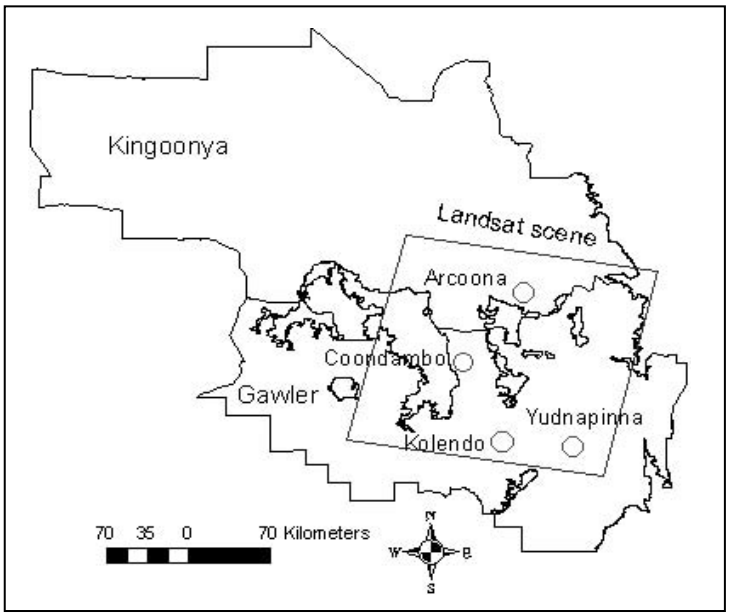

Figure 6.1 Location of study area within the Kingoonya and Gawler Soil Conservation Districts. Shown also are Coondambo, Yudnapinna, Kolendo and Arcoona land systems which were used for land-system scale analysis.

Grazing-induced piospheres are common in the region, with pronounced degradation within 500 m of stock watering points (James *et al.*, 1999; Kinloch *et al.*, 2000), extending up to 1500 m away from water (Department of Water Land Biodiversity and Conservation, 2002) (Figure 6.2). To assist assessment of land degradation, reference sites had been established by the SA pastoral land management authority as benchmark sites for comparison with grazed areas of the same land unit. The reference sites are located far from watering points (approximately 5 km in sheep grazing country) to ensure that grazing domestic stock can not reach them (Fleming *et al.*, 2002). The carrying capacity of the area has been considered to be 5.5 to 11.6 sheep/km^2 (Tynan, 1995; Kingoonya Soil Conservation Board, 1991).

Table 6.1 A brief description of land systems in the study area (Pastoral Board, 2002)

NOTE: This figure is included on page 91 of the print copy of the thesis held in the University of Adelaide Library.

Figure 6.2 Examples of piospheres in the region

6.2.2 Satellite imagery

This component of the research used the January 1991 Landsat TM image from path 99, row 82. The Moving Standard Deviation Index (MSDI) was calculated by passing a 3×3 filter across the image red band (band 3), replacing the moving centre pixel with the standard deviation for any nine pixel window (Tanser and Palmer, 1999). The TM band 3 was used, as did Tanser and Palmer (1999), because compared with other TM bands it displayed a greater range of standard deviation values around watering points (degraded areas) and within reference areas (non-degraded areas). Other studies have shown,

furthermore, that the red band provides more information about spectral contrasts in soil and vegetation cover than other Landsat spectral bands in arid and semi-arid environments (Pilon *et al.*, 1988; Chavez and Mackinnon, 1994). For comparison with MSDI I used the NDVI (Rouse *et al.*, 1974) and PD54 (Pickup *et al.*, 1993) vegetation indices. The PD54 was calculated using Landsat TM band 2 (green) and band 3 (red) (Bastin *et al.*, 1999). A mean 3×3 filter was applied to the PD54 and NDVI to transform data into the same filter size as the MSDI.

6.2.3 Analysis

Watering points and reference sites were used to compare degraded and non-degraded areas, respectively. A reference site and its nearest ten water points in each land system were located on the MSDI, PD54 and NDVI images. The mean MSDI, NDVI and PD54 values were extracted within a 500 m radius buffer around each watering point and the centre of associated reference sites. Fence lines were used to limit the extraction of data within the paddocks. An independent samples t-test was used to test for significant differences between the mean index values for degraded and non-degraded sites. In order to examine changes in the MSDI, PD54 and NDVI values with increasing distances from water points a series of buffers at 50 m intervals ranging from 50 m to 1500 m from the water points was used (Figure 6.3). The buffers formed concentric rings with widths of 50 m.

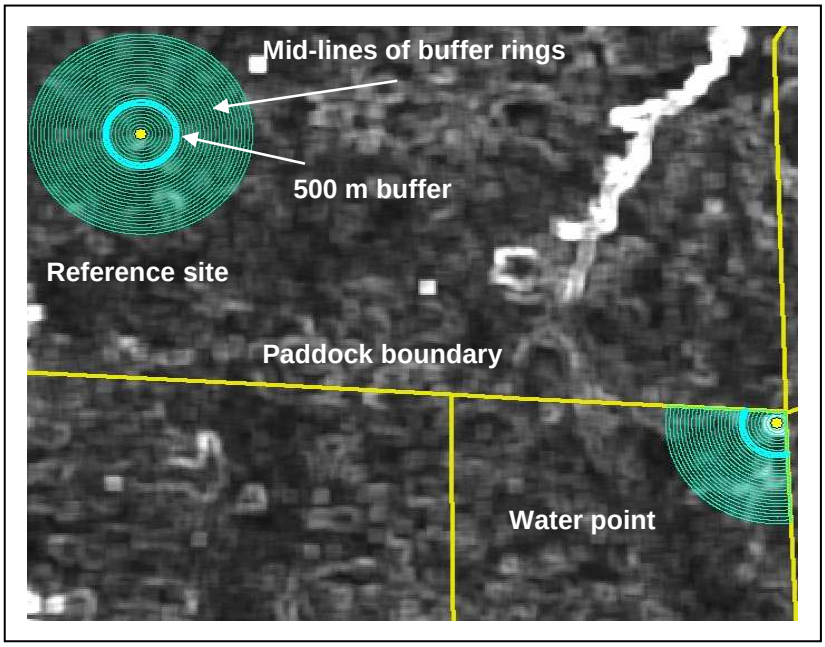

Figure 6.3 The extraction of the MSDI values at a water point and reference site within the Coondambo land system

6.3 Results

6.3.1 Comparison of degraded and non-degraded areas

The mean values of MSDI, PD54 and NDVI within 500 m radius samples of the reference sites and their ten nearest water points in four different land systems are given in Figure 6.4. All degraded sites had higher mean MSDI and generally lower vegetation index values (PD54 and NDVI) than non-degraded areas in the four land systems (Table 6.2). Although all the watering points had the highest and reference sites had lowest MSDI values, these values differed amongst land systems. Coondambo showed the highest MSDI for both watering points and the reference site, followed by Arcoona and Yudnapinna. Watering points and the reference site in Kolendo land system had the lowest MSDI values. In addition, the magnitude of difference between MSDI for degraded and non-degraded areas varied among the land systems. Arcoona showed the highest difference (1.2), followed by Kolendo land system (0.9). The differences in Coondambo and Yudnapinna were similar (0.7). These differences in the MSDI values within and between land systems may result from their different vegetation and land surface characteristics (Table 6.1). For example, the high MSDI for both watering points and the reference site in Coondambo may result from the high contrast between the dominant vegetation types (mulga and myall trees) and the sandy and calcareous soils in this land system.

The NDVI showed different results in the various land systems. There were significant differences ($p<0.001$) between the watering points and reference site in Kolendo land system but these differences were not as strong in Arcoona and Coondambo land systems ($p<0.05$). There was no significant difference in the Yudnapinna land system ($p=0.53$). One of the main reasons for these differences was different vegetation types in different land systems (Table 6.1). The NDVI performs well in land systems with more green plant cover (e.g. woodlands) compared with shrublands (e.g. saltbushes and bluebushes) with grey colour and low near-infrared reflectance (Graetz and Gentle, 1982). In addition, the reference site in Yudnapinna land system was closer to water points than those in other land systems and it appeared to be grazed more than other reference sites. As a result, there was less difference in plant cover between water points and the reference site which the NDVI was not able to capture.

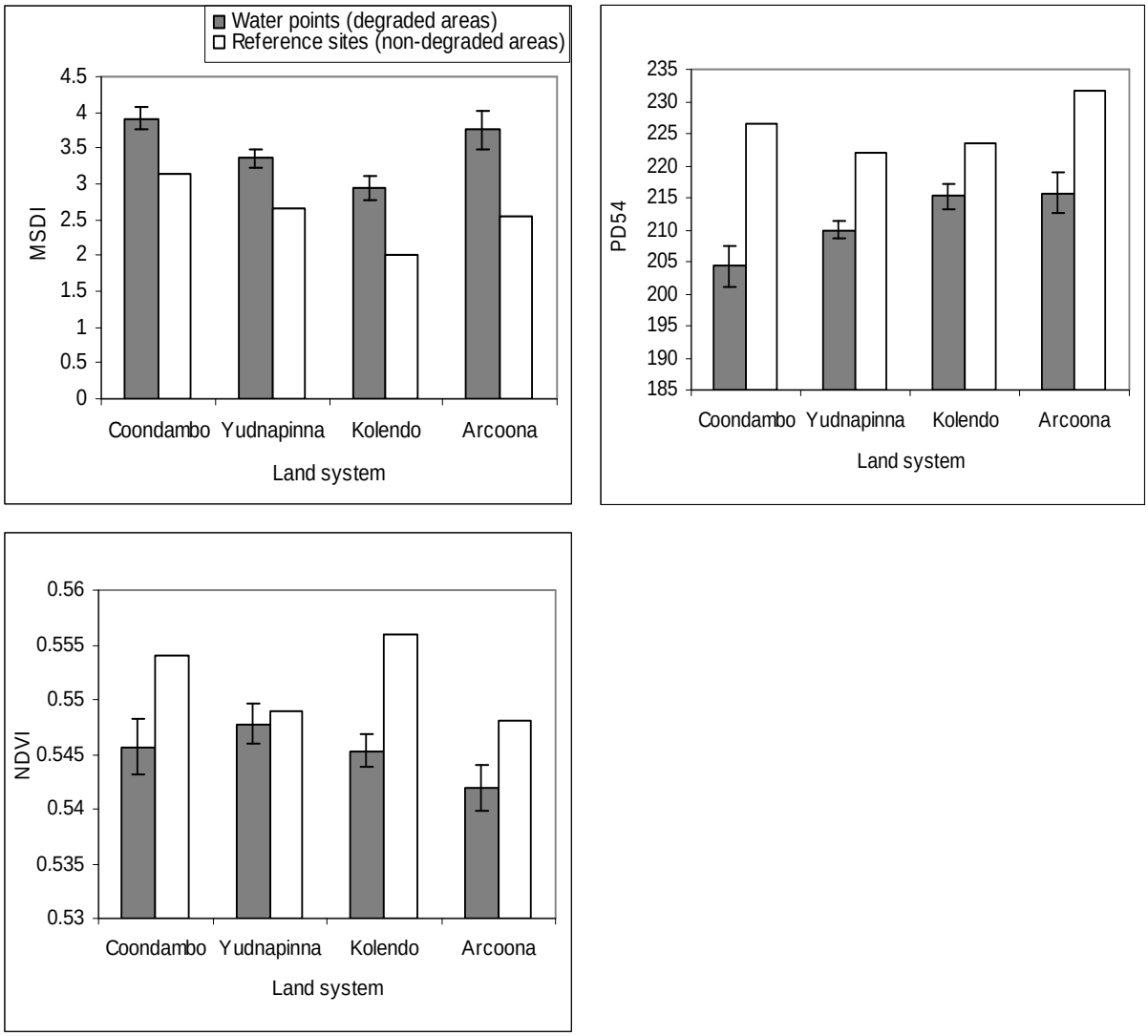

Figure 6.4 Means and standard errors of MSDI, PD54 and NDVI values for ten water points compared with the associated reference site in different land systems

The relative performance of the different indices across all land systems is presented in Table 6.2. The t-statistic is estimated on the difference between mean values for the ten degraded sites and the single reference site relative to the standard deviation of the sample differences. As the same number of sites (n=10) is used, the t-values are directly comparable. Assuming that the main systematic difference between areas around watering points and the adjacent reference areas is degradation through grazing, the t-values are indicators of how well the image indices depict degradation. With the exception of Kolendo, PD54 had the highest t-values. The NDVI did not provide consistent performance, having very variable and low t-values. The MSDI was very consistent, with t-values ranging from 4.4 – 5.9, but the PD54 generally outperformed the MSDI as a land condition indicator.

Table 6.2 Comparison of spectral indices between watering points and reference sites in different land systems. The mean and standard deviation of the degraded conditions is based on the ten nearest watering points around the reference area.

		Land condition				
		Degraded		Non-degraded	T-statistic	P-value
Land system	**Image indices**	Mean	StDev	Mean		
Coondambo	MSDI	3.9	0.5	3.2	4.8	< 0.001
	PD54	204	9.8	227	-7.19	< 0.001
	NDVI	0.545	0.008	0.554	-3.2	0.011
Yudnapinna	MSDI	3.4	0.37	2.7	5.9	< 0.001
	PD54	210	4.5	222	-8.6	< 0.001
	NDVI	0.547	0.005	0.549	-0.65	0.532
Kolendo	MSDI	2.9	0.6	2.0	5.3	< 0.001
	PD54	215	6.0	223	-4.4	< 0.001
	NDVI	0.545	0.004	0.556	-7.0	<0.001
Arcoona	MSDI	3.8	0.9	2.6	4.4	< 0.001
	PD54	215	10.0	231	-5.00	< 0.001
	NDVI	0.541	0.006	0.548	-2.9	<0.018

6.3.2 Trends with distance to water point

Livestock grazing is more intensive near the water points and decreases with distance. Hence distance can be used as a surrogate for intensity of grazing pressure and land degradation. This means that image indices of degradation should show similar trends away from watering points. To examine in more detail how the spectral indices change with different levels of disturbance, the nearest water point to the reference site for all land systems used in the previous section was selected. Using the nearest water point has the advantage that soil, vegetation and land form are most similar to the undisturbed areas for comparison. The means of MSDI, PD54 and NDVI with distance from water points are shown in Figure 6.5 (a-c). All indices showed an effect of disturbance around watering points. However, the examples from different land systems showed marked differences and the performance of the different indices corroborates the previous results. MSDI and PD54 showed clear and consistent changes but NDVI showed only little gradual change with grazing gradients. The high MSDI values near the waterpoint in Coondambo land system may result from spectral contrast between green canopies of

mulga and western myall trees and sandy soils that were dominant features in this land system.

To quantify the change of the indices over distance from water, regression slopes were computed for MSDI, PD54 and NDVI for distance intervals of 500 m (Figure 6.5 d-f). Each point in these figures represents the change of the indices over 10 distance bands (500 m). Grazing gradients are expected to show consistent positive slopes for PD54 and NDVI and it was hypothesised that MSDI would exhibit the opposite trend, namely a decrease along grazing gradients. Most obvious is the clear depiction of grazing gradients in all land systems for the PD54 index. Slope remained positive for distances up to the interval of 950-1400 m for all but the Yudnapinna land system, where no increase in PD54 was detectable above the interval 250-700 m. NDVI, in contrast, only showed increase along the grazing gradient for Coondambo and Kolendo. In Arcoona and Yudnapinna land systems, NDVI decreased away from watering points, hence showing a very limited detection of grazing gradients. MSDI consistently decreased up to the interval of 1050-1500 m for Arcoona, 650-1100 m for Kolendo, 550-1000 m for Yudnapinna and 350-800 m for Coondambo.

6.3.3 Relationships between MSDI diversity index and PD54 vegetation index

The scatterplot of MSDI and PD54 shows clear trajectories away from watering points (Figure 6.6). This further demonstrates a high level of consistency between the two indices. For all but the Coondambo land system the trajectory terminates in a cluster of points, indicating that grazing gradients are limited to the 1500 m radius. For Yudnapinna, MDSI appears to detect a gradual difference away from the watering point, which PD54 does not reveal. The phase diagram representation also suggests the ability of MDSI and PD54 together to clearly separate the different land systems. Reference sites form distinct clusters, as do the tails of the trajectories. Also evident from this representation of the data is that final clusters of the trajectory generally do not end in the reference site cluster. This indicates a high spatial variability of reflectance in the region. It also suggests that even the far points of paddocks, where grazing intensity is least still show a difference in spatial heterogeneity from the undisturbed reference sites. However, both indices show a marked similarity of their response along a grazing gradient independent of large background variability.

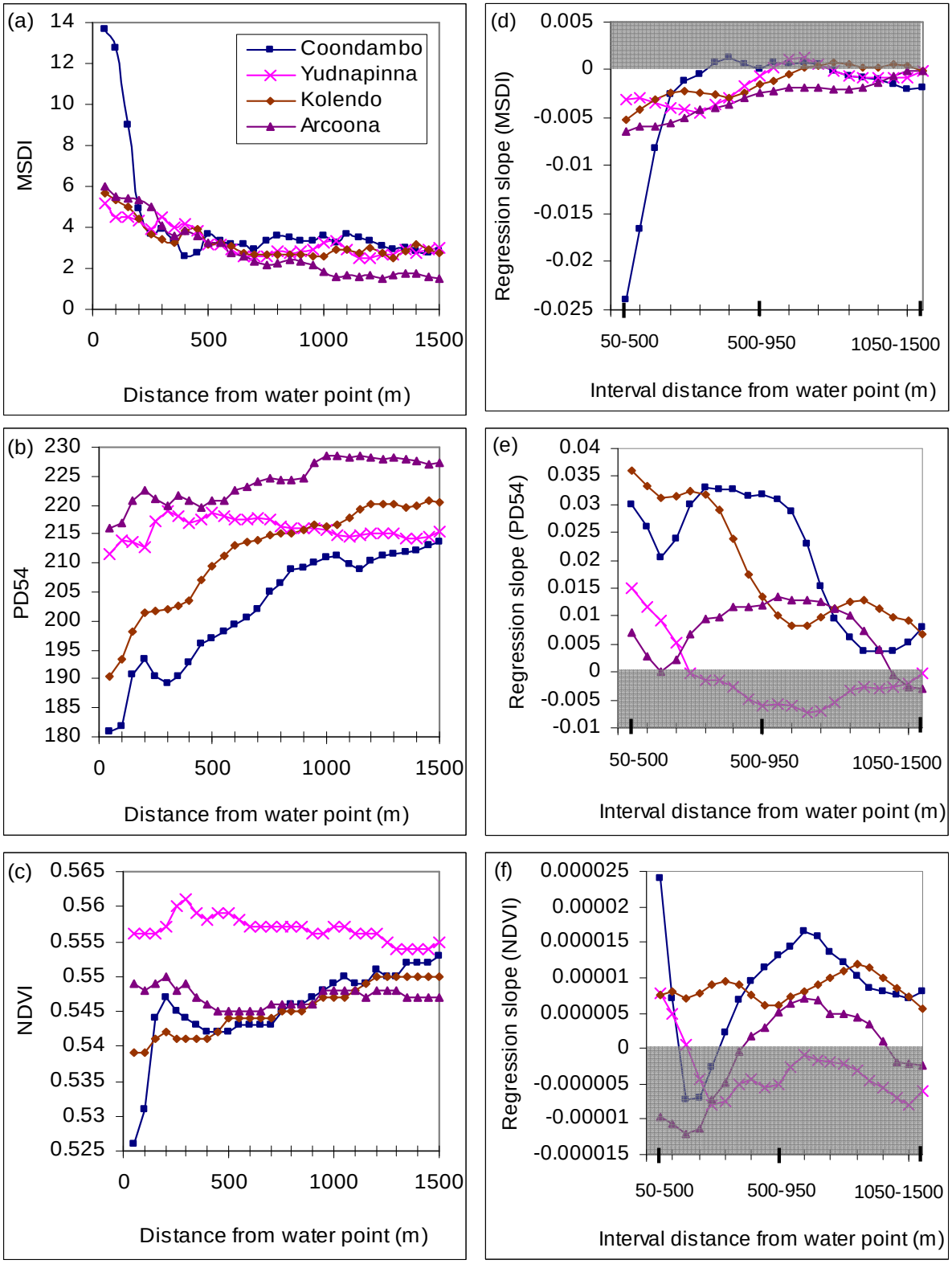

Figure 6.5 Mean and regression slopes of MSDI, PD54 and NDVI with distance from water points in different land systems. The slopes were computed using a linear regression of image indices over distance for a 500 m moving interval. Positive slopes for PD54 and NDVI and negative slopes for MSDI indicate that the image indices are able to correctly detect grazing gradients (shaded grey).

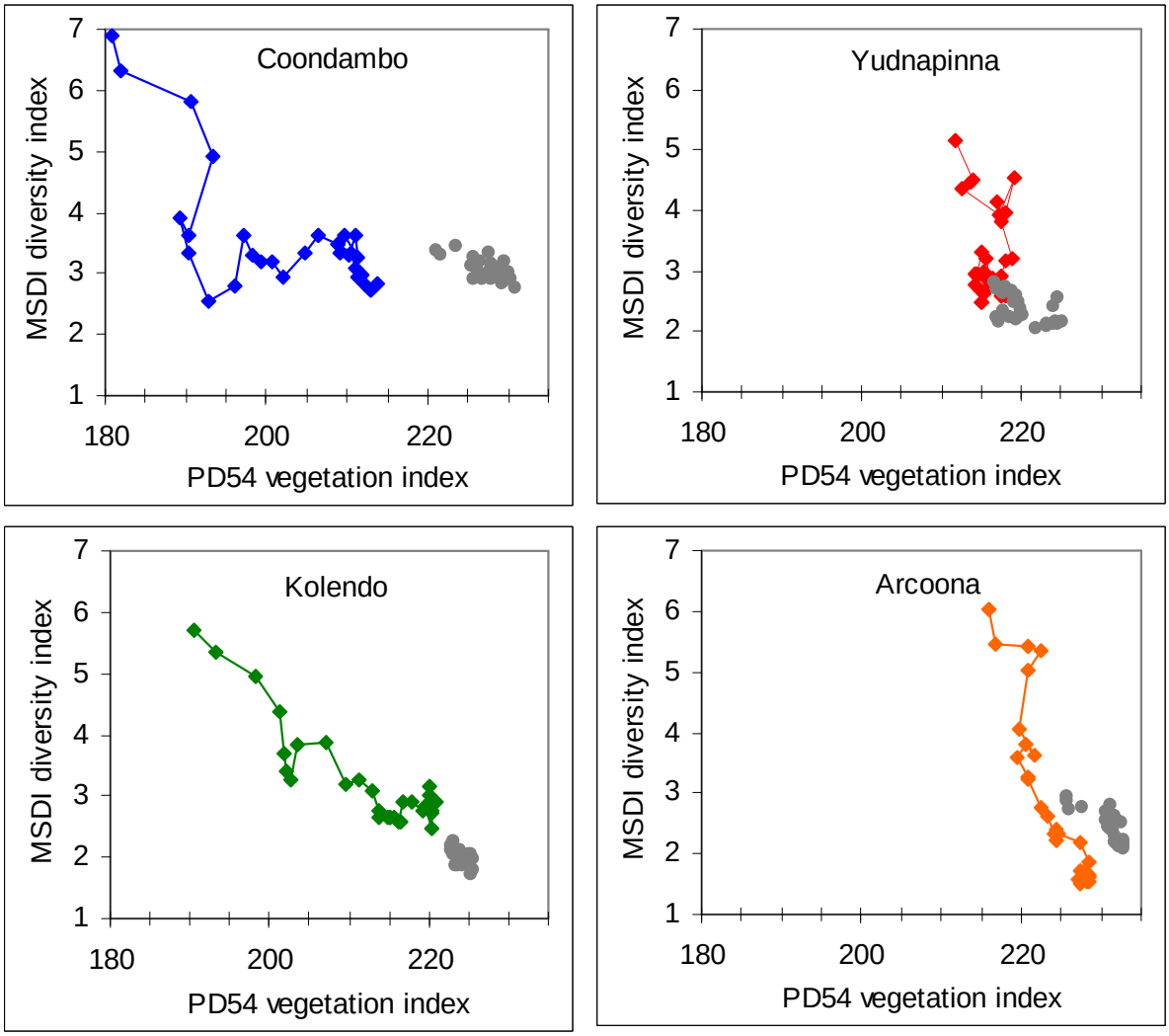

Figure 6.6 The scatter plot of MSDI versus PD54 at different distances from water points and reference sites (50 m interval up to 1500 m) in different land systems. Grey points indicate values for pixels within reference sites in each land system.

6.4 Discussion and conclusions

The effect of degradation is usually more apparent in the piospheres than in areas far from the water points. The results of this study showed that these grazing gradients are detectable using satellite image indices. MSDI showed significantly higher values around the water points compared with the reference sites. Piospheres were thus found to be more heterogeneous in surface reflectance than comparable non-degraded reference areas.

High spatial heterogeneity near stock watering points can result from various factors. Because of the high concentration of animals in these regions, soil condition changes dramatically and this directly influences surface reflectance characteristics. Usually soil compaction, sheep tracks and dung deposition are greater close to water than in areas far

away from water, or in reference areas (Andrew and Lange, 1986a). As a result these regions have higher variation in the soil surface reflectance. In addition to changes in the soil surface, alteration in vegetation cover and composition near watering points is another factor that may add to the reflectance variation. Vegetation in piospheres is often a combination of overgrazed, less-grazed and dead trees and shrubs or litter, and consequently has different reflectance from less-severely grazed or healthy vegetation far from water.

According to previous studies (e.g. Holm *et al*., 2003b) vegetation patchiness in piospheres decreases due to high grazing pressure and potentially this makes degraded regions more homogeneous in appearance than non-degraded areas. Because of the high concentration of animals in piospheres and along preferred paths, however, soil and vegetation diversity are spectrally and spatially more variable than non-degraded or reference areas. This variability decreases gradually with distance from high impact areas.

Detection of variability around watering points depends strongly on the spatial resolution of the imagery and the size of the analysis window. One of the limitations of MSDI, as mentioned by Tanser and Palmer (1999), is that this index can not estimate degradation in an area less than 8100 m^2 due to the filter size (3×3) applied to the Landsat TM imagery with 30 m ground resolution. A high variability is evident if the piosphere is denuded and if the radius of the MSDI window is large enough to include relatively undisturbed, vegetated pixels with different reflectance characteristics. This index is sensitive also to the edges of natural features as well as any disturbance in the landscape. High MSDI is expected at the edge of rivers, salt lakes and any man-made features such as roads.

The PD54 and NDVI vegetation indices that were used as reference indices for comparison with MSDI showed different results. PD54 performed better for all the land systems in the study area and this confirms that this index is more appropriate than NDVI for assessing and monitoring land condition in this arid environment. PD54 had the most consistent differences between degraded and non-degraded areas across the land systems and this confirmed that it can be used as a good indicator of land degradation. This study supports the findings of Chapter 3 that the usefulness of NDVI may be reduced in perennial-dominated arid environments. Whereas the index showed

significant differences between degraded and non-degraded areas in most land systems, its performance was less consistent than PD54. In Yudnapinna, the land system which is dominated by chenopod shrublands in gilgai plains, the low near-infrared reflectance of the vegetation limited the usefulness of NDVI for detecting degradation (Graetz and Gentle, 1982).

As expected, the degradation around the stock watering points was apparent with all the indices studied, though each showed this impact differently along gradients away from water. The MSDI successfully distinguished grazing gradients around the water points. It showed decreasing values with increasing distances from the water points, though these trends were different in various paddocks and land systems due to varying vegetation and soil characteristics and grazing intensities. This index had high values in areas of low vegetation cover and it decreased with increasing vegetation cover or PD54 and NDVI values. The PD54 appeared to perform better and consistently showed an increase with distance from watering points in all land systems. However, in Yudnapinna, the expected increase was weak and limited to a narrow band. The NDVI showed no clear grazing gradient for Yudnapinna and the Arcoona land system.

Despite the good performance of PD54 in land condition assessment and monitoring in Australian perennial-dominated landscapes, it has the disadvantage of subjectivity in its calculation. Hence the relatively good performance of MSDI indicates its potential usefulness as a simple indicator of land condition. It requires less image calibration than vegetation indices and this is a very important factor in remote sensing of land condition over broad areas on a repetitive basis. This index does not depend on the multispectral response of vegetation cover but utilizes spatial pattern in land cover. This component of the study showed that spatial heterogeneity in land surface reflectance may be used as an indicator of land degradation in arid lands of South Australia which are naturally heterogeneous.

7 DISCUSSION AND CONCLUSION

The size, remoteness, and harsh condition of arid lands make it difficult and expensive to assess and monitor condition using field-based techniques. Space-based remote sensing with its broad coverage, repeatability, and cost- and time-effectiveness has been suggested and used as an appropriate tool for this purpose for more than 30 years. Sequences of remote sensing imagery can provide baseline information on vegetation cover, productivity, biomass and also soil status that have essential roles in the determination of land condition. By developing relationships between the imagery and ground measurements and converting the imagery according to the predictive relationships, the imagery allows interpolation of point-based measurements to broader areas, which means land condition could be assessed and monitored efficiently.

This study aimed to evaluate the potential of remote sensing techniques to overcome the limitations of field methods in arid land condition assessment and monitoring. The remote sensing techniques evaluated were vegetation indices, spectral mixture analysis and a landscape diversity index. These techniques were applied to multispectral and hyperspectral imagery of Kingoonya and Gawler Soil Conservation Districts in southern arid lands of South Australia.

Vegetation indices derived from Landsat multispectral imagery were used to investigate their suitability for predicting arid vegetation cover. Strong relationships between vegetation indices and field cover measurements especially at land system scale revealed these spectral indices are good predictors of vegetation cover within stratified land systems in the region (Chapter 3). The most suitable vegetation index, STVI-4, was used in Chapter 4 to monitor vegetation cover and assess land condition. Results showed the STVI-4 detected changes in vegetation cover due to seasonal conditions and management effects. STVI-4 was able also to differentiate the LCI land condition classes in low woodlands, chenopod shrublands and Mt. Eba country, but was limited in non-stratified pasture types. In Chapter 5, the spectral mixture analysis approach was applied to Hyperion hyperspectral imagery to separate vegetation cover from other soil surfaces. My specific aim was to separate vegetation types that have important role in land management. Despite the high resolution of the Hyperion image only two vegetation components were separable and the Hyperion image was unable to provide a meaningful vegetation component for chenopod shrubs that are dominant in the study

area. In contrast with vegetation indices and the spectral mixture analysis, the landscape spatial heterogeneity index depends on the spatial diversity in land cover reflectance for extracting vegetation information. The aim of using this index, derived from Landsat imagery, was to assess land degradation around stock watering points where the highest vegetation disturbance occurs (Chapter 6). This index successfully separated degraded from less degraded or reference areas and also detected grazing gradients near water points.

Following sections review the results and findings of the research for each chapter, highlight the implications of research findings for arid land assessment and monitoring and provide recommendations for future research.

7.1 Review of results and findings

7.1.1 Vegetation indices

Different groups of vegetation indices including slope-based, distance-based, orthogonal transformation, and plant-water sensitive vegetation indices were evaluated across land systems (landscape scale) and within land systems (land systems scale). It was observed generally that all vegetation indices were better predictors of vegetation cover within land systems compared with broader landscape scales.

Slope-based vegetation indices were the best indices for predicting plant cover at regional or landscape scale where 10 different land systems were aggregated. These indices accounted for up to 39% of variation in total cover, followed by plant-water sensitive and orthogonal indices. Distance-based indices did not perform well at this scale. It appeared that different soil types and colours and also different vegetation types between land systems influenced the definition of the soil line in these indices.

At land system scale, most of the vegetation indices were strongly correlated with total plant cover within the two land systems studied and explained 60-90% of the variation in the field measurements. Best indices at this scale were from the orthogonal and plant-water sensitive groups, followed by the distance-based and slope-based indices. Distance-based indices were much better predictors of cover components within the two land systems compared with regional scale because of the greater similarity in soil and vegetation types within land systems. Several distance-based indices (e.g. PD54) have

been used widely for assessing and monitoring perennial-dominated vegetation cover in arid lands of Australia (Pickup *et al.*, 1993). Results here confirmed the use of these indices within land systems rather than across broader areas. One of the limitations of the distance-based indices is, however, the need to define subjectively soil and vegetation-dominated pixels in bi-spectral space, which may lead to inconsistent results in monitoring applications.

Among the vegetation indices evaluated in this study, stress-related indices (e.g. STVI-4) performed best in terms of consistency at both landscape and land system scales. These indices had high to very high correlations with vegetation cover components. Stress-related indices best predicted combined perennial and ephemeral plants, followed by perennial plants at land system and total ground cover at landscape scale. In addition to the lower sensitivity of these indices to the spectral variation in soil and vegetation, they are calculated using arithmetic combination of Landsat image bands, thus are more objective than distance-based indices and can be used in assessment and monitoring vegetation cover, consequently land condition, across broad areas.

Stress-related vegetation indices, designed originally for agricultural applications, have been shown to be better predictors of stressed crops than slope-based vegetation indices (Thenkabail *et al.*, 1994). O'Neill (1996) applied these indices to a semi-arid rangeland in New South Wales, Australia and found that they perform better than slope-based indices in this natural environment. Results of this current study confirmed stress-related indices to be superior to slope-based indices in arid areas. The reason for this good performance of stressed-related indices is that they are not based on solely the red and near-infrared regions of electromagnetic spectrum. In these spectral regions, arid and semi-arid plants due to their xeromorphic adaptations and low chlorophyll levels, like stressed crops, usually have poor spectral contrast. Conversely, because of their low moisture levels and high proportions of woody and dry plant materials, arid plants typically show considerable variation in mid and short-wave infrared reflectance. Consequently indices that include these spectral regions, such as the stress-related vegetation indices, are better recorders of arid perennial plant cover.

7.1.2 Vegetation monitoring and land condition assessment

The application of the STVI-4 to dry season 1991 and 2002 Landsat imagery showed this vegetation index was an appropriate method for detecting vegetation changes. In the

study area, changes in vegetation were highlighted by subtracting 1991 from 2002 STVI-4 images. The vegetation difference image provided useful information about changes in vegetation cover resulting from variations in climate and alterations in land management. It displayed an increase in the STVI-4 values in the east and north east of the study area due to the presence of ephemeral plants in these regions thought to be in response to localised rainfall. Examination of the difference image in relation to paddocks revealed changes in cover within and across boundaries in this region that resulted from management rather than seasonal variations. The impact of management also was observed clearly in this area as there was a high increase in the STVI-4 values around artificial water points where grazing pressure had been removed.

Statistical analysis, however, showed that changes in the STVI-4 did follow trends in cover components (i.e. perennial vegetation cover, total vegetation cover and total ground cover) and also LCI land condition classes from 1991 to 2002. Changes in this vegetation index were in a slight agreement with changes in the cover components and LCI classes. Changes in STVI-4 and total cover had the highest Kappa coefficient (approximately 10%). Kappa coefficients for changes in the STVI-4 versus LCI classes were slightly better than STVI-4 versus cover components. The STVI-4 change accounted for up to 15% of variations in the LCI classes over an eleven-year period.

Despite low agreements between changes in the STVI-4 and LCI classes from 1991 to 2002, the 2005 STVI-4 vegetation index was able to differentiate the LCI classes which were recorded at 885 sites in this year. The STVI-4 discriminated successfully all LCI classes in low open woodlands, good and poor classes in chenopod shrublands and Mt. Eba country. The performance of STVI-4 in non-stratified vegetation cover appeared limited as this index did not show significant differences between different LCI classes. Because STVI-4 is an indicator of vegetation abundance and this component is one of the main criteria for determining land condition in LCI approach, this suggests that the STVI-4 could be used to aid LCI in the assessment of land condition. Before starting a new LCI land condition assessment, for example, the comparison of STVI-4 from last assessment and STVI-4 derived from recent imagery may provide an overview of vegetation condition and changes at last LCI sites as well as entire region.

7.1.3 Arid land characterisation with hyperspectral imagery

Vegetation indices have been used widely to differentiate the reflectance of vegetation cover from other physical materials. Such indices appear to be less applicable in arid environments, however, where vegetation is sparse and soil and other physical features are dominant and contaminate the reflectance of vegetation cover. In this study, for example, the discrimination of vegetation cover in some land types was influenced by the background black and brown surface gravels and stones. Most of the vegetation indices, including one of the most promising vegetation indices (STVI-4), appeared to overestimate vegetation cover. Spectral mixture analysis (SMA) appears to be superior to vegetation indices in arid environments, because it can decompose all components within imagery and thus minimise the effect of different components on one another.

By applying SMA to the Hyperion image, two vegetation and three soil surface end-members were extracted: the soil surface end-members mapped sand plains, sand dunes, eroded areas, and surface gravel and stone. The vegetation end-members discriminated two types of vegetation cover in the region. The first end-member (PVg) mapped all vegetation cover with green and grey green colour (e.g. mulga and western myall) and correlated highly with field estimates of these components. In contrast with PVg, the second end-member (PVc) showed spectral features more characteristic of non-photosynthetic vegetation with lower photosynthetic activity. PVc correlated strongly with field estimates of cottonbush and explained 89% of variation in the sample sites. The spectral signature of this component suggested PVc also mapped other vegetation components such as chenopod shrubs and non-photosynthetic vegetation cover. PVc accounted for up to 23% of variation in these components in the study area.

Despite the favourable hyperspectral resolution of the Hyperion imagery, only two meaningful vegetation end-members were extracted. This may relate to the low vegetation cover of the study area (average 28%), lack of spectral contrast between different vegetation types, background effects of soil, and possibly the high noise content of the Hyperion image. Although the two vegetation end-members extracted from the Hyperion imagery accounted for approximately 70-90% of variations in cover of green and grey green vegetation and cottonbush, no meaningful end-member was produced for chenopod shrubs that are the dominant vegetation in the region and play a key role in management decisions. It seems this limitation of the Hyperion image in the

discrimination of this vegetation type relates mostly to the noisiness of the Hyperion image because of atmospheric or sensor effects and also its moderate spatial resolution (30 m). Research in a similar arid environment (Lewis, 2000) showed it was possible to discriminate chenopod shrubs with hyperspectral CASI (Compact Airborne Spectrographic Imager) imagery with high spatial resolution. The lack of discrimination of these shrubs in the present study thus appears to relate to their low cover relative to the Hyperion spatial resolution, as well as the lower radiometric quality of the satellite imagery.

While spectral mixture analysis is a useful approach in the discrimination of arid landscape components, SMA has limitations for monitoring applications: one of the main limitations is the influence of spectral end-members on one another. Because of the sparseness of vegetation cover in arid environments, the instrument field of view is a mixture of different components and as result of this the availability of a single pixel as a representative of a particular end-member is very rare. Reliance on the image reference spectra thus means that it is difficult to identify "pure" end-member spectra suitable for unmixing. Because of this sensitivity, using this method for monitoring purposes is questionable.

7.1.4 Land degradation assessment with a remotely-sensed heterogeneity index

Due to the dependency of the spatial heterogeneity index (MSDI) on the spatial diversity in ground surface reflectance, this index has high potential in land condition assessments in varied landscapes. To evaluate the usefulness of the MSDI in the study area, spatial heterogeneity in selected piospheres (degraded areas) and nearby reference areas (non-degraded areas) was compared in four different land systems. Results showed piospheres were more heterogeneous in surface reflectance, with high MSDI values compared to non-degraded areas. The higher spatial variations in piospheres seem to result from factors such as soil compaction, sheep tracks and dung deposition, which are usually much greater near water points compared to more distant or reference areas. Another factor that might increase spatial heterogeneity in piospheres may relate to vegetation condition, as overgrazed vegetation in near water has different spectral responses from less-grazed or non-grazed vegetation in reference areas.

The PD54 and NDVI used as comparisons with the spatial diversity index performed differently: the PD54 performed better in all land systems and had consistent

differences between degraded and non-degraded areas, with high values near reference sites. By comparison, the NDVI appeared to be less applicable in the study area. While NDVI showed significant differences between degraded and non-degraded areas in most of the land systems, it could not differentiate these areas in Yudnapinna land system where chenopod shrubs dominated.

The MSDI, PD54, and NDVI indices were able to detect grazing gradients near the artificial stock water points in the study area. MSDI values decreased with increasing distance from water points and showed high values in areas with low vegetation cover. It decreased with increasing vegetation cover as shown by PD54 and NDVI values. The PD54 increased with distance from water in all land systems except Yudnipinna. The NDVI showed no clear grazing gradients either in Yudnapinna or Arcoona land system. These land systems are dominated by chenopod shrubs and the vegetation indices appeared to have limitations for detecting grazing gradients in these landscapes.

7.2 Implications of research findings for arid land assessment and monitoring

As a major land use in arid environments, grazing is the main cause of land degradation. Overgrazing reduces the cover of living and dead vegetation (plant litter) and this promotes soil erosion by water and wind. The continuation of this trend leads land towards desert-like conditions or desertification. High levels of vegetation degradation have been reported widely in Australian's arid lands that cover approximately 75% of the continent. Usually most of the degradation occurs around watering points where grazing pressure is higher than surrounding areas. Because of the broad extent of arid lands, land condition monitoring and assessment using ground-based methods is limited in relation to the information they can provide. Results of this research showed remote sensing techniques, including vegetation indices, spectral mixture analysis and spectral landscape spatial heterogeneity could be used as complementary approaches.

It is clear there are predictive relationships between vegetation indices and quantitative field cover data. While total vegetation cover (perennial and ephemeral plants) was predicted best by image indices, there was a significant correlation between vegetation indices and perennial vegetation cover. Because perennial vegetation is less affected by seasonal variations, it is the most important indicator in land condition assessment and monitoring. These relationships show that certain vegetation indices can be used to

estimate perennial vegetation cover and monitor its variation with time in broad areas where field-based methods are less applicable.

The results showed limitations to the use of vegetation indices in broad areas with different terrains, soils and vegetation types. Vegetation indices were better predictors of field cover data at land system scale rather than regional or landscape scale. Similar results were also obtained when vegetation indices were used to discriminate LCI land condition classes. These indices performed better in stratified compared with non-stratified vegetation cover. This means that stratification into land systems and vegetation cover should be undertaken, and that vegetation indices should be used cautiously across land systems and heterogeneous vegetation cover. As vegetation type in each land system is usually similar, stratification into land systems appears to be adequate.

Despite the extensive use of NDVI, results showed it is not the most sensitive vegetation index in the study area. Its applicability was highly reduced in landscapes dominated by chenopod shrublands. NDVI was, however, the best predictor of total vegetation cover and total vegetation cover plus non-photosynthetic vegetation cover at regional scale. This confirms NDVI is more useful for general vegetation quantification, assessment and monitoring regardless of localized soil and vegetation variation.

Landscape components derived from remote sensing imagery can play an important role in land management. Land managers may, for example, want to know the distribution of different vegetation types and their variations over time resulting from seasonal conditions and management strategies, or they may also want to know the location and distribution of other sensitive land components such as sand dunes. Monitoring sand dunes can help to identify their movement and recognize the most threatened areas early. Image-based components such those derived from Hyperion hyperspectral imagery in this study have high potential for land condition assessment and monitoring. For example, the sandy soil component that clearly mapped all sand dunes could be used as an indicator for monitoring the risk of wind erosion.

As vegetation cover is the most important factor in land condition assessment and monitoring and usually links to both the causes and consequences of land degradation, appropriate image-based techniques are needed to extract vegetation information. Although STVI-4 provided considerable information about vegetation cover and its

variation through time due to seasonal and management effects, the MSDI enhanced land condition assessment, exploiting the spatial patterns in land cover. In this study environment the MSDI detected successfully areas disturbed by overgrazing around stock watering points. The MSDI showed much greater spatial heterogeneity in these areas compared to reference regions. In applying the MSDI more widely the appropriate filter size needs to be chosen in relation to the spatial scale of the landscape pattern and degradation influences: a filter other than the 3×3 moving window used here with Landsat imagery may be more sensitive. In addition, this index needs to be interpreted with caution to exclude artifacts of apparently high spatial heterogeneity at the edges of natural and man-made features such as rivers and roads.

The STVI-4 and MSDI offer the potential to aid field methods in land condition assessment and monitoring. The STVI-4 detected successfully changes in vegetation cover due to seasonal conditions and changes in land management practices and was able to separate LCI land condition classes with high confidence levels within pasture types. The good performance of MSDI in the detection of degradation in perennial-dominated landscapes showed that it may be used as an appropriate indicator of land condition. Because of the simplicity and repeatability of the MSDI heterogeneity index and STVI-4 vegetation index, they could be used as rapid methods for assessing and monitoring land condition of arid lands of South Australia.

7.3 Recommendations for future research

Recommendations span for several decades for the use of remote sensing methods, usually via vegetation indices, in arid land assessment and monitoring. Despite compelling arguments, however, uptake of remote sensing by arid land management agencies has not been universal. Impediments to wider use of the techniques include lack of remote sensing specialists in monitoring and assessment agencies, and lack of understanding amongst land holders about the information that can be derived from remote sensing. There can, additionly, be uncertainty about the interpretation of image indices in relation to more conventional field data in particular environments. The current research has addressed this last question for selected environments in the southern Australian arid lands and showed that information derived from remote sensing imagery using different methods such as vegetation indices, unmixing approaches and the landscape spatial heterogeneity index have high potential in land

condition assessment and monitoring. Such information can assist land management agencies in planning and managing broad areas.

To address some of the limitations of the methods raised in this research and to improve their use and maximise their benefits, the following areas for further research are recommended:

- Land system stratification
- Chenopod shrub discrimination
- Land condition monitoring with the landscape diversity index

Land system stratification would be a logical strategy for vegetation assessment and monitoring in the region. The favourable performance of vegetation indices at land system scale versus broader landscape scales suggests they are land-type dependent indices. At land system scale, vegetation similarity promoted strong relationships with field cover data. It was interesting to see that an index that had the strongest relationship in one land system was weaker in another. This means that according to the definition of vegetation indices, some indices are more suitable for a particular land system. Further research is therefore required to map each land system with the vegetation index that has the strongest relationship with vegetation cover in that land system. Each land system will thus have its specific vegetation index. As the land systems have already been mapped by South Australian government agencies, this mapping in GIS form provides a good basis for stratifying the landscape and developing these relationships for a wider range of the land systems across the South Australian pastoral lands. In order to do this more field data might be needed than were available in this current study. Such data might come from existing programs such as pastoral land monitoring or it might need to be collected specifically for this purpose. Another appropriate way to develop relationships between vegetation index imagery and field cover data is to use stratified pasture types rather than individual land systems. As the results of this study showed vegetation indices performed better in stratified compared with non-stratified pasture types. Using pasture type to establish these relationships appears to be more applicable and quicker and also covers much broader areas.

Use of remote sensing for discrimination of chenopod shrubs, which are the dominant vegetation types in the region, is another important direction for future work. Results from this study showed the Hyperion data were unable to provide a meaningful image vegetation component for chenopod shrubs. Airborne imagery with high spectral and spatial resolution is a good solution for this limitation, though more expensive than satellite imagery. In the near future satellite hyperspectral sensors with high signal to noise ratio may be a cost-effective alternative in arid lands and provide more detailed information about vegetation cover than achieved by Hyperion (Stuffler *et al.*, 2005).

Future work should examine the landscape diversity index for monitoring purposes. If this index can detect changes in land condition over time, its application is highly recommended due to its objectivity and requirement for less image calibration. The MSDI performed as well as widely used vegetation indices, for example PD54, in Australian arid lands. MSDI was able to highlight disturbed areas due to overgrazing with high levels of confidence. Further work is needed to investigate the capability of this index for monitoring land condition.

8 REFERENCES

Adams, J.B., Sabol, D.E., Kapos, V., Almeida Filho, R., Roberts, D.A., Smith, M.O., and Gillespie, A.R., 1995. Classification of multispectral images based on fractions of endmembers: application to land-cover change in the Brazilian Amazon. Remote Sensing of Environment 52(2), 137-154.

Al-Bakri, J.T. and Tayor, T.C., 2003. Application of NOAA AVHRR for monitoring vegetation condition and biomass in Jordan. *Journal of Arid Environments* **54**, 579-593.

Andrew, M.H. and Lange, R.T., 1986a. Development of a new piosphere in arid chenopod shrubland grazed by sheep. 1. Changes to the soil surface. *Australian Journal of Ecology* **11**, 395-409.

Andrew, M.H. and Lange, R.T., 1986b. Development of a new piosphere in arid chenopod shrubland grazed by sheep. 2. Changes to the vegetation. *Australian Journal of Ecology* **11**, 411-424.

Archer, E.R.M., 2004. Beyond the " climate versus grazing" impasse: using remote sensing to investigate the effects of grazing system choice on vegetation cover in the eastern Karoo. *Journal of Arid Environments* **57**, 381-408.

Arnalds, O. and Archer, S. (Editors), 2000. Rangeland desertification. Kluwer Academic Publishers, Dordrecht, Netherlands.

Asner, G.P. and Heidebrecht, K.B., 2002. Spectral unmixing of vegetation, soil and dry carbon cover in arid regions: comparing multispectral and hyperspectral observations. *International Journal of Remote Sensing* **23**(19), 3939-3958.

Asner, G.P. and Heidebrecht, K.B., 2003. Imaging spectroscopy for desertification studies: Comparing AVIRIS and EO-1 Hyperion in Argentina drylands. *IEEE Transactions on Geoscience and Remote Sensing* **41**(6), 1283-1296.

Bannari, A., Morin, D. and Bonn, F., 1995. A review of vegetation indices. *Remote Sensing Review* **13**, 95-120.

Baret, F., Guyot, G., Begue, A., Maurel, P. and Podaire, A., 1988. Complementarity of middle-infrared with visible and near-infrared reflectance for monitoring wheat canopies. *Remote Sensing of Environment* **26**(3), 213-225.

Baret, F., Jaquemound, S. and Hanocq, J.F., 1993. The soil line concept in remote sensing. *Remote Sensing Reviews* **7**, 65-82.

Bastin, G.N., Chewings, V.H., Pearce, G. and McGregor, F., 1999. Assessment of grazing impact on the Barkly tablelands: vegetation index and software. CSIRO Report to NT Department of Land, Planning and Environment, Published on CD-ROM.

Bastin, G.N. and Ludwig, J.A., 2006. Problems and prospects for mapping vegetation condition in Australia's arid rangelands. *Ecological Management and Restoration* **7**(s1), S71-S74.

Bastin, G.N., Pickup, G., Chewings, V.H. and Pearce, G., 1993a. Land degradation assessment in central Australia using a grazing gradient method. *Rangel. J.* **15**(2), 190-216.

Bastin, G.N., Sparrow, A.D. and Pearce, G., 1993b. Grazing gradient in central Australian rangelands: ground verification of remote sensing-based approaches. *Rangel. J.* **15**(2), 217-233.

Bastin, G.N., Tynan, R.W. and Chewings, V.H., 1998. Implementing satellite-based grazing gradient methods for rangeland assessment in South Australia. *Rangel. J.* **20**(1), 61-76.

Bateson, A. and Curtiss, B., 1996. A method for manual endmember selection and spectral unmixing. *Remote Sensing of Environment* **55**(3), 229-243.

Ben-Dor, E., Kruse, F.A., Lefkoff, A.B. and Banin, A., 1994. Comparison of three calibration techniques for utilization of GER 63-channel aircraft scanner data of Makhtesh Ramon, Negev, Israel. *Photogrammetric Engineering and Remote Sensing* **60**(11).

Bierwirth, P.N., 1990. Mineral mapping and vegetation removal via data-calibrated pixel unmixing, using multispectral images. *International Journal of Remote Sensing* **11**(11), 1999-2017.

Boardman, J.W. and Kruse, E., A, 1994. Automated spectral analysis: a geological example using AVIRIS data, ERM Tenth Thematic Conference on Geologic Remote Sensing. Environmental Research Institute of Michigan, Michigan, pp. I-407-I-418.

Booth, D.T. and Tueller, P.T., 2003. Rangeland monitoring using remote sensing. *Arid Land Research and Management* **17**(4), 455-467.

Brits, J., van Rooyen, M.W. and van Rooyen, N., 2002. Ecological impact of large herbivores on the woody vegetation at selected watering points on the eastern basaltic soils in the Kruger National Park. *African Journal of Ecology* **40**(1), 53-60.

Burnside, D.G. and Chamala, S., 1994. Ground-based monitoring: a process of learning by doing. *Rangel. J.* **16**(2), 221-237.

Byrne, G.F., Crapper, P.F. and Mayo, K.K., 1980. Monitoring land-cover change by principal component analysis of multitemporal Landsat data. *Remote Sensing of Environment* **10**(3), 175-184.

Campbell, J.B., 1996. Introduction to remote sensing. Second Edition, Guilford Press, New York.

Caren, C.D., Mladenoff, D.J. and Radeloff, V.C., 2002. Phenological differences in tasselled cap indices improve deciduous forest classification. *Remote Sensing of Environment* **80**, 460-472.

Chavez, P.S. and Mackinnon, D.J., 1994. Automatic detection of vegetation changes in the southern United States using remotely sensed images. *Photogrammetric Engineering and Remote Sensing* **60**(5), 571-583.

Chewings, V.H., Bastin, G.N., Crawford, M.M. and Kinloch, J.E., 2002. Characterisation of vegetation components in the Australian arid zone using Eo-1 Hyperion imagery, Proceedings of the 11th Australasian Remote Sensing and

Photogrammetry Conference. The Remote Sensing and Photogrammetry Association of Australia, 2-6 September, Brisbane, Queensland, Australia, pp. 634-646.

Chisholm, A. and Dumsday, R. (Editors), 1987. land degradation: problems and policies. Cambridge University Press, Cambridge, UK.

Condon, R.W., 1982. Pastoralism. Proceedings of Arid Lands Conference. Australian Conservation Foundation, Broken Hill, New South Wales, Australia, pp. 54-60.

Cook, C.W. and Stubbendieck, J., 1986. Edited, Range research: basic problems and techniques. Society for Range Management, Colorado.

Coppin, P., Jonckheere, I., Nackaerts, K. and Muys, B., 2004. Digital change detection methods in ecosystem monitoring: a review. *International Journal of Remote Sensing* **25**(9), 1565-1596.

Crist, E.P., 1985. A TM tasselled cap equivalent transformation for reflectance factor data. *Remote Sensing of Environment* **17**(3), 301-306.

Danaher, T.G., 1998. The statewide landcover and trees study (SLATS)- Monitoring land cover and greenhouse gas emission in Queensland, Proceedings of the 9th Australasian Remote Sensing Photogrammetry Conference. Remote Sensing and Photogrammetry Association of Australia, Sydney.

Deer, P.J. and Longmore, M.E., 1994. The application of principal components analysis to monitoring the clearance of native forest stands on Kangaroo Island, South Australia, Proceedings of the 7th Australasian Remote Sensing Conference. The Remote Sensing and Photogrammetry Association of Australia, 1-4 March 1994, Melbourne, Australia, pp. 391-398.

Della Torre, B., 2005. Tracking Changes in the Gawler Bioregion, South Australian Department of Water, Land and Biodiversity Conservation, Adelaide, South Australia.

Department for Environment and Heritage, 2007. South Australian fire effected areas. Department for Environment and Heritage, Adelaide, South Australia, [Internet]

Accessed February 2007, Available at URL:http://www.naturemaps.sa.gov.au/imf-ext/imf.jsp?site=NatureMaps.

Department of Water Land Biodiversity and Conservation, 2002. Pastoral lease assessment, technical manual for assessing land condition on pastoral leases in South Australia,1990-2000, Pastoral Program, Sustainable Resources, DWL&BC, Adelaide, South Australia.

Dewidar, K.M., 2004. Detection of land use/land cover changes for the northern part of the Nile delta (Burullus Region), Egypt. *International Journal of Remote Sensing* **25**(20), 4079-4089.

Dregne, H.E., 1983. Desertification of arid lands, advances in desert and arid land technology and development volume 3. Harwood Academic Publishers, New York.

Dregne, H.E., 2002. Land degradation in the drylands. *Arid Land Research and Management* **16**(2), 99-132.

Dusek, D.A., Jackson, R.D. and Musick, J.T., 1985. Winter wheat vegetation indices calculated from combinations of seven spectral bands. *Remote Sensing of Environment* **18**(3), 255-267.

Dutkiewicz, A., 2005. Evaluating Hyperspectral Imagery for Mapping the Surface Symptoms of Dryland Salinity, School of Earth and Environmental Sciences, The University of Adelaide, Adelaide.

Edwards, J., 2001. Monitoring vegetation changes under different arid management regions, near Olympic dam, South Australia, using Landsat TM imagery. Graduate Diploma in Spatial Information Science Thesis, Adelaide University.

Elmore, A.J., Mustard, J.F., Manning, S.J. and Lobell, D.B., 2000. Quantifying vegetation change in semiarid environments: precision and accuracy of spectral mixture analysis and the Normalized Difference Vegetation Index. *Remote Sensing of Environment* **73**(1), 87-102.

ENVI Research Systems Inc, 2000. ENVI User's Guide, the Environment for Visualizing Images, Version 3.4. Research Systems, Inc, Boulder, USA.

Fabbri, A. G., Kushigbor, C. A., Wang, L., Baker, A. B. and Roscoe, S.M., 1989. Integration of remotely sensed and ancillary geological data for assessing mineral resources in the Bathurst Intel area, Canada, Proceeding the 21st Application of Computers and Operations Research in the Mineral Industry. Organizing Committee, Las Vegas (NV), pp. 1109-1120.

Fabricius, C., Palmer, A.R. and Burger, M., 2002. Landscape diversity in a conservation area and commercial and communal rangeland in Xeric Succulent Thicket, South Africa. *Landscape Ecology* **17**, 531-537.

FAO, 1983. Provisional methodology for assessment and mapping of desertification. Food and Agriculture Organization of the United Nations, Rome, Italy.

FAO, 1987. Committee on agriculture, Improving productivity of dryland areas, Rome.

FAO, 1996. AGROSTAT, Statistics Division, FAO, Rome.

Farahpour, M., van Keulen, H., Sharifi, M.A. and Bassiri, M., 2004. A planning support system for rangeland allocation in Iran with case study of Chadegan sub-region. *Rangeland Journal* **26**(2), 225-236.

Fleming, M., Della Torre, B. and Kutsche, F., 2002. Establishing pastoral reference areas, report, Department of Land, Water and Biodiversity Conservation and Department for Environment and Heritage, Adelaide.

Foran, B. and Pearce, G., 1990. The use of NOAA AVHRR and the green vegetation index to assess the 1988/1989 summer growing season in central Australia, Proceeding of Operational Remote Sensing for Developing and Mapping Earth Resources. Committee of the 5th Remote Sensing Conference, Perth, Western Australia, 8-12 October, pp. 198-207.

Foran, B.D. and Pickup, G., 1984. Relationship of aircraft radiometric measurements to bare ground on semi-desert landscapes in central Australia. *Rangel. J.* **6**(2), 59-68.

Fraser, K., 1997. Map of arid lands of the world, Accessed May 2007, [Internet] Accessed May 2007, Available at URL: http://pubs.usgs.gov/gip/deserts/what/world.html.

Friedel, M.H. and Shaw, K., 1987a. Evaluation of methods for monitoring sparse patterned vegetation in arid rangeland, I. Herbage. *Journal of Environmental Management* **25**, 297-308.

Friedel, M.H. and Shaw, K., 1987b. Evaluation of methods for monitoring sparse patterned vegetation in arid rangelands. II. Trees and shrubs. *Journal of Environmental Management* **25**, 306-318.

Friedel, M.H., Sparrow, A.D., Kinloch, J.E. and Tongway, D.J., 2003. Degradation and recovery processes in arid grazing lands of central Australia. part 2: vegetation. *Journal of Arid Environments* **55**, 327-348.

Fung, T. and LeDrew, E., 1987. Application of principal components analysis to change detection. *Photogrammetric Engineering and Remote Sensing* **53**(12), 1649-1658.

Furby, S.L. and Campbell, N.A., 2001. Calibrating images from different dates to 'like-value' digital counts. *Remote Sensing of Environment* **77**(2), 186-196.

Gao, B. and Goetz, A.F.H., 1990. Column Atmospheric water vapour and vegetation liquid water retrievals from airborne imaging spectrometer data. *Journal of Geophysical Research* **95**, 3549-3564.

Garcia-Haro, F.J., Gilabert, M.A. and Melia, J., 1999. Extraction of endmembers from spectral mixtures. *Remote Sensing of Environment* **68**(3), 237-253.

Geerken, R. and Ilaiwi, M., 2004. Assessment of rangeland degradation and development of a strategy for rehabilitation. *Remote Sensing of Environment* **90**, 490-504.

Gilabert, M.A., Gonzalez-Piqueras, J., Garcia-Haro, F.J. and Melia, J., 2002. A generalized soil-adjusted vegetation index. *Remote Sensing of Environment* **82**(2-3), 303-310.

Graetz, R.D., 1987. Satellite remote sensing of Australian rangelands. *Remote Sensing of Environment* **23**, 313-331.

Graetz, R.D. and Gentle, M.R., 1982. Study of the relationships between reflectance in the Landsat wavebands and the composition of an Australian semi-arid shrub rangeland. *Photogrammetric Engineering and Remote Sensing* **48**, 1721-1730.

Graetz, R.D., Gentle, M.R., Pech, R.P., O'Callaghan, J.F. and Drewien, G., 1983. The application of Landsat image data to rangeland assessment and monitoring: an example from South Australia. *Rangel. J.* **5**(2), 63-73.

Green, A.A., Bermon, M., Switzer, P. and Craig, M.D., 1988. A transformation for ordering multispectral data in terms of image quality with implications for noise removal. *IEEE Transactions on Geoscience and Remote Sensing* **26**(1), 65-74.

Green, A.A. and Craig, M.D., 1985. Analysis of aircraft spectrometer data with logaritmic residuals, Proceedings of the airborne imaging spectrometer data analysis workshop. JPL Publication 85-41, Jet Propulsion Laboratory, Pasadena, California, pp. 111-119.

Grunblatt, J., Ottichilo, W.K. and Sinange, R.K., 1992. A GIS approach to desertification assessment and mapping. *Journal of Arid Environments* **23**, 81-102.

Guo, X., Wilmshurst, J., McCanny, S., Fargey, P. and Richard, P., 2004. Measuring spatial and vertical heterogeneity of grasslands using remote sensing techniques. *Journal of Environmental Informatics* **3**(1), 24-32.

Hahn, B.D., Richardson, F.D., Hoffman, M.T., Roberts, R., Todd, S.W. and Carrick, P.J., 2005. A simulation model of long-term climate, livestock and vegetation interactions on communal rangelands in the semi-arid Succulent Karoo, Namaqualand, South Africa. Ecological Modelling 183(2-3), 211-230.

Harison, B.A. and Jupp, D.L.B., 1990. Introduction to image processing. CSIRO, Melbourne, Australia.

Harper, J., George, M. and Tate, K., 1990. Monitoring California' s annual rangeland vegetation, UC/DANR leaflet 21486. Photopoint as a Monitoring Tool, [Internet], Accessed May 2004, Available at URL: http://danr.ucop.edu/uccelr/h16.htm.

Harris, A.T. and Asner, G.P., 2003. Grazing gradient detection with airborne imaging spectroscopy on a semi-arid rangeland. *Journal of Arid Environments* **55**(3), 391-404.

Hatchell, D.C. (Editor), 1999. Technical Guide, Analytical Spectral Devices, Inc (ASD), Boulder, Colorado, USA.

He, D.C. and Wang, L., 1990. Texture unit, texture spectrum, and texture analysis. *IEEE Transactions on Geoscience and Remote Sensing*, **28(**4), 509-512.

Heshmatti, G.A., Facelli, J.M. and Conran, J.G., 2002. The piosphere revisited: plant species patterns close to waterpoints in small, fenced paddocks in chenopod shrublands of South Australia. *Journal of Arid Environments* **51**(4), 547-560.

Hirosawa, Y., Marsh, S.E. and Kliman, D.H., 1996. Application of standardized principal component analysis to land-cover characterization using multitemporal AVHRR data. *Remote Sensing of Environment* **58**(3), 267-281.

Holm, A.M., Cridland, S.W. and Roderick, M.L., 2003a. The use of time-integrated NOAA NDVI data and rainfall to assess landscape degradation in the arid shrubland of Western Australia. *Remote Sensing of Environment* **85**(2), 145-158.

Holm, A.M., Watson, I.W., Loneragan, W.A. and Adams, M.A., 2003b. Loss of patch-scale heterogeneity on primary productivity and rainfall-use efficiency in Western Australia. *Basic and Applied Ecology* **4**, 569-578.

Hostert, P., Roder, A. and Hill, J., 2003a. Coupling spectral unmixing and trend analysis for monitoring long-term vegetation dynamics in Mediterranean rangelands. *Remote Sensing of Environment* **87**, 183-197.

Hostert, P., Roder, A., Hill, J., Udelhoven, T. and Tsiourlis, G., 2003b. Retrospective studies of grazing-induced land degradation: a case study in central Crete, Greece. *International Journal of Remote Sensing* **24**(20), 4019-4034.

Hountondji, Y., Sokpon, N. and Ozer, P., 2006. Analysis of the vegetation trends using low resolution remote sensing data in Burkina Faso for the monitoring of desertification. *International Journal of Remote Sensing* **27**, 871-884.

Huete, A.R., 1988. A soil-adjusted vegetation index (SAVI). *Remote Sensing of Environment* **25**, 295-309.

Huete, A.R., Jackson, R.D. and Post, D.F., 1985. Spectral response of a plant canopy with different soil backgrounds. *Remote Sensing of Environment* **17**(1), 37-53.

Huete, A.R., Miura, T. and Gao, X., 2003. Land cover conversion and degradation analyses through coupled soil-plant biophysical parameters derived from hyperspectral EO-1 Hyperion. *IEEE Transactions on Geoscience and Remote Sensing* **41**(6), 1268-1276.

Huete, A.R., Post, D.F. and Jackson, R.D., 1984. Soil spectral effect on 4-space vegetation discrimination. *Remote Sensing of Environment* **15**, 155-165.

ImSpecLLC, 2004. ACORN 5.0 User Guide, Boulder, Colorado, USA.

Ingebritsen, S.E. and Lyon, R.J.P., 1985. Principal components analysis of multitemporal image pairs. *International Journal of Remote Sensing* **6**(5), 687-696.

Jafari, R., 2001. Use of FAO/UNEP and ICD models for assessing and mapping desertification processes, M. Sc Thesis, Tehran University, Tehran, Iran.

James, C.D., Landsberg, J. and Morton, S.R., 1999. Provision of watering points in the Australian arid zone: a review of effects on biota. *Journal of Arid Environments* **41**(1), 87-121.

Jin, S. and Sader, S.A., 2005. Comparison of time series tasselled cap wetness and the Normalized Difference Moisture Index in detecting forest disturbances. *Remote Sensing of Environment* **94**, 364-372.

Johannsen, C.J. and Sanders, J.L. (Editors), 1982. Remote sensing for resource management. The Soil Conservation of America, Lowa, USA.

Johansen, K., Phinn, S., Dixon, I., Douglas, M. and Lowry, J., 2007. Comparison of image and rapid field assessments of riparian zone condition in Australian tropical savannas. *Forest Ecology and Management* **240**(1-3), 42-60.

Johnson, R.D. and Kasischke, E.S., 1998. Change vector analysis: a technique for the multispecreal monitoring of land cover and condition. *International Journal of Remote Sensing* **19**(3), 411-426.

Karfs, R.A., Daly, C., Beutel, T.S., Peel, L. and Wallace, J.F., 2004. VegMachine-Delivering Monitoring Information to Northern Australian's Pastoral Industry, The 12th Australian Remote Sensing and Photogrammetry Conference. The Remote Sensing and Photogrammetry Association of Australia, Fremantle, Western Australia, 18-22 October 2004, Published on CD-ROM.

Karfs, R.A. and Trueman, M., 2005. Tracking Changes in the Victoria River District Pastoral District, Report to the Australian Collaborative Rangeland Information System (ACRIS) Management Committee, Department of Natural Resources, Environment and the Arts, Northern Territory, Australia.

Kassas, M., 1995. Desertification: a general review. *Journal of Arid Environments* **30**, 115-128.

Kauth, J.R. and Thomas, G.S., 1976. The tasselled cap-A graphic description of the spectral-temporal development of agricultural crop as seen by Landsat, Proceedings of the Symposium Machine Processing of Remotely-sensed Data, Purdue University, West Lafayette, Indiana, 21 June-1 July, pp. 4B41-4B51.

Kimes, D.S., Markham, B.L., Tucker, C.J. and McMurtrey, I., J. E., 1981. Temporal relationships between spectral response and agronomic variables of a corn canopy. *Remote Sensing of Environment* **11**, 401-411.

Khoudiedji, T.A., 1998. Geographic Information Systems and Remote Sensing Methods for Assessing and Monitoring Land Degradation in the Sahel Region: The Case of Southern Mauritania. Ph.D Thesis, Clare University, Worcester, Mauritania.

Kingoonya Soil Conservation Board, 1991. Kingoonya Soil Conservation Board District, general summary of lease assessment findings. Rangeland Assessment Unit, Pastoral Management Branch, Department of Environment and Planning, Adelaide, South Australia.

Kingoonya Soil Conservation Board, 1996. Kingoonya Soil Conservation Board District Plan. Kingoonya Soil Conservation District Board, Primary Industries, Port Augusta, South Australia.

Kinloch, J.E., Bannari, a. and Tongway, D.J., 2000. Measuring landscape function in chenopod shrublands using aerial videography, Proceeding of the 10th Australian Remote Sensing and Photogrammetry Conference. The Remote Sensing and Photogrammetry Association of Australia, Adelaide, South Australia, Australia, pp. 480-491.

Kinloch, J.E. and Friedel, M.H., 2005a. Soil seed reserves in arid grazing lands of central Australia. Part 1: seed bank and vegetation dynamics. *Journal of Arid Environments* **60**(1), 133-161.

Kinloch, J.E. and Friedel, M.H., 2005b. Soil seed reserves in arid grazing lands of central Australia. Part 2: availability of 'safe sites'. *Journal of Arid Environments* **60**(1), 163-185.

Landis, J.R. and Koch, G.G., 1977. The measurement of observer agreement for categorical data. *Biometrics* **33**(1), 159-174.

Lange, R.T., 1969. The Piosphere: Sheep track and dung patterns. *Journal of Range Management* **22**, 396-400.

Lay, B.G. and Evans, B.F., 1973. Rangeland condition assessment, a appraisal of some techniques and their application in pastoral areas of South Australia, Department of Agriculture, Adelaide, South Australia.

Lewis, M.M., 1999. Discriminating arid vegetation composition with multispectral and high spectral resolution imagery. PhD Thesis, University of New South Wales, Australia.

Lewis, M.M., 2000. Discrimination of arid vegetation composition with high resolution CASI imagery. *Rangel. J.* **22**(1), 141-167.

Lewis, M.M., Jooste, V. and deGasparis, A.A., 2001. Discrimination of arid vegetation with airborne multispectral scanner hyperspectral imagery. *IEEE Transactions on Geoscience and Remote Sensing* **39**(7), 1471-1479.

Lewis, M.M. and Wood, B., 1994. Arid land mapping with spectral mixture analysis, Proceedings of the 7th Australasian Remote Sensing Conference, Melbourne, Australia, pp. 565-572.

Lu, D., Mausel, P., Brondizio, E. and Moran, E., 2004. Change detection techniques. *International Journal of Remote Sensing* **25**(12), 2365-2407.

Mas, J.F., 1999. Monitoring land-cover changes: a comparison of change detection techniques. *International Journal of Remote Sensing* **20**(1), 139-152.

Mason, P., 2002. MMTG A-List Hyperspectral Data Processing Software, 920C, CSIRO, Division of Exploration and Mining, Sydney, Australia.

Matlock, W.G., 1981. Realistic planning for arid lands: advances in desert and arid land technology and development, Volume 2. Harwood Academic Publishers, New York.

McGregor, K.F. and Lewis, M.M., 1996. Quantitative spectral change in chenopod shrublands, Proceedings of 9th Biennial Conference, Focus on the Future-the Heat Is on! The Australian Rangeland Society, September 24-27, Port Augusta, South Australia, pp. 153-154.

McKeon, G., Wayne, H., Beverley, H., Grant, S. and Ian, W., 2004. Pasture Degradation and Recovery in Australia's Rangelands: Learning from History, Department of Natural Resources, Mines and Energy, QNRME04130, Queensland.

Mesdaghi, M., 1998. Management of Iran's rangelands. Emam Reza University Press, Mashhad, Iran.

Metternicht, G., 2003. Vegetation indices derived from high-resolution airborne videography for precision crop management. *International Journal of Remote Sensing* **24**, 2855-2877.

Metternicht, G. and Fermont, A., 1998. Estimating erosion surface features by linear mixture modelling. *Remote Sensing of Environment* **64**(3), 254-265.

Metternicht, G., Newby, T., van den Berg, H., Paterson, G. and Booyens, B., 2002. Feasibility of using ASTER data for rapid farm scale soil mapping in South Africa, Proceedings of the 11th Australasian Remote Sensing and Photogrammetry Conference. The Remote Sensing and Photogrammetry Association of Australia, Brisbane, Queensland, Australia, September 2-6, pp. 454-470.

Miller, J.D. and Yool, S.R., 2002. Mapping forest post-fire canopy consumption in several overstory types using multi-temporal Landsat TM and ETM+ data. *Remote Sensing of Environment* **82**(2-3), 481-496.

Minor, T.B., Lancaster, J., Wade, T.G., Wickham, J.D., Whitford, W. and Jones, K.B., 1999. Evaluation change in rangeland condition using multitemporal AVHRR data and Geographic Information System analysis. *Environmental Monitoring and Assessment* 59, 211-223.

Murwira, A. and Skidmore, A.K., 2006. Monitoring change in the spatial heterogeneity of vegetation cover in an African savanna. *International Journal of Remote Sensing* **27**(11), 2255-2269.

Myneni, R.B., Keeling, C.D., Tucker, C.J., Asrar, G. and Nemani, R.R., 1997. Increased plant growth in the northern high latitudes from 1981 to 1991. *Nature* **386**, 698-702.

Nackaerts, K., Vaesen, K., Muys, B. and Coppin, P., 2005. Comparative performance of a modified change vector analysis in forest change detection. *International Journal of Remote Sensing* **26**(5), 839-852.

Nangula, S. and Oba, G., 2004. Effects of artificial water points on the Oshana ecosystem in Namibia. *Environmental Conservation* **31**(1), 47-54.

Nash, M.S., Jackson, E. and Whitford, W.G., 2003. Soil microtopography on grazing gradients in Chihuahuan desert grasslands. *Journal of Arid Environments* **55**(1), 181-192.

O' Neill, A.L., 1996. Satellite-derived vegetation indices applied to semi-arid shrublands in Australia. *Australian Geographer* **27**(2), 185-199.

Okin, G.S., Roberts, D.A., Murray, B. and Okin, W.J., 2001. Practical limits on hyperspectral vegetation discrimination in arid and semiarid environments. *Remote Sensing of Environment* **77**(2), 212-225.

Ostir, K., Veljannovski, T., Podobnikar, T. and Stanc, Z., 2003. Application of satellite remote sensing in natural hazard management. *International Journal of Remote Sensing* **24**(20), 3983-4002.

Pastoral Board, 2002. (CD-ROM), Pastoral Board, Department of Water, Land Biodiversity and Conservation, Adelaide, South Australia.

Pearlman, J.S. et al., 2003. Hyperion, a space-based imaging spectrometer. *IEEE Transactions on Geoscience and Remote Sensing* **41**(6), 1160-1173.

Pearson, R.L. and Miller, L.D., 1972. Remote sensing of standing crop biomass for estimation of the productivity of the shortgrass Prairie, Pawnee national grasslands, Colorado, The 8th International Symposium on Remote Sensing of the Environment, 2-6 October, Ann Arbor, Michigan, pp. 1355-1379.

Perry, C.R., Lautenschlager, J.R. and Lautenschlager, L.F., 1984. Functional equivalence of spectral vegetation indices. *Remote Sensing of Environment* **14**, 169-182.

Peters, A.J. and Eve, M.D., 1995. Satellite monitoring of desert plant community response to moisture. *Environmental Monitoring and Assessment* **37**, 273-287.

Pickup, G., 1989. New land degradation survey techniques for arid Australia: problems and prospects. *Rangel. J.* **11**(2), 74-82.

Pickup, G., 1990. Impact of soil erosion on Australia' s rangelands, Proceedings of the 6th Australian Rangeland Society Conference, Carnarvon, Western Australia. Australian Rangeland Society, Perth, Western Australia, pp. 159-170.

Pickup, G., Bastin, G.N. and Chewings, V.H., 1994. Remote-sensing-based condition assessment for nonequilibrium rangeland under large-scale commercial grazing. *Journal of Ecological Applications* **4**(3), 497-517.

Pickup, G. and Chewings, V.H., 1988. Forecasting patterns of soil erosion in arid lands from Landsat MSS data. *International Journal of Remote Sensing* **9**(1), 69-84.

Pickup, G. and Chewings, V.H., 1994. A grazing gradient approach to land degradation assessment in arid areas from remotely-sensed data. *International Journal of Environmental Studies* **15**, 597-617.

Pickup, G., Chewings, V.H. and Nelson, D.J., 1993. Estimating changes in vegetation cover over time in arid rangelands using Landsat MSS data. *Remote Sensing of Environment* **43**, 243-263.

Pickup, G. and Foran, B.D., 1987. The use of spectral and spatial variability to monitor cover change on inert landscapes. *Remote Sensing of Environment* **23**, 351-363.

Pickup, G. and Nelson, D.J., 1984. Use of Landsat radiance parameters to distinguish soil erosion, stability, and deposition in arid central Australia. *Remote Sensing of Environment* **16**, 195-209.

Pilon, P.G., Howarth, P.j. and Adeniyi, P.O., 1988. An enhanced classification approach to change detection in arid and semi-arid environments. *Photogrammetric Engineering and Remote Sensing* **54**, 1709-1716.

Price, K.P., Guo, X. and Stiles, J.M., 2002. Optimal Landsat TM band combinations and vegetation indices for discrimination of six grassland types in eastern Kansas. *International Journal of Remote Sensing* **23**(23), 5031-5042.

Purevdorgy, T., Tateishi, R., Ishigama, T. and Honda, Y., 1998. Relationships between percent vegetation cover and vegetation indices. *International Journal of Remote Sensing* **19**(18), 3519-3535.

Queensland Department of Natural Resources Mines and Water, 2006. The Australian Grassland and Rangeland Assessment by Spatial Simulation project (Aussie GRASS). Department of Natural Resources, Mines and Water, Queensland, [Internet] Accessed September 2006, Available at URL: http://www.longpaddock.qld.gov.au/AboutUs/ResearchProjects/AussieGRASS/index.html.

Qi, J., Chehbouni, A., Huete, A.R., Kerr, Y.H. and Sorooshian, S., 1994. A modified soil adjusted vegetation index. *Remote Sensing of Environment* **48**(2), 119-126.

Quigley, M., Mason, P. and Huntington, 2004. Image Restoration and Atmospheric Correction of 'Hyperion' Hyperspectral EO-1 Satellite Data, 1218F, CSIRO, Division of Exploration and Mining, Sydney, Australia.

Ramsey, E., Rangoonwala, A., Nelson, G., Ehrlich, R. and Martella, K., 2005. Generation and validation of characteristic spectra from EO1 Hyperion image data for detecting the occurrence of the invasive species, Chinese tallow. *International Journal of Remote Sensing* **26**(8), 1611-1636.

Rangeland Assessment Unit, 1988. Land systems description. Rangeland assessment unit, Department of lands, The government of South Australia, Adelaide.

Research Systems Inc, 2000. ENVI User's Guide, the Environment for Visualizing Images, Version 3.4. Research Systems, Inc, Boulder, USA.

Reynolds, J.F. and Stafford Smith, D.M. (Editors), 2002. Global desertification, do humans cause deserts? Dehlem University Press, Berlin, Germany.

Ribed, P.S. and Lopez, A.M., 1995. Monitoring burnt areas by principal components analysis of multi-temporal TM data. *International Journal of Remote Sensing* **1**(9), 1577-1587.

Richards, G. and Furby, S.L., 2002. Sub-hectare land cover monitoring: Developing a national scale time-series program, Proceedings of the 11th Australasian Remote Sensing and Photogrametry Conference. The Remote Sensing and Photogrammetry Association of Australia, Brisbane, Australia.

Richards, J.A., 1984. Thematic mapping from multitemporal image data using the principal components transformation. *Remote Sensing of Environment* **16**(1), 35-46.

Richardson, A.J. and Wiegand, C.L., 1977. Distinguishing vegetation from soil background information. *Photogrammetric Engineering and Remote Sensing* **43**(12), 1541-1552.

Robinove, C.J., Chavez, P.S., Gehring, D. and Holmgren, R., 1981. Arid land monitoring using Landsat albedo difference images. *Remote Sensing of Environment* **11**, 133-156.

Rogan, J., Franklin, J. and Roberts, D.A., 2002. A comparison of methods for monitoring multitemporal vegetation change using Thematic Mapper imagery. *Remote Sensing of Environment* **80**(1), 143-156.

Rondeaux, G., Steven, M. and Baret, F., 1996. Optimization of soil-adjusted vegetation indices. *Remote Sensing of Environment* **55**, 95-107.

Rouse, J.W., Haas, R.W., Schell, J.A., Deering, D.W. and Harlan, J.C., 1974. Monitoring the vernal advancement and retrogradation (green ware effect) of natural vegetation. NASA/GSFCT, Type 3, Final Report, Greenbelt, MD, USA.

Rubio, J.L. and Bochet, E., 1998. Desertification indicators as diagnosis criteria for desertification risk assessment in Europe. *Journal of Arid Environments* **39**, 113-120.

Runnstorm, M.C., 2003. Rangeland development of Muus sandy land in semi-arid China: an analysis using Landsat and NOAA remote sensing data. *Land Degradation and Development* **14**, 189-202.

Ruthven III, D.C., 2007. Grazing effects on forb diversity and abundance in a honey mesquite parkland. *Journal of Arid Environments* **68**(4), 668-677.

Satterwhite, M.B. and Henley, J.P., 1987. Spectral characteristics of selected soils and vegetation in northern Nevada and their discrimination using band ratio techniques. *Remote Sensing of Environment* **23**, 155-175.

Sattle, J.J. and Drake, N., 1993. Linear mixing and the estimation of ground cover propertions. *International Journal of Remote Sensing* **14**(6), 1159-1177.

Schlesinger, W.H. et al., 1990. Biological feedbacks in global desertification. *Science* **247**, 1043-1048.

Schmidt, H. and Karnieli, A., 2001. Sensitivity of vegetation indices to substrate brightness in hyper-arid environment: the Markhtesh Ramon Crater (Israel) case study. *International Journal of Remote Sensing* **22**(17), 3503-3520.

Sharma, K.D., 1998. The hydrological indicators of desertification. *Journal of Arid Environments* **39**(2), 121-132.

Sidahmed, A., 1996. The rangelands of the arid/semi-arid areas: challenges and hopes for the 2000s, The International Conference on Desert Development in the Arab Gulf Countries. KISR, Kuwait, 23-26 March, pp. 1-15.

Singh, A., 1989. Digital change detection techniques using remotely sensed data. *International Journal of Remote Sensing* **10**, 989-1003.

Small, C., 2004. The Landsat ETM+ spectral mixing space. *Remote Sensing of Environment* **93**, 1-17.

Smith, G.M. and Milton, E.J., 1999. The use of the empirical line method to calibrate remotely sensed data to reflectance. *International Journal of Remote Sensing* **20**(13), 2653-2662.

Smith, M.O., Ustin, S.L., Adams, J.B. and Gillespie, A.R., 1990. Vegetation in deserts: I. A regional measure of abundance form multispectral images. *Remote Sensing of Environment* **31**(1), 1-26.

Stanley, R.J., 1982. Soils and vegetation: an assessment of current status. Proceedings of National Arid Lands Conference, What Future for Australia' Arid Lands. Australian Conservation Foundation, Broken Hill, New South Wales, May 21-25, pp. 8-18.

Stuffler, T., Kaufmann, H., Hofer, S., Forster, K.P., Graue, R., Kampf, D., Mehl, H., Schreir, G., Mueller, A., Arnold, G., Bach, H., Benz, U., Jung-Rothenhausler, F. and Haydn, R., 2005. The Advanced German Hyperspectral Mission EnMAP, In the Proceeding of the 31st International Symposium on Remote Sensing of Environment, Istanbul.

Symeonakis, E. and Drake, N., 2004. Monitoring desertification and Land degradation over Sub-Saharan Africa. *International Journal of Remote Sensing* **25**(3), 573-592.

Tanser, F.C. and Palmer, A.R., 1999. The application of remotely-sensed diversity index to monitor degradation patterns in a semi-arid, heterogeneous, South Africa landscape. *Journal of Arid Environments* **43**, 477-484.

Thenkabail, P.S., Ward, A.D., Lyon, J.G. and Maerry, C.J., 1994. Thematic Mapper vegetation indices for determining Soybean and Corn growth parameters. *Photogrammetric Engineering and Remote Sensing* **60**(4), 437-442.

Thiam, A. and Eastman, J.R., 2001. Vegetation indices in IDRISI 32 release 2, guide to GIS and image processing volume 2. Clark University, USA.

Tompkins, S., Mustard, J.F., Pieters, C.M. and Forsyth, D.W., 1997. Optimization of endmembers for spectral mixture analysis. *Remote Sensing of Environment* **59**(3), 472-489.

Tongway, D.J., Sparrow, A.D. and Friedel, M.H., 2003. Degradation and recovery processes in arid lands of central Australia. Part 1: soil and land resources. *Journal of Arid Environments* **55**, 301-326.

Townshend, J.R.G. and Justice, C.O., 1986. Analysis of the dynamics of African vegetation using the normalized difference vegetation index. *International Journal of Remote Sensing* **7**, 1435-1446.

Tromp, M. and Epema, G.F., 1999. Spectral mixture analysis for mapping land degradation in semi-arid areas. *Geologie en Mijnbouw* **77**, 153-160.

Tucker, C.J., Vanpraet, C., Boerwinkel, E. and Gaston, A., 1983. Satellite remote sensing of total dry matter production in the Senegalese Sahel. *Remote Sensing of Environment* **13**(6), 461-474.

Tueller, P.T., 1987. Remote sensing science applications in arid environment. *Remote Sensing of Environment* **23**(2), 143-154.

Tynan, R., 1995. Lease assessment overview report, Gawler Ranges Soil Conservation District(GRSCD), Department of Environment and Natural Resources, Adelaide.

UNCED, 1992. Agenda 21, United Nations Conference on Environment and Development, United Nations, New York.

Ungar, S.G., Pearlman, J.S., Mendenhall, J.A. and Reuter, D., 2003. Overview of the Earth Observing One (EO-1) mission. *IEEE Transactions on Geoscience and Remote Sensing* **41**(6), 1149-1159.

University of Arizona, 2001. Arizona rangelands: rangeland inventory, monitoring and evaluation. [Internet], Accessed May 2004, Available at URL: http://cals.arizona.edu/agnic/az/inventorymonitoring.

Walker, B.H., 1970. An evaluation of eight methods of botanical analysis on grasslands in Rhodesia. *Applied Energy* **7**, 403-416.

Wallace, J., Behn, G. and Furby, S., 2006. Vegetation condition assessment and monitoring from sequences of satellite imagery. *Ecological Management and Restoration* **7**(s1), S31-S36.

Wang, J., Rich, P.M., Price, K.P. and W.D, K., 2004. Relationships between NDVI and tree productivity in the central great plains. *International Journal of Remote Sensing* **25**(16), 3127-3138.

Wessels, K.J., Prince, S.D., Frost, P.E. and Zyl, D.V., 2004. Assessing the effects of human-induced land degradation in the former homelands of northern South Africa. *Remote Sensing of Environment* **91**, 47-67.

Wessels, K.J., Prince, S.D., Malherbe, J., Small, J., Frost, P.E. and VanZyl, D., 2007. Can human-induced land degradation be distinguished from the effects of rainfall variability? A case study in South Africa. Journal of Arid Environments 68(2), 271-297.

White, J. and Gould, P., 2002. Gawler Bioregion vegetation monitoring, Pastoral Program, Sustainable Resources, The Department of Conservation, Adelaide, South Australia.

Wilson, A.D., Abraham, N.A., Barratt, R., Choate, J., Green, D.R., Harland, R.J., Oxley, R.E. and Stanley, R.J., 1987. Evaluation of methods of assessing vegetation change in the semi-arid rangelands of southern Australia. *Rangel. J.* **9**(1), 5-13.

Woods, L.E., 1983. Land degradation in Australia. Australian Government Publishing Service, Canberra, Australia.

Wu, D., 2000. Comparison of tree different methods to select feature for discriminating forest cover types using SAR imagery. *International Journal of Remote Sensing* **21**(10), 2089-2099.

Yool, S.R., 2001. Enhancing fire scar anomalies in AVHRR NDVI time series data. *GeoCarto International* **16**, 5-12.

Yool, S.R., Makaio, M.J. and Watts, J.M., 1997. Techniques for computer-assisted mapping of rangeland change. *Journal of Range Management* **50**(3), 307-314.

Zhao, H.-L., Zhao, X.-Y., Zhou, R.-L., Zhang, T.-H. and Drake, S., 2005. Desertification processes due to heavy grazing in sandy rangeland, Inner Mongolia. *Journal of Arid Environments* **62**(2), 309-319.

Zhao, W.Y., Li, J.L. and Qi, J.G., 2007. Changes in vegetation diversity and structure in response to heavy grazing pressure in the northern Tianshan mountains, China. *Journal of Arid Environments* **68**(3), 465-479.

APPENDIX 1

Examples of vegetation species in the study area

Maireana sedifolia (Pearl bluebush)

Maireana astrotricha (Low bluebush)

Atriplex vesicaria (Bladder saltbush)

Maireana aphylla (Cottonbush)

Acacia aneura (Mulga)

Acacia papyrocorpa (Western myall)

Senna. ft. petiolaris (Desert cassia)

Callitris glaucophylla (Native pine)

Halosarcia pergranulata (Samphire)

Acacia tetragonophylla (Dead finish)

Eragrostis eriopoda (Woollybutt)

Sand dune with dry sandhill canegrass

APPENDIX 2

Atmospheric correction parameters

ACORN input parameters for Hyperion

Image format	1
Integer format	0
Image dimensions (bands, samples, lines, offset)	191 256 3412 0
Longitude (degree, minute, second)	-30° 55' 33"
Date (day, month, year)	29 12 2005
Time (UTC) (hour, minute, second)	02 36 20
Elevation	150 m
Altitude	705000 m
Model	Mid-latitude-summer (1)
Derive water vapour	1140 nm (2)
Include path in water fit	1
Visibility	100000 m
Estimate visibility	1
Artifact suppression (type1, type2, type3)	1 1 1

Hyperion wavelength, FWHM and gain values for ACORN. Offset values of all bands were null.

Band number	Wavelength	FWHM	Gain
10	447.17	11.3871	0.025
11	457.34	11.3871	0.025
12	467.52	11.3871	0.025
13	477.69	11.3871	0.025
14	487.87	11.3784	0.025
15	498.04	11.3538	0.025
16	508.22	11.3133	0.025
17	518.39	11.258	0.025
18	528.57	11.1907	0.025
19	538.74	11.1119	0.025
20	548.92	11.0245	0.025
21	559.09	10.9321	0.025
22	569.27	10.8368	0.025
23	579.45	10.7407	0.025
24	589.62	10.6482	0.025
25	599.8	10.5607	0.025
26	609.97	10.4823	0.025
27	620.15	10.4147	0.025
28	630.32	10.3595	0.025
29	640.5	10.3188	0.025
30	650.67	10.2942	0.025
31	660.85	10.2857	0.025
32	671.02	10.298	0.025
33	681.2	10.3349	0.025
34	691.37	10.3909	0.025
35	701.55	10.4591	0.025
36	711.72	10.5322	0.025
37	721.9	10.6004	0.025
38	732.07	10.6562	0.025
39	742.25	10.6933	0.025
40	752.43	10.7058	0.025
41	762.6	10.7276	0.025
42	772.78	10.7907	0.025
43	782.95	10.8833	0.025
44	793.13	10.9938	0.025
45	803.3	11.1045	0.025
46	813.48	11.198	0.025
47	823.65	11.26	0.025
48	833.83	11.2823	0.025
49	844	11.2821	0.025
50	854.18	11.2815	0.025
51	864.35	11.2809	0.025
52	874.53	11.2796	0.025
53	884.7	11.2782	0.025
54	894.88	11.2771	0.025
55	905.05	11.2764	0.025
56	915.23	11.2756	0.025
57	925.41	11.2754	0.025

Band number	Wavelength	FWHM	Gain
79	932.64	11.0457	0.0125
80	942.73	11.0457	0.0125
81	952.82	11.0457	0.0125
82	962.91	11.0457	0.0125
83	972.99	11.0457	0.0125
84	983.08	11.0457	0.0125
85	993.17	11.0457	0.0125
86	1003.3	11.0457	0.0125
87	1013.3	11.0457	0.0125
88	1023.4	11.0451	0.0125
89	1033.5	11.0423	0.0125
90	1043.59	11.0371	0.0125
91	1053.69	11.0302	0.0125
92	1063.79	11.0218	0.0125
93	1073.89	11.0122	0.0125
94	1083.99	11.0013	0.0125
95	1094.09	10.9871	0.0125
96	1104.18	10.9732	0.0125
97	1114.18	10.9572	0.0125
98	1124.28	10.9418	0.0125
99	1134.38	10.9248	0.0125
100	1144.48	10.9064	0.0125
101	1154.58	10.8884	0.0125
102	1164.68	10.8696	0.0125
103	1174.77	10.8513	0.0125
104	1184.87	10.8335	0.0125
105	1194.97	10.8154	0.0125
106	1205.07	10.7979	0.0125
107	1215.17	10.7822	0.0125
108	1225.17	10.7662	0.0125
109	1235.27	10.752	0.0125
110	1245.36	10.7385	0.0125
111	1255.46	10.727	0.0125
112	1265.56	10.7174	0.0125
113	1275.66	10.7091	0.0125
114	1285.76	10.7022	0.0125
115	1295.86	10.697	0.0125
116	1305.96	10.6946	0.0125
117	1316.05	10.6937	0.0125
118	1326.05	10.6949	0.0125
119	1336.15	10.6996	0.0125
120	1346.25	10.7058	0.0125
121	1356.35	10.7163	0.0125
122	1366.45	10.7283	0.0125
123	1376.55	10.7437	0.0125
124	1386.64	10.7612	0.0125
125	1396.74	10.7807	0.0125
126	1406.84	10.8034	0.0125

Band number	Wavelength	FWHM	Gain
127	1416.94	10.8267	0.0125
128	1426.94	10.8534	0.0125
129	1437.04	10.8818	0.0125
130	1447.14	10.911	0.0125
131	1457.23	10.9422	0.0125
132	1467.33	10.9743	0.0125
133	1477.43	11.0073	0.0125
134	1487.53	11.0414	0.0125
135	1497.63	11.0759	0.0125
136	1507.73	11.1108	0.0125
137	1517.83	11.1461	0.0125
138	1527.92	11.1811	0.0125
139	1537.92	11.2155	0.0125
140	1548.02	11.2496	0.0125
141	1558.12	11.2826	0.0125
142	1568.22	11.3146	0.0125
143	1578.32	11.3461	0.0125
144	1588.42	11.3753	0.0125
145	1598.51	11.4037	0.0125
146	1608.61	11.4302	0.0125
147	1618.71	11.4538	0.0125
148	1628.81	11.476	0.0125
149	1638.81	11.4958	0.0125
150	1648.91	11.5133	0.0125
151	1659.01	11.5286	0.0125
152	1669.1	11.5404	0.0125
153	1679.2	11.5505	0.0125
154	1689.3	11.558	0.0125
155	1699.4	11.5621	0.0125
156	1709.5	11.5634	0.0125
157	1719.6	11.5617	0.0125
158	1729.7	11.5562	0.0125
159	1739.69	11.5477	0.0125
160	1749.79	11.5346	0.0125
161	1759.89	11.5193	0.0125
162	1769.99	11.5002	0.0125
163	1780.09	11.4789	0.0125
164	1790.19	11.4548	0.0125
165	1800.29	11.4279	0.0125
166	1810.38	11.3994	0.0125
167	1820.48	11.3688	0.0125
168	1830.58	11.3366	0.0125
169	1840.58	11.3036	0.0125
170	1850.68	11.2696	0.0125
171	1860.78	11.2363	0.0125
172	1870.87	11.2007	0.0125
173	1880.97	11.1666	0.0125
174	1891.07	11.1334	0.0125
175	1901.17	11.1018	0.0125
176	1911.27	11.0714	0.0125

Band number	Wavelength	FWHM	Gain
177	1921.37	11.0424	0.0125
178	1931.47	11.0155	0.0125
179	1941.57	10.9913	0.0125
180	1951.56	10.9698	0.0125
181	1961.66	10.9508	0.0125
182	1971.76	10.9355	0.0125
183	1981.86	10.923	0.0125
184	1991.96	10.9139	0.0125
185	2002.06	10.9083	0.0125
186	2012.16	10.9069	0.0125
187	2022.25	10.9057	0.0125
188	2032.35	10.9013	0.0125
189	2042.45	10.895	0.0125
190	2052.45	10.8854	0.0125
191	2062.55	10.8739	0.0125
192	2072.65	10.8591	0.0125
193	2082.75	10.8429	0.0125
194	2092.84	10.8243	0.0125
195	2102.94	10.8039	0.0125
196	2113.04	10.782	0.0125
197	2123.14	10.7591	0.0125
198	2133.24	10.7341	0.0125
199	2143.34	10.7092	0.0125
200	2153.34	10.6834	0.0125
201	2163.43	10.6572	0.0125
202	2173.53	10.6313	0.0125
203	2183.63	10.6052	0.0125
204	2193.73	10.5804	0.0125
205	2203.83	10.556	0.0125
206	2213.93	10.5328	0.0125
207	2224.02	10.5101	0.0125
208	2234.12	10.4904	0.0125
209	2244.22	10.4722	0.0125
210	2254.22	10.4552	0.0125
211	2264.32	10.4408	0.0125
212	2274.42	10.4285	0.0125
213	2284.52	10.4197	0.0125
214	2294.62	10.4129	0.0125
215	2304.71	10.4088	0.0125
216	2314.81	10.4077	0.0125
217	2324.91	10.4077	0.0125
218	2335.01	10.4077	0.0125
219	2345.11	10.4077	0.0125
220	2355.21	10.4077	0.0125
221	2365.21	10.4077	0.0125

APPENDIX 3

Representative examples of field spectra collected with ASD Field Spectrometer in April 2006

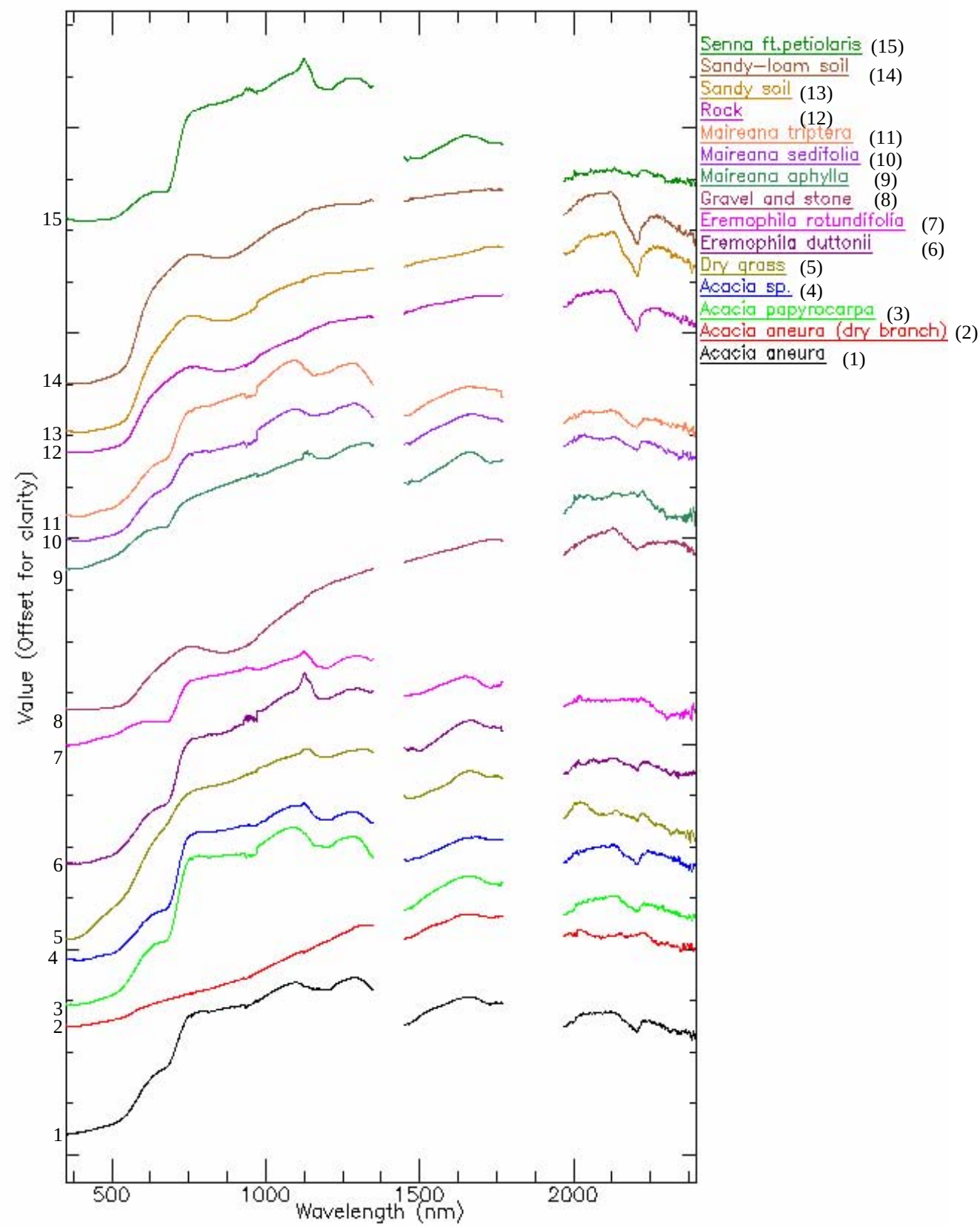

APPENDIX 4

Percentage cover collected from approximately 1000 points at each site in January 2006 (Sample size= 52)

Sites	**1**	**2**	**3**	**4**	**5**	**6**	**7**	**8**	**9**	**10**	**11**	**12**	**13**	**14**	**15**	**16**	**17**	**18**	**19**	**20**	**21**	**22**	**23**	**24**	**25**	**26**
Coordinates (Easting & Northing) Components	565346 6616504	565941 6616370	566817 6615687	567371 6612869	566740 6611508	566412 6610766	566294 6608143	567146 6607513	567618 6607266	568297 6607279	566244 6604898	569107 6603626	569166 6603063	568632 6603730	568671 6603056	567997 6603497	567272 6603595	566395 6602761	566056 6601073	566030 6598573	566008 6596288	566423 6594009	569545 6606884	570664 6606762	569964 6606730	569266 6606909
Bare soil	45.3	54.9	53.2	49.8	40.8	41.9	50.1	23.1	58.5	54.5	33.9	35.4	44.0	47.4	49.1	52.6	35.0	28.3	50.0	22.7	24.4	40.7	61.7	52.7	40.6	55.3
Gravel and stone	17.8	25.0	33.3				0.6													40.7	38.2	10.6		27.4		2.4
Litter	9.2	2.6	5.5	45.7	43.8	43.0	4.3	57.8	23.4	38.0	43.1	44.3	7.9	21.1	11.8	10.6	44.4	23.6	30.4	8.4	9.2	26.9	35.9	6.8	35.4	24.9
Cryptogams							0.4														0.8					
Ephemeral (Grass+Herbs)	2.2	4.2	0.5	0.4	6.5		4.4	5.8	1.3	1.9	18.3	9.2	0.5	7.4	4.7	0.9	13.5	37.2	10.3	5.6	0.3	15.4	0.7		9.0	10.8
Acacia aneura		0.8	1.4	1.8	9.0	15.1	3.1	1.7	3.5	4.4	4.6	11.1		3.2	8.3	6.7	7.2	7.6	4.9	15.8	27.1	6.3	1.7	7.4	2.2	3.8
Acacia burkittii																										
Acacia kempeana																										
Acacia papyrocarpa			0.2	2.3			11.7	9.2	0.7	1.2			24.1		12.3	15.9				1.7						0.5
Acacia tetragonophylla	1.7	1.3	1.1																0.5							
Atriplex vesicaria	8.8	0.8	1.4				21.3	1.2					0.8		3.9	1.1										
Casuarina pauper																								2.9		1.7
Chenopodium nitrariaceum									9.8																	
Dissocarpus biflorus																										
Eremophila duttonii			0.6																							
Eremophila latrobei																										
Eremophila longifolia																										
Eremophila rotundifolia																										
Eremophila scoparia																										
Grevillea juncifolia									2.9																	
Lawrencia squamata	1.4																									
Maireana aphylla																										
Maireana appressa	0.1																									
Maireana astrotricha	9.2	3.3					0.6																			
Maireana pentatropis																										
Maireana pyramidata																										
Maireana sedifolia		2.2					2.6						22.6	1.1	6.9	10.1										
Maireana triptera	3.4	5.0	0.5																							
Melaleuca glomerata																										
Sclerolaena obliquicuspis	0.8																									
Senna artemisioides																										
Senna ft.gawlerensis																										
Senna ft.oligophylla			1.2																							
Senna ft.petiolaris			0.4				0.9	1.2							2.9	2.0		3.4	3.8	5.2				2.7	12.8	0.7
Senna sp.			0.7																							

Sites	**27**	**28**	**29**	**30**	**31**	**32**	**33**	**34**	**35**	**36**	**37**	**38**	**39**	**40**	**41**	**42**	**43**	**44**	**45**	**46**	**47**	**48**	**49**	**50**	**51**	**52**
Coordinates (Easting & Northing) Components	566387 6607586	568098 6613270	568715 6612000	569643 6611125	571414 6610138	567156 6594013	566154 6592061	565981 6591346	566647 6590926	566782 6590572	566015 6589521	567866 6608016	566459 6606127	566739 6601580	566724 6597857	566042 6587922	567254 6613508	566779 6613234	566810 6614551	570302 6614721	571631 6614863	567729 6619022	570021 6626301	567859 6618170	567891 6619419	570902 6619622
Bare soil	33.6	28.1	26.3	47.0	37.7	42.4	32.9	29.3	27.3	31.3	32.1	41.0	25.4	29.5	19.8	27.7	62.4	47.2	9.9	40.5	29.0	29.2	28.5	26.7	40.0	56.2
Gravel and stone		26.3		41.0				3.3			10.3		30.3	16.4	30.6	17.1	3.6	32.7	41.8	1.4	15.5			25.8	10.2	13.1
Litter	21.1	34.0	35.4	2.4	49.4	30.5	40.5	23.4	29.1	21.3	29.6	39.9	12.1	26.6	20.6	29.5	13.2	1.1	13.6	17.5	9.4	29.7	13.2	10.6	13.6	11.5
Cryptogams								11.3		3.6			4.4		7.1	3.6									0.8	
Ephemeral (Grass+Herbs)	14.7	7.3	23.3	5.8	7.3	13.6	9.9	12.2	32.0	9.0	8.6	5.3	5.6	5.5	11.5	9.3	1.2	7.7	6.4	5.2	8.8	10.8	8.1	4.5	6.4	1.8
Acacia aneura	3.0	4.2	14.8	2.2	2.4	2.8	1.3	2.3	3.3	1.1	1.6		2.1	5.5	7.7	2.9					1.9		14.3	2.8		1.9
Acacia burkittii										11.5	1.1					3.2										
Acacia kempeana																		3.9								
Acacia papyrocarpa	4.3				1.2					1.7		9.1	2.7			0.8	17.6	3.6								
Acacia tetragonophylla						0.8				0.3														2.5	0.4	1.7
Atriplex vesicaria																								2.5	15.3	
Casuarina pauper											1.5					2.3										
Chenopodium nitrariaceum																										
Dissocarpus biflorus						3.7								1.3												
Eremophila duttonii								1.5							1.0				3.7	15.2	2.0					
Eremophila latrobei															1.7	2.7				5.2						
Eremophila longifolia														8.7												
Eremophila rotundifolia																			19.3		27.1					
Eremophila scoparia																		2.6		1.5						
Grevillea juncifolia						2.3	15.4		2.2		12.4															
Lawrencia squamata																										
Maireana aphylla										14.5									4.1	7.5	6.3	30.3	31.2	22.1	10.2	12.2
Maireana appressa																										
Maireana astrotricha																										
Maireana pentatropis						0.9			0.9		1.1															
Maireana pyramidata																									0.4	
Maireana sedifolia								2.3		1.4	1.5	1.2	17.4	0.9											2.7	1.7
Maireana triptera																			1.3							
Melaleuca glomerata	21.8																						4.8			
Sclerolaena obliquicuspis																										
Senna artemisioides									5.2											6.1						
Senna ft.gawlerensis								14.6		1.4					1.1											
Senna ft.oligophylla																										
Senna ft.petiolaris	1.6			1.4	1.9	1.0						1.4		5.5			1.9	1.1						2.5		
Senna sp.						1.8				2.8		2.1														